Medizinische Fakultät
der
Universität Duisburg-Essen

Aus dem Institut für Pharmakologie

The role of NLRP3-inflammasome signaling

in different forms of atrial fibrillation

I n a u g u r a l d i s s e r t a t i o n
zur
Erlangung des Doktorgrades der Medizin
durch die Medizinische Fakultät
der Universität Duisburg-Essen

Vorgelegt von
Tina Veleva
aus Stara Zagora, Bulgarien
2021

DOI: 10.17185/duepublico/77159
URN: urn:nbn:de:hbz:465-20230419-124124-7

Dekan: Herr Univ.- Prof. Dr. med. J. Buer

1. Gutachter/in: Herr Univ.- Prof. Dr. med. D. Dobrev

2. Gutachter/in: Herr Univ.- Prof. Dr. med. M. Totzeck

3. Gutachter/in: Frau Prof. Dr. med. C. Schmidt

Tag der mündlichen Prüfung: 10. August 2022

‘Играта прави шампиона’

Посветено на моите родители

TABLE OF CONTENTS

1 INTRODUCTION

1.1 Inflammation

Inflammation underlies a wide range of coordinated processes, triggered by infection and tissue injury. The immune-competent cells form an adaptive response to noxious stimuli in order to maintain tissue homeostasis. Primed with a variety of germline-encoded immune signaling receptors (pattern recognition receptors; PRRs), these cells can detect infections or non-infectious instigators (Mangan et al., 2018). The triggers are derived either from different pathogens (pathogen-associated molecular patterns; PAMPs), or from the host itself (danger-associated molecular patterns; DAMPs). Activation of PRRs leads to a variety of transcriptional changes and therefore to the initiation of a proinflammatory immune response, activating the innate immune defenses (von Moltke et al., 2013).

A distinct group of intracellular PRRs, known as NOD-like receptors (NLRs), recognizes a wide range of both endogenous and exogenous triggers (PAMPs and DAMPs). They assemble in high molecular weight complexes inside the cell, where they facilitate the maturation of proinflammatory cytokines (Schroder & Tschopp, 2010). Already extensively studied in other systems, cytokines have recently received significant scientific attention in the cardiovascular field, particularly the interleukin-1 family (Medzhitov, 2008). The Canakinumab Anti-inflammatory Thrombosis Outcomes Study (CANTOS) put a spotlight on interleukin-1β (IL-1β), establishing that inhibition of a major product of the NLRP3 inflammasome with canakinumab reduces the incidence of cardiovascular events and might alter cancer incidence in patients with atherosclerosis, a previous myocardial infarction and elevated C-reactive protein (CRP) levels (Ridker et al., 2017). Besides interleukin-18 (IL-18), IL-1β is secreted predominantly from macrophages and monocytes. They differ from the other cytokine family members being synthesized as inactive precursors, and being processed by an intracellular cysteine protease, caspase-1 (Casp1), into active forms (van de Veerdonk et al., 2011).

1.2 Inflammasomes

The multiprotein complexes formed in the cytosol, originally known as caspase-1 activation platforms, were first described in 2002 and were subsequently designated as inflammasomes (Martinon et al., 2002). The inflammasomes originated from the NLR family and commonly carry a central nucleotide-binding and oligomerization (NACHT) domain, which enables the binding of a small adaptor protein – the apoptosis-associated speck-like protein containing a C-

terminal caspase activation and recruitment domain (CARD), also known as ASC. These supramolecular complexes are responsible for the proximity-induced self-cleavage of activator caspases and gasdermin family proteins, as well as the subsequent secretion of proinflammatory cytokines (Latz, 2010; Monie, 2017; Schroder et al., 2010).

1.2.1 NLRP3 inflammasome

The NLRP3 inflammasome complex is the most studied member of the NLR family (**Figure 1**). It consists of a receptor (NACHT, LRR, and PYD domains containing protein 3; NLRP3), an adaptor (ASC) and an effector protein (Casp1) (Monie, 2017; Schroder et al., 2010). The leucine-rich repeats (LRR) domain in the C-terminus of the NLRP3, function in ligand sensing and autoregulation. The N-terminal side contains a pyrin domain (PYD), which acts as a mediator of homotypic protein-protein interactions with the PYD domain of ASC. It enables the recruitment of the precursor of Casp1 (pro-Casp1) (Latz, 2010; Schroder et al., 2010). As a dynamic molecular structure, the activation of the NLRP3 inflammasome requires two steps or signals. The first step is the so-called priming (transcriptional control of the expression of numerous genes) and the second step is known as triggering (assembly of the NLRP3 inflammasome). The assembly of these 3 proteins in a wheel-shaped signaling hub in the cytosol mediates the spatial proximity of the inactive zymogen caspases, enabling their auto-cleavage into active Casp1. Once activated, Casp1 triggers the maturation of the inactive isoforms (pro-IL-1β, pro-IL-18) into active IL-1β and IL-18. Additionally, Casp1 cleaves the full-length gasdermin D (GSDMD-FL), removing its inhibiting C-terminus (GSDMD-CT), facilitating the release of the N-terminus (GSDMD-NT) which forms pores in the plasma membrane of cells. These pores allow the products of the inflammasome cascade (IL-1β, IL-18 and others) to leave the cell and further propagate the activation of the same or similar cascades in the neighboring cells (Gaidt & Hornung, 2016b). Nevertheless, the secretion of cytokines can also be accompanied by inflammatory programmed cell death (pyroptosis), executed via both Casp1 (canonical NLRP3 pathway) and caspase-11 (Casp11 in mice = caspase-4/5 in humans; non-canonical NLRP3 pathway; see below).

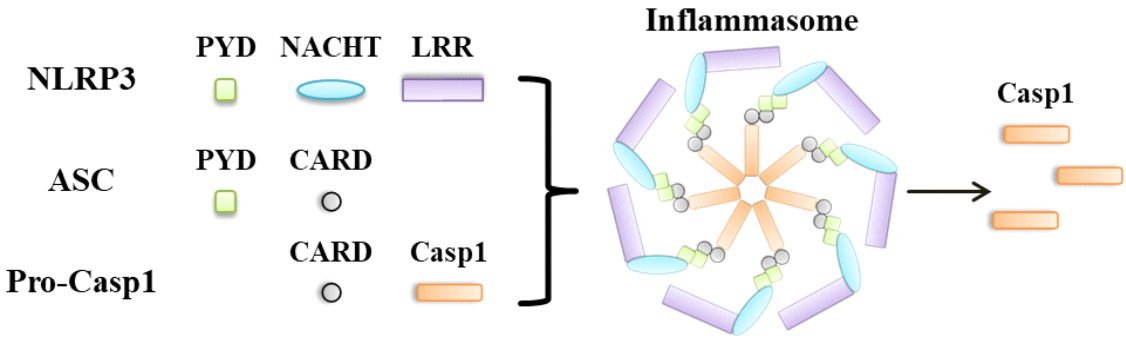

Figure 1: The NLRP3 inflammasome complex. Upon triggering, the components of the NLRP3 inflammasome form a propeller in the cytosol, enabling Casp1 auto-cleavage. ASC = apoptosis-associated speck-like protein containing a CARD; CARD = caspase activation and recruitment domain; Casp1 = active caspase-1; LRR = leucine rich repeats; NLRP3 = NACHT, LRR and PYD domains containing binding protein 3; Pro-Casp1 = pro-caspase-1; PYD = pyrin.

1.2.2 Priming of the NLRP3 inflammasome

The first signal to activate the NLRP3 inflammasome involves priming of the components of the three-domain structure. Toll-like receptor (TLR), tumor necrosis factor receptor (TNFR), interleukin-1 receptor (IL-1R), anaphylatoxin C3a and C5a receptors or angiotensin-II receptor (AGTR), all can activate the nuclear factor 'kappa-light-chain-enhancer' of activated B-cells (NFκB) transcription pathway (**Figure 2**) (Bauernfeind et al., 2009; Bauernfeind et al., 2016; Franchi et al., 2009; Groslambert & Py, 2018; Sutterwala et al., 2014). This results in enhanced transcription of target genes including NLRP3 and pro-IL-1β (Scott et al., 2019). Additionally, priming without involving transcription could be facilitated through TLR and IL-1R, which accelerate the de-ubiquitination of NLRP3, a process depending on mitochondrial reactive oxygen species (mtROS). Depending on which priming is executed (transcriptional or non-transcriptional), inflammasome activation could take from 10-30 min to more than 3 h (Bauernfeind et al., 2016; Fernandes-Alnemri et al., 2013; Juliana et al., 2012; Lin et al., 2014; Schroder et al., 2012). The TLR4/NFκB pathway is a major driver of NLRP3-inflammasome priming. Ligand binding activates TLR4 and triggers the myeloid differentiation primary response 88 (MyD88), the MyD88/IL-1R-associated kinase 4 (IRAK4) pathway, as well as TIR domain-containing adapter-inducing interferon-β (TRIF). Finally, NFκB dissociates from its endogenous inhibitor in the cytoplasm (IκB) and translocates to the nucleus (Scott et al., 2019). These cytosolic interactions rely on the production of mtROS, which play an important role in both priming and triggering of the NLRP3 inflammasome (Groslambert et al., 2018; Sutterwala et al., 2014).

Upon priming, cytosolic Casp1 and NLRP3 are recruited to the mitochondria. The mitochondrial protein cardiolipin relocates from the inner to the outer mitochondrial membrane

in order to interact with both proteins (Groslambert et al., 2018; Iyer et al., 2013; Sharma & Kanneganti, 2016).

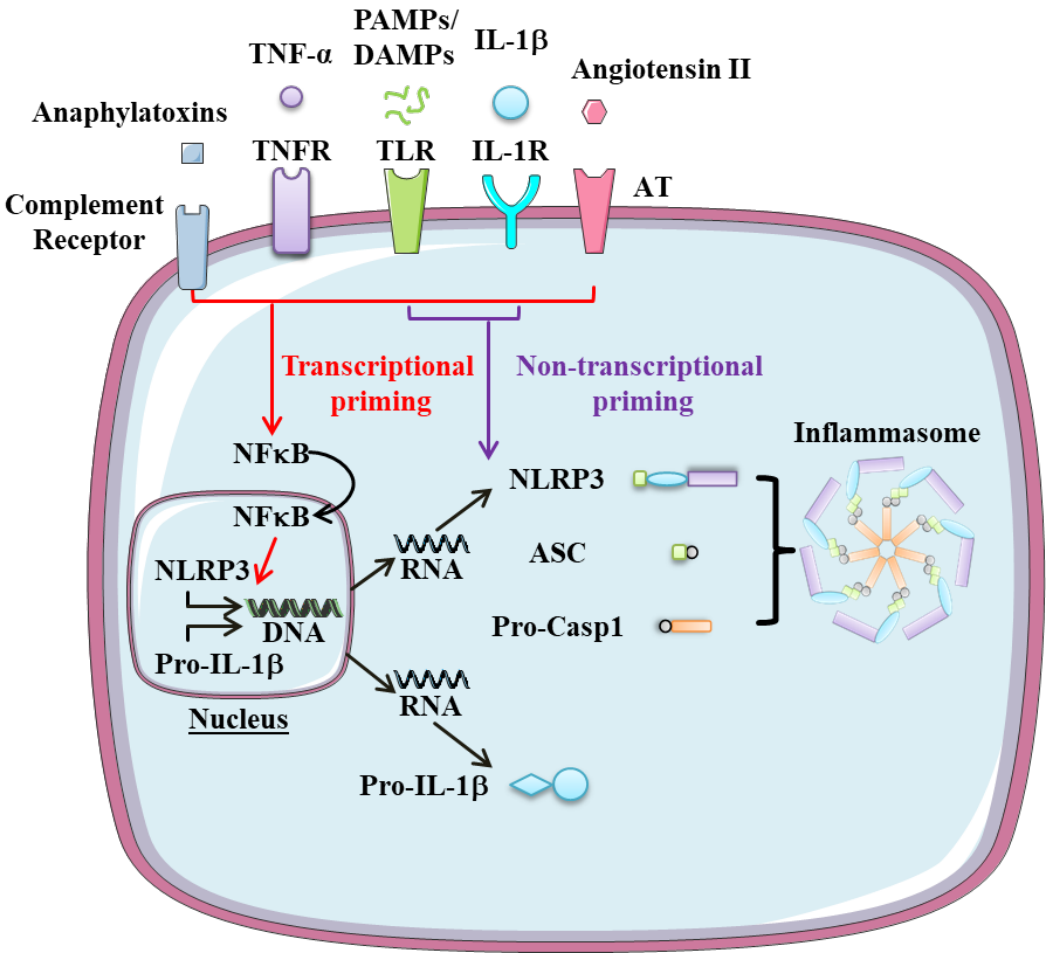

Figure 2: Priming of the NLRP3 inflammasome. Downstream signaling pathways of different receptors lead to either transcriptional or non-transcriptional priming of the NLRP3 inflammasome complex. PAMPs/DAMPs and cytokines activate rapid non-transcriptional modification of the inflammasome's sensor - NLRP3. Additionally, NFκB activation and its translocation into the nucleus of the cell facilitates NLRP3 and IL-1β transcriptional priming. AT = angiotensin-II receptor; ASC = apoptosis-associated speck-like protein containing a CARD domain. DAMPs = damage-associated molecular patterns; DNA = deoxyribonucleic acid; (Pro-)IL-1β = (pro-)interleukin-1β; NFκB = nuclear factor 'kappa-light-chain-enhancer' of activated B-cells; NLRP3 = NACHT, LRR and PYD domains containing binding protein 3; PAMPs = pathogen-associated molecular patterns; Pro-Casp1 = pro-caspase-1; RNA = ribonucleic acid; TLR = toll-like receptor; TNF-α = tumor necrosis factor α; TNFR = tumor necrosis factor receptor. (Adapted from Groslambert et al., 2018; Willeford et al., 2018)

1.2.3 Triggering of the NLRP3 inflammasome

The assembly of the sensor with the effector proteins, facilitated by ASC, is called triggering of the NLRP3 inflammasome complex. This step leads to formation of the catalytically active Casp1 in the center of the NRLP3 inflammasome propeller with subsequent maturation and secretion of cytokines (Broz & Dixit, 2016). A change in the K^+ homeostasis is considered the

main event controlling the multicomplex formation in the cytosol of immune-competent cells (Groslambert et al., 2018; Sutterwala et al., 2014).

NLRP3 is a cytosolic protein, which under basal conditions is inactive and resides in endoplasmic reticulum of resting mouse bone marrow-derived macrophages (BMDM) and other immune cells (Groslambert et al., 2018; Misawa et al., 2013; Zhou et al., 2011). Stress stimuli enable the oligomerization of the NLRP3 NACHT domain, allowing it to form a wheel-shaped signaling hub. The LRR domain is located on the outside of this propeller, whereas the inner side contains the PYDs, which form a disk promoting the recruitment of ASC molecules. The ASC protein is predominantly located in the nucleus, but occurs also in the cytosol in close association with the mitochondria (Bryan et al., 2009; Groslambert et al., 2018; Misawa et al., 2013). ASC forms typical structures, ~1-2 μm in size, called 'specks'. ASC itself is considered as a proinflammatory stimulus, with ASC specks being able to leave the cell as large insoluble aggregates, thereby propagating the inflammatory signal in phagocytic cells (Baroja-Mazo et al., 2014; Broz et al., 2010; Dick et al., 2016; Fernandes-Alnemri et al., 2007; Masumoto et al., 1999).

1.2.3.1 Canonical NLRP3 pathway

Canonical activation of the NLRP3 inflammasome in immune cells is mediated by cellular K^+ depletion (Munoz-Planillo et al., 2013). Activation of the purinergic receptor subtype 7 (P2X7R), pannexin-1 receptor, or pore-forming units can facilitate K^+ efflux (**Figure 3**). The pannexin-1 channel or connexin-43 hemi-channels can also release adenosine triphosphate (ATP) from the cell in the extracellular space, where it could act as a paracrine transmitter. Binding of exogenous ATP within milliseconds opens the ligand-gated ion channel P2X7R channel for small cations, including K^+, Na^+ and Ca^{2+} (Burnstock, 2016; Burnstock & Knight, 2018; Volonte et al., 2012). Crystals, crystal-like structures, mtROS and lysosomal-derived cathepsin B activate the NLRP3 inflammasome through the canonical pathway (**Table 1**).
Previous studies identified that pro-Casp1, which requires a biochemical change to become an active enzyme, is a tetramer composed of two p20 and two p10 subunits (Lavrik et al., 2005). Recently it was reported that a transient species also exists, the catalytically active heterodimer p33/p10, with the p33 complex being formed from the CARD domain and p20, while the proteolytically active p10 remains bound to ASC (Swanson et al., 2019). The p33/p10 self-cleavage generates p20/p10 thereby terminating the protease activity (Boucher et al., 2018). Since the stability of the p33/p10 heterodimers is different for different cell types, this limits

the activity of caspase-1 in a time-dependent manner. This intrinsic shutdown of the inflammasome signal highlights the transient and time coordinated nature of inflammasome-dependent inflammatory responses (Boucher et al., 2018).

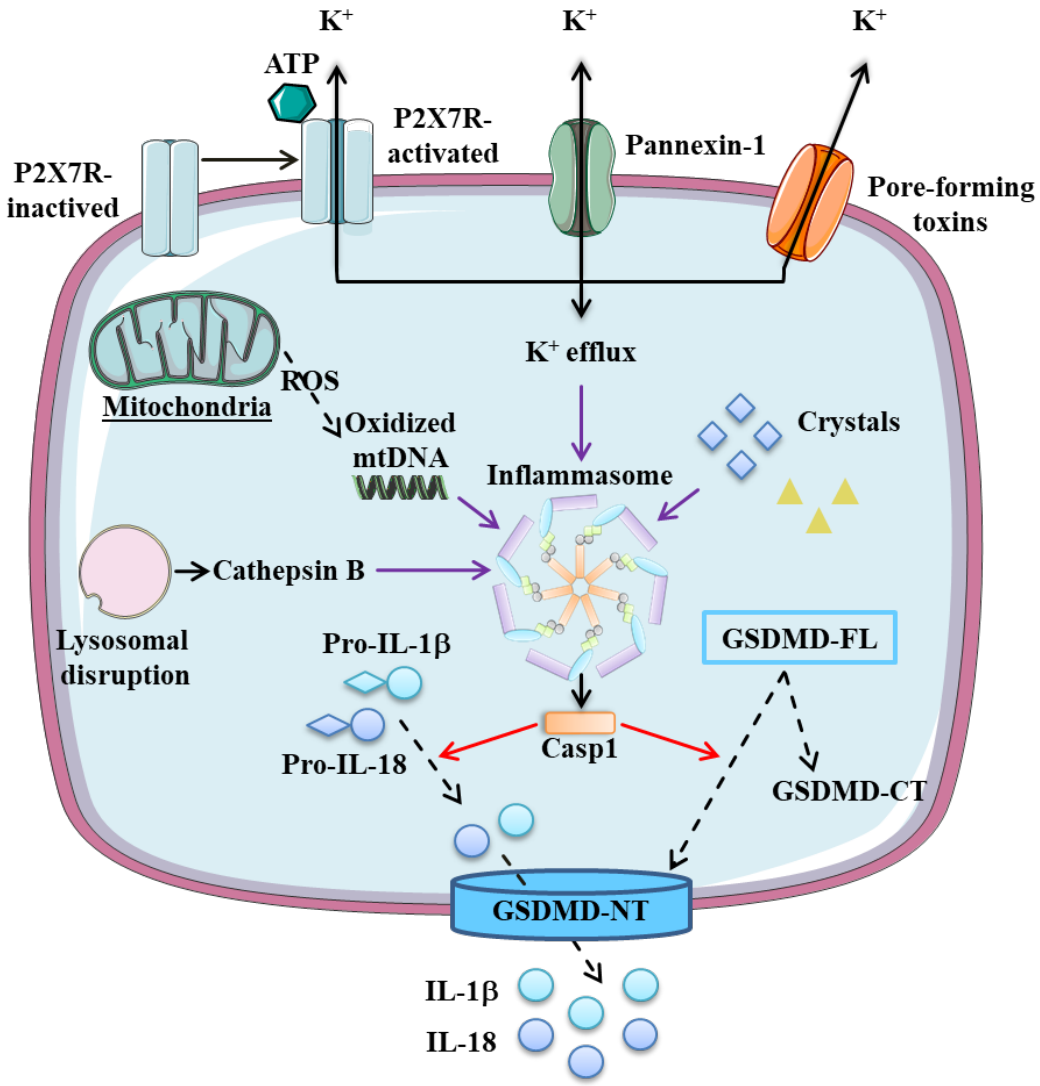

Figure 3: Canonical activation of the NLRP3 inflammasome. K^+ efflux through either ATP-dependent P2X7R activation, pannexin-1 receptor activation or pore-forming units leads to cellular K^+ depletion, resulting in canonical activation of the NLRP3 inflammasome. In addition, mtROS, several crystals and lysosomal-derived cathepsin B can also activate the NLRP3 inflammasome through the canonical pathway. Activated Casp1 leads to maturation of pro-IL-1β and pro-IL-18. Casp1 also cleaves GSDMD-FL to its pore-forming unit GSDMD-NT by removing its inhibiting C-terminus. The activated cytokines IL-1β and IL-18 are able to leave the cell through the GSDMD pore, further propagating the inflammatory signaling. ATP = Adenosine triphosphate; Casp1 = active caspase-1; GSDMD-CT = C-terminus of gasdermin D; GSDMD-FL = full-length gasdermin D; GSDMD-NT = N-terminus of gasdermin D; (Pro-)IL-1β = (pro-)interleukin-1β; (Pro-)IL-18 = (pro-)interleukin-18; mtDNA = mitochondrial deoxyribonucleic acid; mtROS = mitochondria-derived reactive oxygen species; NLRP3 = NACHT, LRR and PYD domains containing binding protein 3; P2X7R = purinergic receptor subtype 7. (Adapted from Sutterwala et al., 2014)

Table 1: Triggers of the NLRP3 inflammasome complex (Swanson et al., 2019).

Activator	Source	Triggers
DAMP	Self-derived	ATP, cholesterol crystals, monosodium urate crystals, calcium pyrophosphate dehydrate crystals, calcium oxalate crystals, soluble uric acid, neutrophil extracellular traps, cathelicidin, α-synuclein, amyloid- β, serum amyloid A , prion protein, biglycan, hyaluronan, islet amyloid polypeptide, hydroxyapatite, haeme, oxidized mitochondrial DNA , membrane attack complex, cyclic GMP–AMP, lysophosphatidylcholine, ceramides, oxidized phospholipid 1-palmitoyl-2-arachidonoyl-sn-glycero-3-phosphorylcholine, sphingosine
	Foreign-derived	Alum, silica, aluminium hydroxide, nanoparticles, carbon nanotubes, chitosan, palmitate (also self-derived), UVB, imiquimod (R837)/CL097, resiquimod (R848)
PAMP	Bacterial	Lipopolysaccharide, peptidoglycan, muramyl dipeptide, trehalose-6,6'-dibehenate, c-di-GMP–c-di-AMP, bacterial RNA and RNA–DNA hybrid; Toxins: nigericin, gramicidin , α/β-haemolysin, tetanolysin O, pneumolysin, leucocidin etc.
	Viral	Double-stranded RNA, single-stranded RNA
	Fungal	β-Glucans, hyphae, mannan, zymosan

1.2.3.2 Non-canonical pathway

There is an additional mechanism of NLRP3 complex activation, which involves cleavage of other cysteine proteases, including Casp4/Casp5 in humans and Casp11 in mice (**Figure 4**) (Gaidt et al., 2016a; Groslambert et al., 2018; Jamilloux et al., 2018; Netea et al., 2009; Piccini et al., 2008). Casp11 recognizes a strong lipopolysaccharide (LPS) signal from Gram-negative bacteria with its CARD domain and cleaves GSDMD-FL. The GSDMD-NT affinity for phosphatidylinositol lipid species found in the plasma membrane promotes pore formation (Sanders et al., 2015).

Caspase-11/4/5 are unique in terms of their high selectivity for GSDMD and their inability to directly maturate cytokines (Man & Kanneganti, 2016). However, Caspase-11/4/5 could control cytokine secretion by increasing plasma membrane permeabilization through formation of GSDMD pores. This mechanism indirectly activates the canonical pathway, most likely

because of disturbances in K^+ homeostasis. It has recently been shown that Casp11 also cleaves pannexin-1 upon intracellular LPS stimulation, mediating ATP release leading to P2X7R activation and activating the NLRP3 inflammasome complex in a non-canonical manner (Kayagaki et al., 2013; Yang et al., 2015).

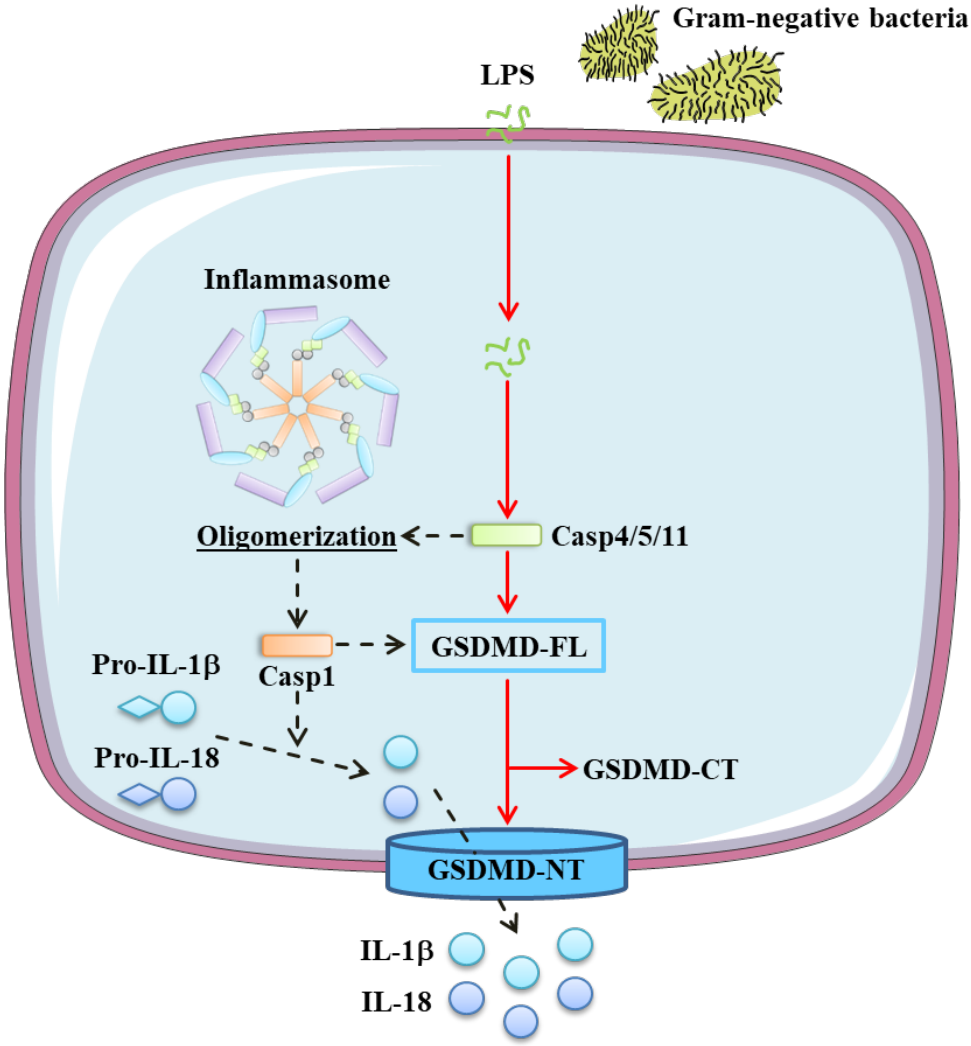

Figure 4: Non-canonical pathway of NLRP3 inflammasome activation. Non-canonical activation of the NLRP3 inflammasome is mediated by Casp4/5/11. TLR-independent downstream signaling of Gram-negative bacteria-derived LPS elicits Casp1 processing along with a cleavage of GSDMD-FL. GSDMD-NT pore formation allows activated cytokines IL-1β and IL-18 to leave the cell. Non-canonical activation of the NLRP3 inflammasome may induce inflammatory programmed cell death (pyroptosis) Casp1/4/5/11= active caspase-1/4/5/11; GSDMD-CT = C-terminus of gasdermin D; GSDMD-NT = N-terminus of gasdermin D; GSDMD-FL = full-length gasdermin D; (Pro-)IL-1β = (pro-)interleukin-1β; (Pro-)IL-18 = (pro-)interleukin-18; LPS = lipopolysaccharides; mtDNA = mitochondrial deoxyribonucleic acid; NLRP3 = NACHT, LRR and PYD domains containing binding protein 3; P2X7R = purinergic receptor subtype 7; TLR4 = toll-like receptor 4. (Adapted from Man et al., 2016)

1.2.3.3 Alternative activation of the NLRP3 inflammasome

In human monocytes, the triggering of NLRP3 requires no K^+ depletion or is K^+-independent. This alternative activation is executed through the TIR-domain-containing adapter-inducing interferon-β (TRIK) / receptor-interacting serine/threonine-protein kinase-1 (RIPK1) / Fas-associated protein with death domain (FADD) and caspase-8 (Casp8) signaling pathway. It results in a weaker IL-1β response in comparison to the canonical mechanism of activation. Casp8 suppresses receptor-interacting serine/threonine-protein kinase-3 (RIPK3), which participates in signaling processes leading to apoptosis (Wallach et al., 2016). Pathogens may disinhibit RIPK3 from Casp8, which results in the generation of mtROS, potentially activating the NLRP3 inflammasome (Wallach et al., 2016).

1.2.4 Membrane pore formation and pyroptosis

Pore formation mediated by GSDMD could associate with inflammatory cell death (pyroptosis). Cell swelling, cell membrane disruption and release of cytoplasmic content including cytokines secretion during pyroptosis can lead to tissue damage, organ failure and septic shock (Aziz et al., 2013; Miao et al., 2010).

Pyroptosis is primarily executed by Casp4/5/11-mediated GSDMD cleavage with subsequent GSDMD-NT-pores formation and cell membrane permeabilization (Aglietti et al., 2016; Ding et al., 2016; Liu et al., 2016). GSDMD has been recently visualized with pores having a circular shape and variable size of ~20-22 nm with inner diameter of 10-15 nm (Man et al., 2017). The IL-1 family cytokines are 4.5 nm in diameter, supporting the theory that GSDMD is required for the release of IL-1β from the cell (Evavold et al., 2018; Sborgi et al., 2016). It is interesting to note that canonical NLRP3 inflammasome activation and release of IL-1β can occur in the absence of pyroptosis (Chen et al., 2014; Karmakar et al., 2015; Karmakar et al., 2016; Karmakar et al., 2020).

1.3 Atrial fibrillation

Atrial fibrillation (AF) is the most common clinically relevant arrhythmia, frequently associated with inflammation, cardiac diseases and comorbidities (Harada et al., 2015; Zoni-Berisso et al., 2014). Despite the clear clinical association between inflammation and AF, the exact mechanisms of inflammatory signaling in the pathophysiology of AF are elusive. AF influences not only the patients' quality of life but can also lead to hemodynamic instability, stroke, heart failure and is associated with increased morbidity and mortality. The symptoms of AF include shortness of breath, palpitations, fatigue, dyspnea and sleeping disorders. However, one third of AF patients are asymptomatic (Kirchhof et al., 2016). The evolution of AF is progressive and AF is usually classified according to the duration of the episodes. Episodes lasting less than 7 days, which convert spontaneously to sinus rhythm, are referred to as paroxysmal AF (PAF). AF with episodes longer than 7 days is designated as persistent. When no further attempts are made to achieve sinus rhythm, AF is considered permanent (Heijman et al., 2014). Generally, PAF occurs in patients of younger age. Permanent AF is considered to be the most common form of AF in the general populations (around 50 % of patients) (Zoni-Berisso et al., 2014). In this work, long-standing persistent AF and permanent AF would be referred as "chronic" (CAF).

A secondary form of AF is post-operative AF (POAF), which develops after surgery with peak incidence between the 2nd and the 4th day. POAF increases the duration of hospital stay, and as with common AF forms increases risk for stroke, morbidity and mortality (Dobrev et al., 2019; Maesen et al., 2012).

1.4 Inflammatory signaling in atrial fibrillation

Increasing evidence suggests that inflammation plays an important role in the promotion of ectopic firing and reentry-promoting atrial remodeling (Scott et al., 2019). Ectopic activity can emerge from delayed afterdepolarizations (DADs) due to Ca^{2+}-handling abnormalities in the atria. It can act as a trigger to initiate reentry in a vulnerable substrate (electrical and/or structural abnormalities). Structural and electrical remodeling of the atria support sustained AF and are promoted by cardiovascular risk factors and AF itself (Wakili et al., 2011). Inflammatory signaling may be closely associated with the development and maintenance of AF by contributing to atrial remodeling. However, whether inflammation is a cause or a consequence of AF remains unclear (Van Wagoner & Chung, 2018). Various inflammatory markers (e.g. C-reactive protein, CRP) have been associated with the occurrence of AF and

were used to predict the prevalence of AF, but their clinical predictive value is limited (Harada et al., 2015).

Proinflammatory tumor necrosis factor α (TNF-α) signaling has been associated with electrical and structural remodeling, leading to AF initiation and progression (Ren et al., 2015). Other inflammatory proteins like TLR4, MyD88 and NFκB (total and phosphorylated) where found to be increased in atrial tissue from patients with AF (Xu et al., 2018). Oxidative stress and ROS generation are known contributors to AF pathophysiology, promoting the activation of NFκB and thereby promoting proinflammatory signaling. They also enhance myeloperoxidase (MPO) generation, a well-known contributor to structural remodeling and atrial fibrosis (Friedrichs et al., 2012). Expression and activation of NLRP3 inflammasome, promoting IL-1β and IL-18 formation and secretion, are also clearly associated with the pathogenesis of AF. In a mouse model, cardiac-restricted constitutive activation of the NLRP3 inflammasome in atrial cardiomyocytes was sufficient to promote atrial ectopic activity, thereby enhancing the inducibility of AF (Yao et al., 2018). Atrial ectopic activity, as a consequence of NLRP3 inflammasome activation, likely resulted from enhanced sarcoplasmic reticulum Ca^{2+} release from dysfunctional ryanodine receptor type-2 (RyR2) (Yao et al., 2018). In addition, these mice developed an arrhythmogenic substrate for reentry characterized by action potential duration (APD) shortening due to augmented ultra-rapid delayed-rectifier K^+ current (I_{Kur}), atrial hypertrophy and fibrosis (Scott et al., 2019). However, the upstream mechanisms leading to NLRP3 inflammasome activation in clinical AF are unknown.

2 SCOPE OF THESIS

The aim of the present work was to investigate the expression and activation of the NLRP3 inflammasome in right atrial (RA) appendages from patients undergoing open-heart surgery. For this purpose, we examined patients with previously diagnosed PAF or CAF, as well as those who developed first-onset POAF after surgery. Patients who were in sinus rhythm (SR) prior to and after cardiac surgery served as controls (Ctl). Antibodies suitable for detection of the components and products of the NLRP3 inflammasome activation were validated using specific blocking peptides, recombinant proteins and adenoviral knockdown of proteins of interest. The proteins levels of the components and products of the NLRP3 inflammasome system were quantified in both whole-tissue atrial lysates and human atrial cardiomyocytes (HAM). This thesis addressed the hypothesis that the NLRP3-inflammasome complex is more active in patients with AF, especially in patients prone to POAF. We discovered that the NLRP3 inflammasome was activated in the AF groups vs. the Ctl group, but its activation was much stronger in cardiomyocytes compared to whole-tissue lysates. Of note, the POAF group showed the strongest activation in both whole-tissue lysates and cardiomyocytes. Our results position human atrial cardiomyocytes as a major source of inflammatory signaling and indicate that cardiomyocyte NLRP3-inflammasome signaling may contribute to the formation of the AF-promoting vulnerable substrate.

3 MATERIALS AND METHODS

3.1 Chemicals and laboratory equipment

The chemicals and laboratory equipment used in this study are listed in **Table 2- 3**.

Table 2: Chemicals.

Substance	Company	Catalog Number
2,3-butanedione monoxime (BDM)	Sigma-Aldrich	31550
3-[(3-cholamidopropyl)dimethylammonio]-1-propanesulfonate (CHAPS)	Carl Roth	1479.3
3-(N-morpholino)propanesulfonic acid (MOPS)	Sigma-Aldrich	M1254
3-hydroxy-4-(2-sulfo-4-[4-sulfophenylazo]phenylazo)-2,7-naphthalenedisulfonic acid sodium salt (Ponceau S)	Carl Roth	5938.1
4-(2-hydroxyethyl)-1-piperazineethanesulfonic acid (HEPES)	Carl Roth	9105.4
Acrylamide	Carl Roth	3029.1
Ammonium persulfate (APS)	Carl Roth	9592.1
Bromophenol blue (BPB)	Carl Roth	A512.1
Bovines serum albumin (BSA)	Sigma-Aldrich	A6003
Claycomb medium	Sigma-Aldrich	51800C
Dithiothreitol (DTT)	Carl Roth	6908.3
Ethylenediaminetetraacetic acid (EDTA)	Sigma-Aldrich	EDS-500G
Fetal calf serum (FCS)	Pan Biotech	P30-3304
Glucose	Sigma-Aldrich	G7528
Glycerol	Carl Roth	3783.1
Glycin	Carl Roth	3187.4
L-glutamine	Sigma-Aldrich	G7513-100ml
Methanol	J.T.Baker	8045
Monopotassium phosphate (KH_2PO_4)	Merck Millipore	104873
Magnesium sulfate heptahydrate ($MgSO_4X7H_2O$)	Sigma	230391
Norepinephrine-bitartrate salt	Sigma	N5785
Odyssey blocking buffer in PBS	Li-cor Bioscience	927-50003
Penicillin-Streptomycin liquid	Invitrogen	15140-122
Phosphatase Inhibitor Cocktail (PhosSTOP)	Roche	04996837N4P14
Phosphate buffered saline (PBS)	Thermo Scientific	14190094
Polysorbate 20 (Tween-20)	Sigma-Aldrich	P7949
Potassium chloride (KCL)	Carl Roth	HNO2.2
Protease Inhibitor Cocktail (cOmplete Mini)	Roche	04693124N4P14
Sodium chloride (NaCl)	Carl Roth	P029.3
Sodium dodecyl sulfate (SDS)	Carl Roth	CN30.3
Sodium floride (NaF)	Sigma-Aldrich	S7920
Sodium orthovanadate (Na_3VO_4)	Sigma-Aldrich	S6508
Taurin	Carl Roth	4721.2

Tris (hydroxymethyl) aminomethane (Tris-HCl)	Carl Roth	9090.3
Tris(hydroxymethyl)aminomethane (Tris ultrapure)	AppliChem	A1086.5000 A
Triton X-100	Carl Roth	3051.2

Table 3: Laboratory equipment.

Device	Company
Cell culture flasks	Starlab
Centrifuge	Thermo Scientific, NeoLab, Eppendorf
Homogenizer	IKA
Freezer -20°C	Liebherr
Freezer -80°C	Thermo Scientific
Incubator	Thermo Scientific
Laminar Flow	Thermo Scientific
Magnetic stirrer	NeoLab, IKA
Magnetic stirring bar	NeoLab
Microplate reader	Tecan
Microscope	Nikon
Mini-protean comb 10/15 well,1.5 mm	Bio-Rad
Odyssey® CLx imaging system	Li-Cor
pH meter	SI Analytics
Pipettes	Ependorf
Pippetor	Hirschmann
Power supply	Bio-Rad
Precision balance	Kern EG, Sartorius
Refridgerator	Liebherr
Rocking shaker	IKA
Scanner	Epson
Termomixer compact	Eppendorf
Sonicator	Hielscher

3.2 Human atrial tissue

Human RA appendages (**Figure 5**) were collected from patients undergoing open-heart surgery for valve replacement or coronary bypass grafting. The tip of the RA appendage was removed during routine cannulation to extracorporeal circulation through the heart-lung machine. Each patient provided written informed consent before surgery. Experimental protocols were approved by the local ethics committees of the Medical Faculty of the University Duisburg-Essen (No. 12 5268-BO) and Medical Faculty Carl Gustav Carus of the Technical University Dresden (No. EK790799). The tissue was transferred in cold Tyrode solution (**Table 4**) to the laboratory, where it was frozen immediately in liquid nitrogen and stored at -80°C.

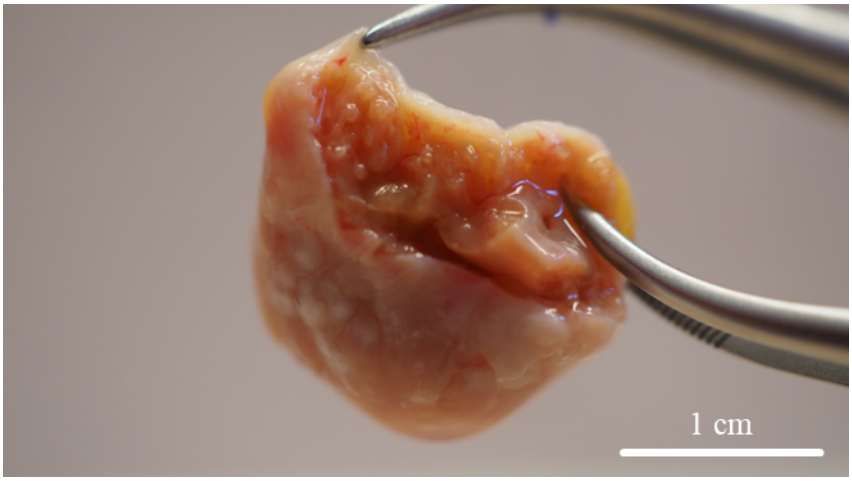

Figure 5: Human right atrial (RA) appendage. An example of a human RA appendage obtained from a patient who underwent open-heart surgery.

Table 4: Composition of transport solution.

	Substance	Quantity
Tyrode solution (pH 7)	BDM	30 mM
	Glucose	20 mM
	KCl	10 mM
	KH_2PO_4	1.2 mM
	$MgSO_4 .7H_2O$	5 mM
	MOPS	5 mM
	NaCl	100 mM
	Taurin	50 mM

3.3 Protein isolation

3.3.1 Whole-tissue homogenates from human RA appendages

To prepare whole-tissue homogenates (HMG), RA appendages were pulverized with a mortar while frozen in liquid nitrogen. A 5-fold amount of Kranias buffer was added relative to the weight of the tissue (**Table 5**). Once fixed with the buffer the samples were homogenized and sonicated two times for 10 s with an ultrasonic processor. After being vortexed, the samples were centrifuged at 900 g for 15 min at 4°C. The formed supernatant containing protein lysate was transferred into reaction tubes and stored at -80°C.

Table 5: Composition of Kranias buffer.

	Substance	Concentration
Kranias stock solution (pH 8.86)	EDTA	5 nM
	Glycerol	10 %
	NaF	30 mM
	SDS	3 %
	Tris ultrapure	30 mM

3.3.2 Isolation of atrial cardiomyocytes using BSA gradients

The HAM fractions used in this work are from the biobank of the Institute of Pharmacology (Prof. Dobrev). Cardiomyocytes were separated from non-cardiomyocyte-cells as previously described (Graf et al., 2005; Heijman et al., 2018). This approach was based on Ca^{2+}-free Tyrode's solution containing 0.1 % bovine serum albumin (BSA). The cells were left to sediment for 45 min over a 6 % BSA gradient. The upper fraction of the gradient was formed mostly from cell debris and tissue fragments. The non-cardiomyocytes, predominantly fibroblasts, were located between the 2 % and 6 % BSA gradient phase. Cardiomyocytes were primarily located at the bottom of the gradient, which was verified using light-microscopy (Yao et al., 2018)). Lysates were isolated from cardiomyocyte-enriched fractions and prepared for immunoblotting as described in 3.3.1.

3.3.3 Protein determination

Total protein concentration was determined using the Pierce™ bicinchoninic acid (BCA) protein assay kit according to the manufacturer's protocol. Referring to the Biuret reaction, the protein in the samples reduces Cu^{2+} to Cu^{1+} in an alkaline medium. This gives rise to a water soluble chelate complex of two BCA molecules with one cupper cation. The formation of a purple chelate complex is linear to the protein concentration over a broad concentration range using Bovine serum albumin (BSA) standard curve (20-2000 µg/mL). The photometric measurement of the absorbance, at 562 nm, was accomplished by a Microplate Reader Infinite M200 Pro (Tecan).

3.3.4 Sample preparation for immunoblotting

Prior to pipetting, every sample was prepared with 6:1 Leammli buffer and heated in a dry cabinet for 5 min at 95°C. Leammli buffer contained bromophenol blue (BSB) as a dye and dithiothreitol (DDT) to disrupt the bindings between the proteins (**Table 6**). It consisted of glycerol to increase density, sodium dodecyl sulfate (SDS) as negative detergent and Tris-buffered saline with Tween20 (TBST) to keep the pH physiologically similar.

Table 6: Composition of Leammli buffer.

	Substance	Concentration
Leammli buffer	BSB	1 mM
	DDT	603 mM
	Glycerol	652 mM
	SDS	12 %
	Tris ultrapure	60 mM

3.3.5 Virus infection of HL-1 cells

For the validation of the GSDMD antibody HL-1 cells (an immortalized mouse cardiac cell line) were infected with adenovirus serotype 5, downregulating GSDMD (Sh-GSDMD). The virus was produced by Vector BioLabs while the HL-1 Cardiac Muscle Cell Line was acquired from Sigma-Aldrich (SCC065). The cells were infected and cultured for 72 h in Claycomb medium with 10 % fetal calf serum (FCS) (**Table 7**). Thereafter, the HL-1 cells were lysed and prepared for immunoblotting using the standard protocol described in 3.3.4.

Table 7: Composition of Claycomb medium.

	Substance	Concentration
Claycomb medium	FCS	10 %
	L-glutamine	4 mM
	Penicilin/Streptomycin	100 µg/ml
	Norepinephrine	100 µg

3.4 Immunoblotting

3.4.1 Gel preparation

Gels used for electrophoresis were made in a 1.5 mm spacer plate and an aligned short plate clamped together. The gel consisted of ¾ separating gel buffer and ¼ stacking gel buffer. Acrylamide was used to build the pores of the gel. The size of the pores depends on the percentage of acrylamide. SDS is a strongly anionic detergent, which disrupts the non-covalent interactions among the proteins. Tris (hydroxymethyl) aminomethane (Tris), a component of the buffers with close-to-physiological pH, enabled a better permeability of the gel. The polymerization of the acrylamide was initiated by ammonium persulfate (APS) and the catalyst tetramethylethylendiamin (TEMED). The compositions used to prepare gels of different concentrations are mentioned in **Table 8**. Loading pocket cells (10 or 15) were formed by placing a gel comb.

Table 8: Composition of gels.

	Substance	10 %	12 %	15 %
Separating gel	Distilled water	4.0 ml	3.3 ml	2.3 ml
	30 % Acrylamide	3.3 ml	4.0 ml	5.0 ml
	10 % APS	0.1ml	0.1ml	0.1ml
	10 % SDS	0.1ml	0.1ml	0.1ml
	TEMED	0.008 ml	0.008 ml	0.008 ml
	1.5 M Tris (pH 8.8)	2.5 ml	2.5 ml	2.5 ml
Stacking gel	Distilled water	2.8 ml	2.8 ml	2.8 ml
	30 % Acrylamide	0.85 ml	0.85 ml	0.85 ml
	10 % APS	0.05 ml	0.05 ml	0.05 ml
	10 % SDS	0.05 ml	0.05 ml	0.05 ml
	TEMED	0.005 ml	0.005 ml	0.005 ml
	0.5 M Tris (pH 6.8)	1.25	1.25	1.25

3.4.2 Gel electrophoresis

Sodium dodecyl sulfate-polyacrylamide gel electrophoresis (SDS-PAGE) is an analytical method developed by U. K. Leammli in 1970 for separating proteins according to their molecular weight in an electric field (Laemmli, 1970).

The pockets of the gel were filled with the same amount of denaturated protein concentration and a pre-stained protein marker (**Table 9**). The electrophoresis was executed in a tank filled with running buffer (**Table 10**) at a constant voltage of 80 V for 15 min followed by 150 V for 60 min using Power PAC HC high-current power supply from Bio-Rad. The negatively charged proteins migrated through the gel towards the anode. The smaller the proteins, the farther they moved through the gel.

Table 9: Pre-stained protein markers.

Marker	Company
Precision plus protein dual xtra pre-stained standard	Bio-Rad
Chameleon duo pre-stained protein ladder	Li-cor

Table 10: Composition of electrophoresis buffer.

	Substance	Concentration	Company
Running buffer	Glycin	960 mM	Carl Roth
	SDS	0.5 %	Serva
	Tris ultrapure	125 mM	AppliChem
	ad. 1000 ml Distilled water		Braun

3.4.3 Transfer

The gel was carefully removed from the glass plate and positioned in a blotting chamber, which consists of the following components: four layers of filter paper, two fiber sponges, one nitrocellulose membrane, one black and white cartridge. The cartridge was subsequently inserted in a cassette holder and put in a buffer tank together with an ice block. A precooled blotting buffer (**Table 11**) filled up the tank. The transfer was run in a fridge at 0.3 A for 1.5 h. The proteins were transferred onto the membrane as a consequence of their negative charge being drawn by the positively charged anode.

Table 11: Composition of blotting buffer.

	Substance	Concentration
Blotting buffer	Glycin	192 nM
	Methanol	20 %
	Tris ultrapure	25 nM
	ad. 1000 ml Distilled water	

3.4.4 Blocking

After the transfer, the membrane underwent total protein staining with Ponceau S. Washing buffer (**Table 12**) was used to remove any staining. The membrane was labeled and trimmed accordingly. Blocking buffer (**Table 13**) was applied for 1 h at room temperature to minimize the amount of non-specific binding. The membrane was incubated at 4°C overnight with a primary antibody against the protein of interest. The antibody was diluted accordingly to the desired concentration in TBST and blocking buffer in a ratio of 10 to 1. The incubation of the secondary antibody requires a non-transparent box, because of the use of a fluorescent chemical compound. After 1 h incubation at room temperature and preparation with washing buffer, the membrane's densitometry was measured with an Odyssey scanner.

Table 12: Composition of washing buffer.

	Substance	Concentration
TBST buffer	NaCl	0.15 M
(pH 7.4)	Tris ultrapure	0.01 M
	Tween 20	0.2 %
	ad. 1000 ml Distilled water	

Table 13: Composition of blocking buffer.

	Substance	Relation
Blocking buffer (pH 7.4)	TBST	1
	Odyssey blocking buffer in PBS	3

3.5 List of antibodies

Once the proteins from the tissue lysates were transferred onto the membrane, the membranes were incubated with different types of antibodies targeting the proteins of interest (**Table 14**). Blocking peptides were used for the validation of the primary antibodies (**Table 15**). For visualization an additional incubation with an appropriate fluorescent secondary antibody was performed (**Table 16**).

Table 14: Primary antibodies.

Primary Antibody (AB)	Concentration	Host	Company	Catalog Number
ASC	1:500	rabbit	Santa Cruz	sc-22514-R
ASC (B-3)	1:500	mouse	Santa Cruz	sc-514414
Calsequestrin	1:2500	rabbit	Thermo Fisher	PA1-913
Caspase-1	1:500; 1:1000	rabbit	Bio Vision	3019-100
CD11b	1:500	rabbit	Abcam	ab52478
CD68	1:200	mouse	Abcam	ab201973
CD206	1:500	rabbit	Abcam	ab64693
F4/80	1:500	rat	Abcam	ab16911
IL-1β	1:250; 1:500	rabbit	Abcam	ab9722
IL-18	1:500	mouse	MBL	D046-3
GAPDH	1:20000	mouse	HyTest	5G4 6C5
Gasdermin D	1:500	rabbit	Thermo Fisher	PA5-30823
Gasdermin D	1:500	rabbit	Sigma	G7422
NFκB-Total	1:500	mouse	Novusbio	NB100-56712 p65
Ser536-NFκB	1:500	rabbit	Novusbio	NB100-82088 Ser536
NLRP3	1:500	rabbit	Novusbio	NBP1-77080
P2X7R	1:1000	rabbit	Abcam	ab94717
P2X7R	1:250; 1:500	goat	Santa Cruz	sc-15200
TLR4	1:250	mouse	Novusbio	NB100-56566

Table 15: Blocking peptides.

Blocking Peptide (BP)	Primary AB/ BP	Host	Company	Catalog Number
ASC (B-3)	1:5	mouse	Santa Cruz	sc-514414 P

Caspase-1	1:5	rabbit	Bio Vision	3019BP-50
NLRP3	1:5	rabbit	Novusbio	NBP1-77080PEP

Table 16: Secondary antibodies.

Secondary Antibody	Concentration	Company
IRDye 680RD goat anti-mouse IgG	1:20 000	Li-cor
IRDye 680RD goat anti-rabbit IgG	1:20 000	Li-cor
IRDye 800RD goat anti-rat IgG	1:20 000	Li-cor
IRDye 800RD goat anti-mouse IgG	1:20 000	Li-cor
IRDye 800RD goat anti-rabbit IgG	1:20 000	Li-cor
IRDye 800RD donkey anti-goat IgG	1:20 000	Li-cor

3.6 Statistics

Statistical analyses were performed using GraphPad Prism 7. Normality was tested using the D'Agostino&Pearson omnibus test. Data following a normal distribution were analyzed using parametric (unpaired) tests. A standard Student's *t*-test was used to determine significant differences between two groups and one-way analysis of variance (ANOVA) with Dunnett's multiple comparisons post-hoc test was used for multiple comparisons. For non-normally distributed data, the non-parametric Mann-Whitney U-test or Kruskal-Wallis with Dunn's multiple comparisons post-hoc test were used. Continuous variables are presented as either mean±SD or as median and interquartile ranges. Categorical data were analyzed using Chi-squared tests, with Bonferroni correction in case of > 2 groups. Probability values (P-values) of these tests are reported and $P<0.05$ was considered statistically significant. * indicates $P<0.05$; ** indicates $P<0.01$; and *** indicates $P<0.001$. All data in this work were processed and statistically evaluated using the software programs listed in **Table 17**.

Table 17: Employed software programs.

Program	Company
Image Studio	Li-cor
GraphPad Prism Version 7	GraphPad software
Medical ART	Servier
Microsoft office package	Microsoft
Tecan i-control	Tecan
Epson Scan	Epson

4 RESULTS

4.1 Patients

In order to determine the contribution of the NLRP3 complex in the development of AF, we obtained RA appendages from patients undergoing open-heart surgery. An overview of the clinical characteristics of all the patient groups included in this study is provided in **Table 18** for HMG and in **Table 19** for HAM. Since different control groups were used for pair-wise comparisons with POAF, PAF and CAF, clinical characteristics of the subsets of patients whose samples were directly compared in HMG experiments are given in **Tables 20-22**. Similarly, clinical characteristics of the subsets of patients whose samples were directly compared in HAM experiments are provided in **Tables 23-25.**

There were no significant differences in gender, age, body mass index (BMI) and comorbidities between the four groups. In the case of the atrial whole-tissue, the statistical analyses showed that there were no differences except in POAF for use of angiotensin-converting enzyme (ACE) inhibitors. Left ventricular ejection fraction (LVEF) and left atrial diameter (LAD) differences were detected in both PAF and CAF samples. Additionally, PAF patients were more frequently prescribed lipid-lowering drugs (LLD), but were less frequently given nitrates compared to Ctl patients, whereas CAF patients more often used digitalis. **Table 23** summarized comparisons in isolated cardiomyocytes involving POAF samples, showing reduced prevalence of hyperlipidemia (HLP). PAF and CAF patients had increased LAD and took more often β-blockers, but less frequent dihydropyridines (DHP) compared to Ctl patients. However, there was a trend towards increased use of β-blockers in CAF cardiomyocytes' samples (**Tables 24-25**).

Table 18: Clinical characteristics of patients used for biochemistry experiments on atrial whole-tissue homogenates (HMG).

	Ctl HMG	POAF HMG	PAF HMG	CAF HMG
Patients, n	68	33	28	34
Female gender, n (%)	20 (30)	15 (47)	8 (29)	11 (34)
Age, y	66±1.3	69±1.2	72±0.8	71±0.6
Body mass index, kg/m	28±0.6	28±0.5	30±0.6	27±0.4
CAD, n (%)	20 (31)	5 (15)	10 (37)	8 (24)
AVD/MVD, n (%) ##	31 (48)	18 (55)	11 (41)	17 (52)
CAD+AVD/MVD, n (%)	12 (18)	10 (30)	6 (22)	8 (24)
Other	2 (3)	0 (0)	0 (0)	0 (0)
Hypertension, n (%)	53 (84)	21 (68)	25 (96)	27 (93)
Diabetes, n (%)	15 (29)	6 (19)	6 (30)	11 (50)
Hyperlipidemia, n (%)	26 (58)	9 (32)	14 (88)	13 (72)
LVEF, % ##	60±1.1	62±1.1	55±0.8	54±1.0
LAD, mm ###	39±0.9	40±0.6	49±0.4	54±2.5
Digitalis, n (%) ###	1 (2)	0 (0)	1 (4)	7 (21)
ACE inhibitors, n (%)	29 (44)	8 (24)	12 (43)	16 (48)
AT1 blockers, n (%)	8 (12)	6 (18)	7 (25)	5 (15)
β-blockers, n (%)	35 (53)	15 (45)	19 (68)	22 (67)
Dihydropyridines, n (%)	16 (24)	12 (36)	8 (29)	11 (33)
Diuretics, n (%)	22 (33)	10 (30)	11 (39)	17 (52)
Nitrates, n (%)	4 (6)	2 (6)	0 (0)	5 (15)
Lipid-lowering drugs, n (%)	22 (33)	10 (30)	17 (61)	15 (45)

Continuous variables are presented as mean±SD. Categorical data are given as number of patients (%). ACE = angiotensin-converting enzyme; AT = angiotensin receptor; AVD = aortic valve disease; CAD = coronary artery disease; LAD = left atrial diameter; LVEF = left ventricular ejection fraction; POAF = post-operative atrial fibrillation; #P<0.05, ##P<0.01, ###P<0.001 vs. Ctl (patients in sinus rhythm); n indicates number of patients. CAD, AVD/MVD and CAD+AVD/MVD reflect the indications for cardiac surgery (bypass surgery, valve replacement or a combination of both). Details on missing information for each variable are provided in the legends of **Tables 20-22**.

Table 19: Clinical characteristics of patients used for biochemistry experiments on human atrial cardiomyocytes (HAM).

	Ctl HAM	POAF HAM	PAF HAM	CAF HAM
Patients, n	34	17	8	15
Female gender, n (%)	16 (47)	6 (35)	5 (63)	10 (67)
Age, y	65±1.1	64±1.1	71±0.5	73±1.0
Body mass index, kg/m	27±0.4	27±0.5	27±0.6	26±0.3
CAD, n (%)	12 (35)	7 (41)	1 (13)	0 (0)
AVD/MVD, n (%)	13 (38)	3 (18)	3 (38)	6 (40)
CAD+AVD/MVD, n (%)	9 (26)	6 (35)	4 (50)	9 (60)
Other	0 (0)	1 (6)	0 (0)	0 (0)
Hypertension, n (%)	30 (88)	14 (82)	7 (88)	12 (80)
Diabetes, n (%)	11 (32)	6 (35)	1 (13)	5 (33)
Hyperlipidemia, n (%) [#]	22 (69)	7 (41)	7 (88)	5 (33)
LVEF, %	59±1.3	48±2.0	63±1.1	55±1.0
LAD, mm	39±0.5	41±0.6	47±0.4	47±0.4
Digitalis, n (%) [##]	2 (6)	1 (6)	2 (25)	6 (40)
ACE inhibitors, n (%)	18 (53)	12 (71)	5 (63)	9 (60)
AT1 blockers, n (%)	6 (18)	3 (18)	0 (0)	2 (13)
β-blockers, n (%)	17 (50)	13 (76)	7 (88)	12 (80)
Dihydropyridines, n (%) [#]	13 (38)	1 (6)	0 (0)	2 (13)
Diuretics, n (%)	5 (15)	6 (35)	2 (25)	6 (40)
Nitrates, n (%)	7 (21)	4 (24)	0 (0)	1 (7)
Lipid-lowering drugs, n (%)	11 (32)	10 (59)	2 (25)	1 (7)

Continuous variables are presented as mean±SD. Categorical data are given as number of patients (%). ACE = angiotensin-converting enzyme; AT = angiotensin receptor; AVD = aortic valve disease; CAD = coronary artery disease; LAD = left atrial diameter; LVEF = left ventricular ejection fraction; POAF = post-operative atrial fibrillation; [#]P<0.05, [##]P<0.01, [###]P<0.001 vs. Ctl (patients in sinus rhythm); n indicates number of patients. CAD, AVD/MVD and CAD+AVD/MVD reflect the indications for cardiac surgery (bypass surgery, valve replacement or a combination of both). Details on missing information for each variable are provided in the legends of **Tables 23-25**.

Table 20: Clinical characteristics of patients used for POAF biochemistry experiments in whole-tissue homogenates (HMG).

	Ctl HMG	POAF HMG
Patients, n	44	33
Female gender, n (%) [1]	14 (32)	15 (47)
Age, y	66±1.4	69±1.2
Body mass index, kg/m^2 [2]	29±0.6	28±0.5
CAD, n (%) [3]	10 (23)	5 (15)
AVD/MVD, n (%) [3]	25 (58)	18 (55)
CAD+AVD/MVD, n (%) [3]	6 (14)	10 (30)
Other [3]	2 (5)	0 (0)
Hypertension, n (%) [4]	32 (80)	21 (68)
Diabetes, n (%) [5]	11 (33)	6 (19)
Hyperlipidemia, n (%) [6]	18 (56)	9 (32)
LVEF, % [7]	61±1.1	62±1.1
LAD, mm [8]	40±0.9	40±0.6
Digitalis, n (%) [9]	1 (2)	0 (0)
ACE inhibitors, n (%) [7]	21 (47)	8 (24) *
AT1 blockers, n (%) [10]	4 (9)	6 (18)
β-blockers, n (%) [7]	25 (57)	15 (45)
Dihydropyridines, n (%) [11]	9 (20)	12 (36)
Diuretics, n (%) [7]	17 (39)	10 (30)
Nitrates, n (%) [7]	1 (2)	2 (6)
Lipid-lowering drugs, n (%) [9]	17 (39)	10 (30)

Continuous variables are presented as mean±SD. Categorical data are given as number of patients (%). ACE = angiotensin-converting enzyme; AT = angiotensin receptor; AVD = aortic valve disease; CAD = coronary artery disease; LAD = left atrial diameter; LVEF = left ventricular ejection fraction; POAF = post-operative atrial fibrillation; *P<0.05 vs. Ctl (patients in sinus rhythm); n indicates number of patients. CAD, AVD/MVD and CAD+AVD/MVD reflect the indications for cardiac surgery (bypass surgery, valve replacement or a combination of both). Data were not available for [1] 1 POAF patient, [2] 4 Ctl and 4 POAF patients, [3] 1 POAF patient [4] 4 Ctl and 2 POAF patients, [5] 1 Ctl and 1 POAF patients, [6] 12 Ctl and 5 POAF patients, [7] 6 Ctl and 6 POAF patients, [8] 20 Ctl and 14 POAF patients, [9,] 6 Ctl and 7 POAF patients, [10] 7 Ctl and 5 POAF patients, [11] 6 Ctl and 5 POAF.

Table 21: Clinical characteristics of patients used for PAF biochemistry experiments in whole-tissue homogenates (HMG).

	Ctl HMG	PAF HMG
Patients, n	38	28
Female gender, n (%) [1]	15 (41)	8 (29)
Age, y [1]	68±1.0	72±0.8
Body mass index, kg/m [2]	29±0.7	30±0.6
CAD, n (%) [3]	13 (36)	10 (37)
AVD/MVD, n (%) [3]	15 (42)	11 (41)
CAD+AVD/MVD, n (%) [3]	7 (19)	6 (22)
Other [3]	1 (3)	0 (0)
Hypertension, n (%) [4]	31 (84)	25 (96)
Diabetes, n (%) [5]	8 (28)	6 (30)
Hyperlipidemia, n (%) [6]	14 (52)	14 (88) *
LVEF, % [7]	61±1.0	55±0.8 *
LAD, mm [8]	39±1.0	49±0.4*
Digitalis, n (%) [9]	0 (0)	1 (4)
ACE inhibitors, n (%) [10]	16 (43)	12 (43)
AT1 blockers, n (%) [12]	5 (14)	7 (25)
β-blockers, n (%) [10]	21 (57)	19 (68)
Dihydropyridines, n (%) [9]	8 (22)	8 (29)
Diuretics, n (%) [10]	10 (27)	11 (39)
Nitrates, n (%) [9]	4 (11)	0 (0) *
Lipid-lowering drugs, n (%) [9]	10 (27)	17 (61) **

Continuous variables are presented as mean±SD. Categorical data are given as number of patients (%). ACE = angiotensin-converting enzyme; AT = angiotensin receptor; AVD = aortic valve disease; CAD = coronary artery disease; LAD = left atrial diameter; LVEF = left ventricular ejection fraction; PAF = paroxysmal atrial fibrillation; *P<0.05, **P<0.01 vs. Ctl (patients in sinus rhythm); n indicates number of patients. CAD, AVD/MVD and CAD+AVD/MVD reflect the indications for cardiac surgery (bypass surgery, valve replacement or a combination of both). Data were not available for [1] 1 Ctl patient, [2] 11 Ctl and 4 PAF patient, [3] 2 Ctl and 1 PAF patients, [4] 1 Ctl and 4 PAF patients, [5] 9 Ctl and 9 PAF patients, [6] 11 Ctl and 15 PAF patients, [7] 3 Ctl and 2 PAF patients, [8] 20 Ctl and 24 PAF patients, [9] 4 Ctl and 5 PAF patients, [10] 4 Ctl and 4 PAF patients, [12] 5 Ctl and 4 PAF patients.

Table 22: Clinical characteristics of patients used for CAF biochemistry experiments in whole-tissue homogenates (HMG).

	Ctl HMG	CAF HMG
Patients, n	30	34
Female gender, n (%) [1]	13 (46)	11 (34)
Age, y [2]	69±1.1	71±0.6
Body mass index, kg/m [3]	30±0.7	27±0.4
CAD, n (%) [2]	10 (36)	8 (24)
AVD/MVD, n (%) [2]	11 (39)	17 (52)
CAD+AVD/MVD, n (%) [2]	6 (21)	8 (24)
Other [2]	1 (4)	0 (0)
Hypertension, n (%) [4]	25 (89)	27 (93)
Diabetes, n (%) [5]	8 (36)	11 (50)
Hyperlipidemia, n (%) [6]	11 (61)	13 (72)
LVEF, % [7]	63±1.0	54±1.0 **
LAD, mm [8]	32±1.4	54±2.5 *
Digitalis, n (%) [9]	0 (0)	7 (21) *
ACE inhibitors, n (%) [10]	12 (43)	16 (48)
AT1 blockers, n (%) [11]	5 (18)	5 (15)
β-blockers, n (%) [10]	16 (57)	22 (67)
Dihydropyridines, n (%) [12]	8 (29)	11 (33)
Diuretics, n (%) [12]	8 (29)	17 (52)
Nitrates, n (%) [10]	2 (7)	5 (15)
Lipid-lowering drugs, n (%) [10]	8 (29)	15 (45)

Continuous variables are presented as mean±SD. Categorical data are given as number of patients (%). ACE = angiotensin-converting enzyme; AT = angiotensin receptor; AVD = aortic valve disease; CAD = coronary artery disease; CAF = chronic atrial fibrillation; LAD = left atrial diameter; LVEF = left ventricular ejection fraction; *P<0.05, **P<0.01 vs. Ctl (patients in sinus rhythm); n indicates number of patients. CAD, AVD/MVD and CAD+AVD/MVD reflect the indications for cardiac surgery (bypass surgery, valve replacement or a combination of both). Data were not available for [1] 2 Ctl and 2 CAF patients, [2] 2 Ctl and 1 CAF patient, [3] 8 Ctl and 3 CAF patients, [4] 2 Ctl and 5 CAF patients, [5] 8 Ctl and 12 CAF patients, [6] 12 Ctl and 16 CAF patients, [7] 2 Ctl and 3 CAF patients, [8] 19 Ctl and 23 CAF patients, [9] 4 Ctl and 8 CAF patients, [10] 4 Ctl and 5 CAF patients, [12] 5 Ctl and 5 CAF patients, [12] 4 Ctl and 4 CAF.

Table 23: Clinical characteristics of patients used for POAF biochemistry experiments in human atrial cardiomyocytes (HAM).

	Ctl HAM	POAF HAM
Patients, n	23	17
Female gender, n (%)	12 (52)	6 (35)
Age, y	64±1.2	64±1.1
Body mass index, kg/m	27±0.5	27±0.5
CAD, n (%)	9 (39)	7 (41)
AVD/MVD, n (%)	10 (43)	3 (18)
CAD+AVD/MVD, n (%)	4 (17)	6 (35)
Other	0 (0)	1 (6)
Hypertension, n (%)	19 (83)	14 (82)
Diabetes, n (%)	8 (35)	6 (35)
Hyperlipidemia, n (%) [1]	17 (77)	7 (41) *
LVEF, % [2]	58±1.4	48±2.0
LAD, mm [3]	38±0.5	41±0.6
Digitalis, n (%)	1 (4)	1 (6)
ACE inhibitors, n (%)	13 (57)	12 (71)
AT1 blockers, n (%)	5 (22)	3 (18)
β-blockers, n (%)	16 (70)	13 (76)
Dihydropyridines, n (%)	1 (4)	1 (6)
Diuretics, n (%) [1]	3 (13)	6 (35)
Nitrates, n (%)	2 (09)	4 (24)
Lipid-lowering drugs, n (%)	11 (48)	10 (59)

Continuous variables are presented as mean±SD for normal-distributed data or median and interquartile ranges. Categorical data are given as number of patients (%). ACE = angiotensin-converting enzyme; AT = angiotensin receptor; AVD = aortic valve disease; CAD = coronary artery disease; LAD = left atrial diameter; LVEF = left ventricular ejection fraction; POAF = post-operative atrial fibrillation; *P<0.05 vs. Ctl (patients in sinus rhythm); n indicates number of patients. CAD, AVD/MVD and CAD+AVD/MVD reflect the indications for cardiac surgery (bypass surgery, valve replacement or a combination of both). Data were not available for [1] 1 Ctl patient, [2] 1 Ctl and 1 POAF patients, [3] 14 Ctl and 7 POAF patients.

Table 24: Clinical characteristics of patients used for PAF biochemistry experiments in human atrial cardiomyocytes (HAM).

	Ctl HAM	PAF HAM
Patients, n	20	8
Female gender, n (%)	10 (50)	5 (63)
Age, y [1]	66±1.2	71±0.5
Body mass index, kg/m	26±0.2	27±0.6
CAD, n (%)	5 (25)	1 (13)
AVD/MVD, n (%)	7 (35)	3 (38)
CAD+AVD/MVD, n (%)	8 (40)	4 (50)
Other	0 (0)	0 (0)
Hypertension, n (%)	16 (80)	7 (88)
Diabetes, n (%)	5 (25)	1 (13)
Hyperlipidemia, n (%) [1]	13 (68)	7 (88)
LVEF, % [2]	61 ±1.4	63±1.1
LAD, mm[4]	39±0.6	47±0.4 *
Digitalis, n (%)	1 (5)	2 (25)
ACE inhibitors, n (%)	8 (40)	5 (63)
AT1 blockers, n (%)	3 (15)	0 (0)
β-blockers, n (%)	12 (60)	7 (88) *
Dihydropyridines, n (%)	8 (40)	0 (0) *
Diuretics, n (%) [2]	3 (15)	2 (25)
Nitrates, n (%)	3 (15)	0 (0)
Lipid-lowering drugs, n (%)	2 (10)	2 (25)

Continuous variables are presented as mean±SD. Categorical data are given as number of patients (%). ACE = angiotensin-converting enzyme; AT = angiotensin receptor; AVD = aortic valve disease; CAD = coronary artery disease; LAD = left atrial diameter; LVEF = left ventricular ejection fraction; PAF = paroxysmal atrial fibrillation; *P<0.05 vs. Ctl (patients in sinus rhythm); n indicates number of patients. CAD, AVD/MVD and CAD+AVD/MVD reflect the indications for cardiac surgery (bypass surgery, valve replacement or a combination of both). Data were not available for [1] 1 Ctl patient, [2] 1 Ctl and 1 PAF patients, [3] 11 Ctl and 4 PAF patients.

Table 25: Clinical characteristics of patients used for CAF biochemistry experiments in human atrial cardiomyocytes (HAM).

	Ctl HAM	CAF HAM
Patients, n	20	15
Female gender, n (%)	10 (50)	10 (67)
Age, y	70±0.8	73±1.0
Body mass index, kg/m	27±0.2	26±0.3
CAD, n (%)	8 (40)	0 (0)
AVD/MVD, n (%)	3 (15)	6 (40)
CAD+AVD/MVD, n (%)	9 (45)	9 (60)
Other	0 (0)	0 (0)
Hypertension, n (%)	18 (90)	12 (80)
Diabetes, n (%)	7 (35)	5 (33)
Hyperlipidemia, n (%) [1]	11 (61)	5 (33)
LVEF, % [2]	61 ±1.5	55±1.0
LAD, mm [3]	39±0.4	47±0.4 *
Digitalis, n (%)	2 (10)	6 (40) *
ACE inhibitors, n (%)	10 (50)	9 (60)
AT1 blockers, n (%)	4 (10)	2 (13)
β-blockers, n (%) [4]	6 (30)	12 (80) *
Dihydropyridines, n (%)	9 (45)	2 (13) *
Diuretics, n (%) [5]	3 (12)	6 (40)
Nitrates, n (%)	5 (25)	1 (7)
Lipid-lowering drugs, n (%)	5 (25)	1 (7)

Continuous variables are presented as mean±SD. Categorical data are given as number of patients (%). ACE = angiotensin-converting enzyme; AT = angiotensin receptor; AVD = aortic valve disease; CAD = coronary artery disease; CAF = chronic atrial fibrillation; LAD = left atrial diameter; LVEF = left ventricular ejection fraction; *P<0.05 vs. Ctl (patients in sinus rhythm); n indicates number of patients. CAD, AVD/MVD and CAD+AVD/MVD reflect the indications for cardiac surgery (bypass surgery, valve replacement or a combination of both). Data were not available for [1] 2 Ctl patient, [2] 1 Ctl and 1 CAF patient, [3] 10 Ctl and 9 CAF patients, [4] 12 Ctl patients, [5] 1 Ctl patient.

4.2 Protein levels of the NLRP3 inflammasome system in whole-tissue homogenates from patients with different forms of AF

4.2.1 Validation of antibodies

4.2.1.1 NLRP3

We performed Western blots using whole-tissue lysates from Ctl patients. We were able to detect two bands at 100 kDa and 125 kDa. According to recent findings suggesting that the LRR domain is not essential for the activation and self-regulation of NLRP3, the 100 kDa band likely corresponds to a protein fragment lacking the LRR, while the 125 kDa band may represent a full-length NLRP3 (Hafner-Bratkovic et al., 2018). A third band at 250 kDa was also present, which presumably represents the dimers of the NLRP3 protein (**Figure 6**). For the validation of the antibody, we used a compatible blocking peptide. The decrease in intensity of the detected bands in the presence of the blocking peptide confirmed the specificity of three bands.

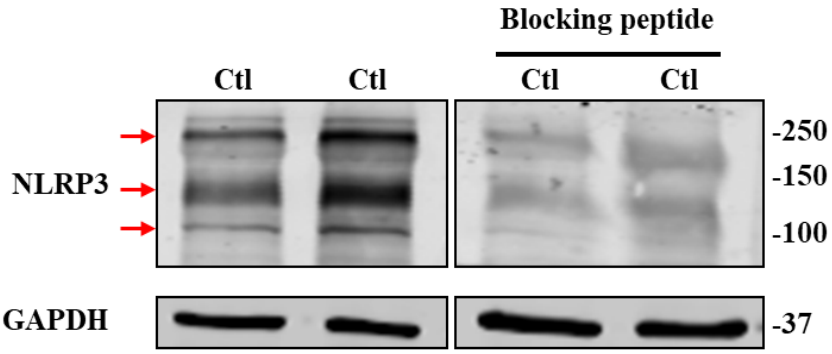

Figure 6: Validation of the NLRP3 antibody. Representative Western blots showing the NLRP3 bands in whole-tissue lysates from patients in SR. On the left, the blot was incubated with the specific antibody. On the right, an identical Western blot was performed with the NLRP3 antibody being bound and inactivated by the compatible blocking peptide. GAPDH was used as a loading control. Ctl = patients in sinus rhythm. NLRP3 = NACHT, LRR and PYD domains containing binding protein 3; GAPDH = Glyceraldehyde 3-phosphate dehydrogenase.

4.2.1.2 GSDMD

For the validation of the GSDMD antibody, we detected GSDMD-FL as well as its N-terminus (GSDMD-NT) and C-terminus (GSDMD-CT) in HL-1 cells with adenoviral GSDMD (Sh-GSDMD) knockdown (**Figure 7**). The decrease in intensity of the detected bands in HL-1 cells ad-Sh-GSDMD confirmed their specificity.

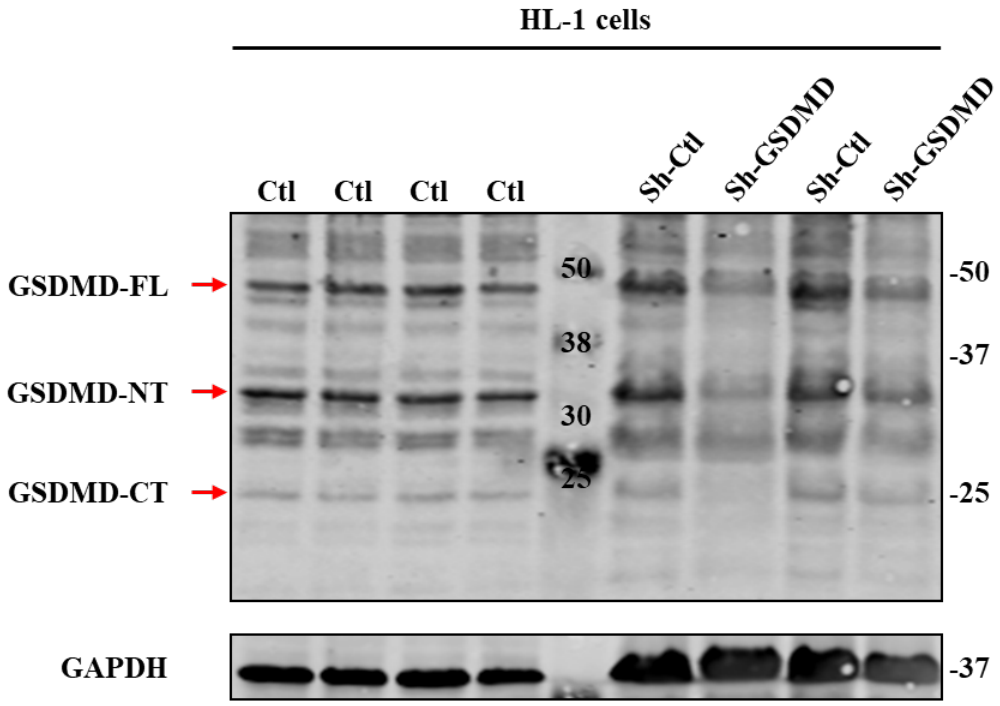

Figure 7: Protein expression of GSDMD. Representative Western blot showing GSDMD-FL, its N-terminus (GSDMD-NT) and C-terminus (GSDMD-CT) in control (Ctl, left) and ad-Sh-GSDMD infected HL-1 cells (right). GAPDH was used as a loading control. Ctl = HL-1 cells lysates. GAPDH = Glyceraldehyde 3-phosphate dehydrogenase; GSDMD-CT = C-terminus of gasdermin D; GSDMD-FL = full-length gasdermin D; GSDMD-NT = N-terminus of gasdermin D.

4.2.1.3 ASC

A compatible blocking peptide was used for the validation of the ASC antibody. The decrease in intensity of the detected bands in the presence of the blocking peptide confirmed the specificity of the bands. It was possible to detect ASC monomers at 22-24 kDa in human atrial whole-tissue lysates (**Figure 8**).

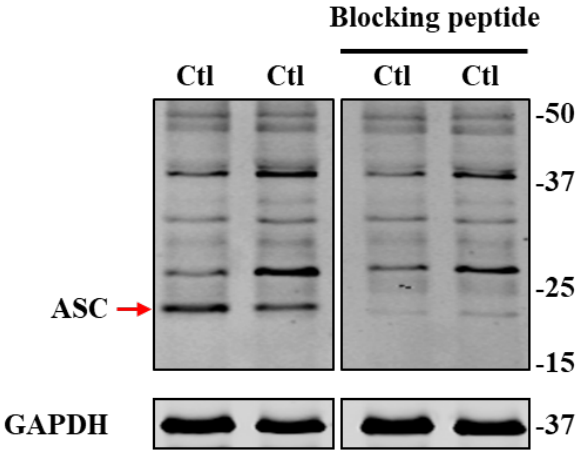

Figure 8: Validation of ASC antibody. Left, representative Western blots showing ASC monomers in atrial whole-tissue lysates from Ctl patients. Right, the same blot incubated with

1:5 ASC antibody and blocking peptide showing a strong decrease in the intensity of the ASC band at 22-24 kDa. GAPDH was used as a loading control. Ctl = patients in sinus rhythm. ASC = apoptosis-associated speck-like protein containing a CARD domain; GAPDH = Glyceraldehyde 3-phosphate dehydrogenase.

4.2.1.4 IL-1β

By applying different concentrations of IL-1β recombinant protein we were able to verify the expected size of its precursor and active form in human atrial lysates from Ctl patients (**Figure 9**).

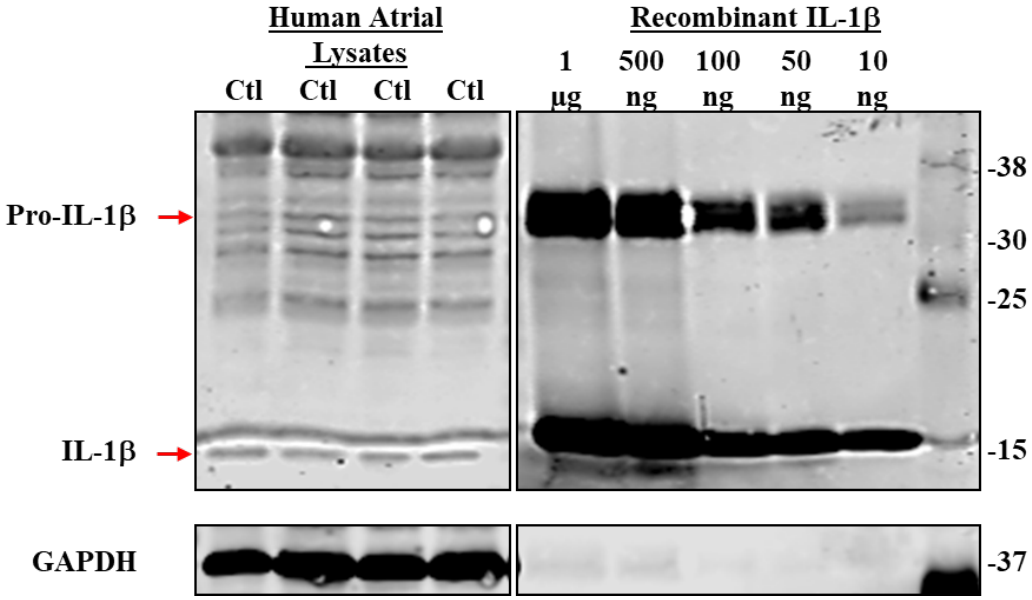

Figure 9: Validation of IL-1β antibody. Left, representative Western blot showing IL-1β in in whole-tissue lysates from patients in SR. Right, a blot incubated with different concentrations (1 µg, 500 ng, 100 ng, 50 ng and 10 ng) of a recombinant IL-1β protein showing the bands equivalent to the Pro-IL-1β and its active form on the membrane. GAPDH was used as a loading control. Ctl = patients in sinus rhythm. (Pro-)IL-1β = (pro-)interleukin-1β; GAPDH = Glyceraldehyde 3-phosphate dehydrogenase.

4.2.2 NLRP3 inflammatory signaling in atrial whole-tissue lysates from POAF patients

POAF is the most important type of secondary AF. It occurs in approximately 40 % of patients undergoing cardiac surgery with peak incidence between the 2nd and 4th day post-surgery (Filardo et al., 2018). POAF is associated with hemodynamic instability and increased stroke risk, as well as substantial increases in hospital costs, intensive care unit time and hospital stay (Ahlsson et al., 2010; Dobrev et al., 2019; Melduni et al., 2015). Systemic inflammation is

considered an important contributor to the pathophysiology of POAF, but the precise underlying mechanisms remain incompletely understood (Dobrev et al., 2019; Maesen et al., 2012; Ucar et al., 2007).

4.2.2.1 NLRP3 inflammasome components in atrial whole-tissue lysates from POAF patients

Since the NLRP3 inflammasome plays a critical role in the immune response, we compared protein levels of its major components in patients who developed POAF or who remained in SR (Ctl) after surgery (**Figure 10**). Immunoblots showed increased protein expression of NLRP3 (100 kDa: Ctl: 1.000 ± 0.110, n = 19 vs. POAF: 1.703 ± 0.305, n = 15; P = 0.024; 125 kDa: Ctl: 1.000 ± 0.105, n = 19 vs. POAF: 1.309 ± 0.192, n = 15; P = 0.146) and active Casp1 isoforms (Casp1-p33: Ctl: 1.000 ± 0.091, n = 13 vs. POAF: 1.396 ± 0.115, n = 8; P = 0.024; Casp1-p20: Ctl: 1.000 ± 0.060, n = 13 vs. POAF: 1.719 ± 0.294, n = 8; P = 0.036). Pro-Casp1 remained unchanged (Ctl: 1.000 ± 0.077, n = 13 vs. POAF: 1.218 ± 0.123, n = 8; P = 0.132). ASC protein expression also tended to increase in POAF vs. Ctl patients (Ctl: 1.000 ± 0.123, n = 9 vs. POAF: 2.160 ± 0.529, n = 11; P = 0.068).

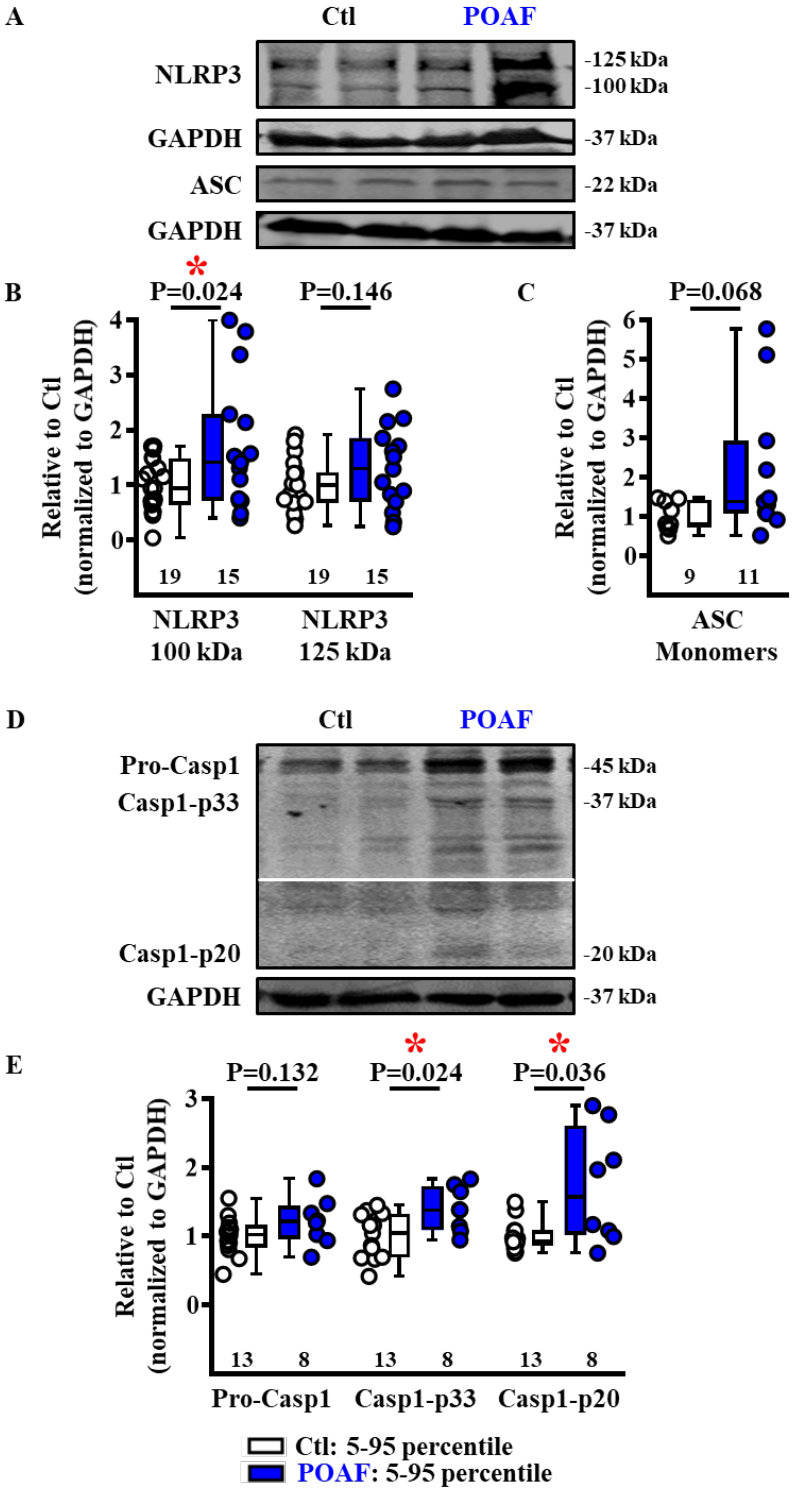

Figure 10: Components of the NLRP3 inflammasome in POAF atrial whole-tissue homogenates. Representative Western blots of NLRP3 and ASC (**A**), pro-Casp1 and its active forms Casp1-p33and Casp1-p20 (**D**), as well as quantitative analysis of whole-atrial tissue lysates from patients with POAF compared to Ctl (**B**, **C** and **E**). GAPDH was used as a loading control. *P<0.05, **P<0.01 vs. Ctl (= patients in sinus rhythm); numbers indicate number of patients. ASC = apoptosis-associated speck-like protein containing a CARD domain; Casp1-p33/p20 = active caspase-1; GAPDH = Glyceraldehyde 3-phosphate dehydrogenase; NLRP3 = NACHT, LRR and PYD domains containing binding protein 3; POAF = post-operative atrial fibrillation; Pro-Casp1 = pro-caspase-1.

4.2.2.2 Activation of GSDMD in atrial whole-tissue lysates from POAF patients

Upon LPS the CARD domain of Casp11 cleaves GSDMD into its N-terminus (NT) that forms pores in the plasma membrane. The NT-pore allows ions like Na^+, Ca^{2+} and K^+ to enter or leave the cell which impairs ion homeostasis, indirectly triggering the NLRP3 inflammasome (Huang et al., 2019; Kayagaki et al., 2011). Since GSDMD is responsible for the formation of the pores and enables the propagation of NLRP3 inflammatory signaling, we studied whether its protein levels were regulated in patients with POAF compared to Ctl patients (**Figure 11**). Indeed, the protein expressions of GSDMD-FL (Ctl: 1.000 ± 0.082, n = 14 vs. POAF: 1.402 ± 0.112, n = 11; P = 0.007) and GSDMD-NT (Ctl: 1.000 ± 0.088, n = 14 vs. POAF: 1.407 ± 0.124, n = 11; P = 0.011) were both increased in POAF patients, whereas those of GSDMD-CT (Ctl: 1.000 ± 0.123, n = 14 vs. POAF: 1.124 ± 0.115, n = 11; P = 0.403) were similar.

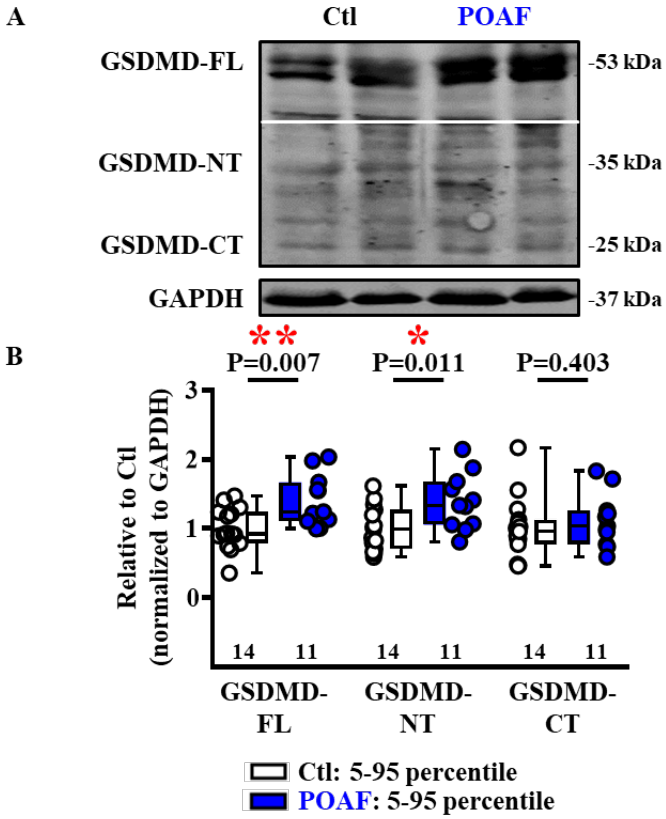

Figure 11: GSDMD in atrial whole-tissue homogenates from POAF patients. Representative Western blots of GSDMD-FL, GSDMD-NT and GSDMD-CT (**A**), as well as quantitative analysis of atrial whole-tissue lysates from patients with POAF compared to Ctl (**B**). GAPDH was used as a loading control. *P<0.05, **P<0.01 vs. Ctl (= patients in sinus rhythm); numbers indicate number of patients. GAPDH = Glyceraldehyde 3-phosphate dehydrogenase; GSDMD-CT = C-terminus of gasdermin D; GSDMD-FL = full-length gasdermin D; GSDMD-NT = N-terminus of gasdermin D; POAF = post-operative atrial fibrillation.

4.2.2.3 Maturation of cytokines in atrial whole-tissue lysates from POAF patients

The proinflammatory mediator IL-1β is a key regulator of the innate immune response (Van Tassell et al., 2013). Adverse remodeling is often associated with its upregulation. Together with IL-18 it elevates the expression chemokines and adhesion molecules (Xiao et al., 2018). Therefore, we next studied the protein levels of IL-1β and IL-18 (**Figure 12**). There were no significant differences between the protein levels of the premature and active isoforms of IL-1β (pro-IL-1β: Ctl: 1.000 ± 0.083, n = 14 vs. POAF: 0.825 ± 0.094, n = 11; P = 0.178; IL-1β: Ctl: 1.000 ± 0.087, n = 14 vs. POAF: 0.809 ± 0.201, n = 11; P = 0.360) and IL-18 (pro-IL-18: Ctl: 1.000 ± 0.129, n = 14 vs. POAF: 1.049 ± 0.178, n = 11; P = 0.822; IL-18: Ctl: 1.000 ± 0.250, n = 14 vs. POAF: 0.712 ± 0.233, n = 11; P = 0.419) in POAF patients.

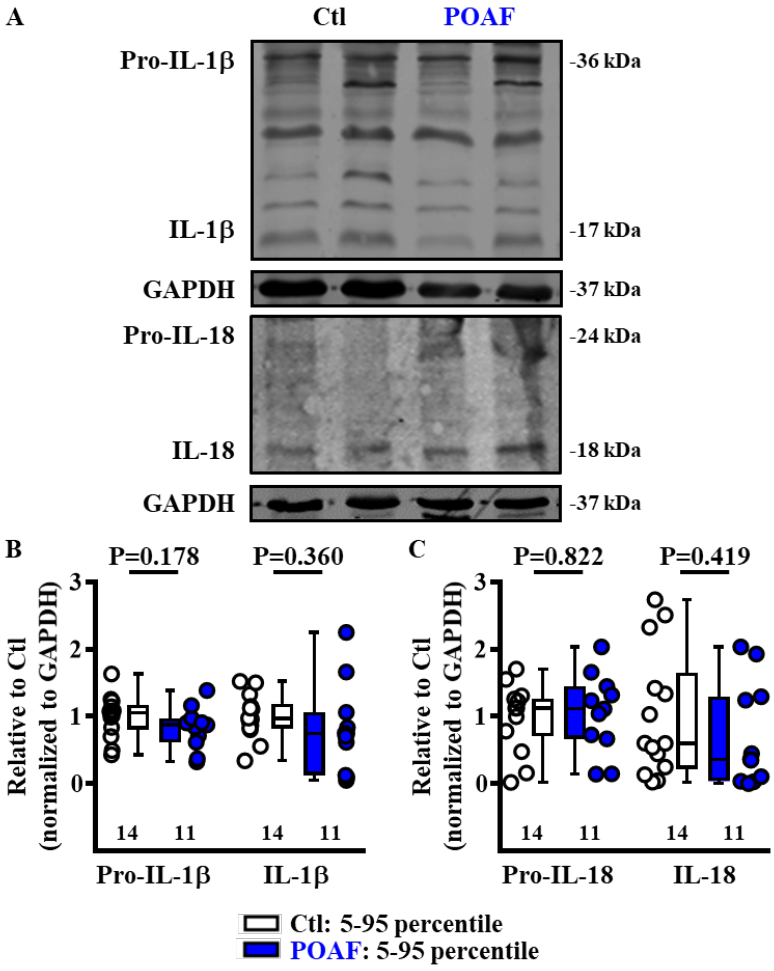

Figure 12: Maturation of IL-1β and IL-18 in atrial whole-tissue homogenates from POAF patients. Representative Western blots of IL-1β and IL-18 and their precursors (pro-IL-1β; pro-IL-18) (**A**), as well as quantitative analysis of atrial whole-tissue lysates from patients with POAF compared to Ctl (**B**). GAPDH was used as a loading control. Ctl = patients in sinus rhythm; numbers indicate number of patients. GAPDH = Glyceraldehyde 3-phosphate dehydrogenase; (Pro-)IL-18 = (pro-)interleukin-18; (Pro-)IL-1β = (pro-)interleukin-1β; POAF = post-operative atrial fibrillation.

4.2.2.4 Priming of the NLRP3 inflammasome complex in POAF atrial whole-tissue homogenates

Upon activation of various receptors, there is both transcriptional or non-transcriptional priming of the components of the NLRP3 inflammasome (Groslambert et al., 2018). Therefore, we studied two key upstream regulators of the TLR4/NFκB priming pathway (**Figure 13**). The protein levels of TLR4 (Ctl: 1.000 ± 0.133, n = 13 vs. POAF: 1.953 ± 0.373, n = 11; P = 0.017) and NFκB-Total (Ctl: 1.000 ± 0.065, n = 22 vs. POAF: 1.482 ± 0.185, n = 13; P = 0.006) were significantly increased in POAF. The protein expression of phosphorylated NFκB remained unchanged (Ser536-NFκB: Ctl: 1.000 ± 0.088, n = 22 vs. POAF: 1.219 ± 0.216, n = 13; P = 0.468). Similarly, there were no significant differences in relative Ser536-NFκB phosphorylation levels (Ser536/Total: Ctl: 1.000 ± 0.076, n = 22 vs. POAF: 0.890 ± 0.119, n = 13).

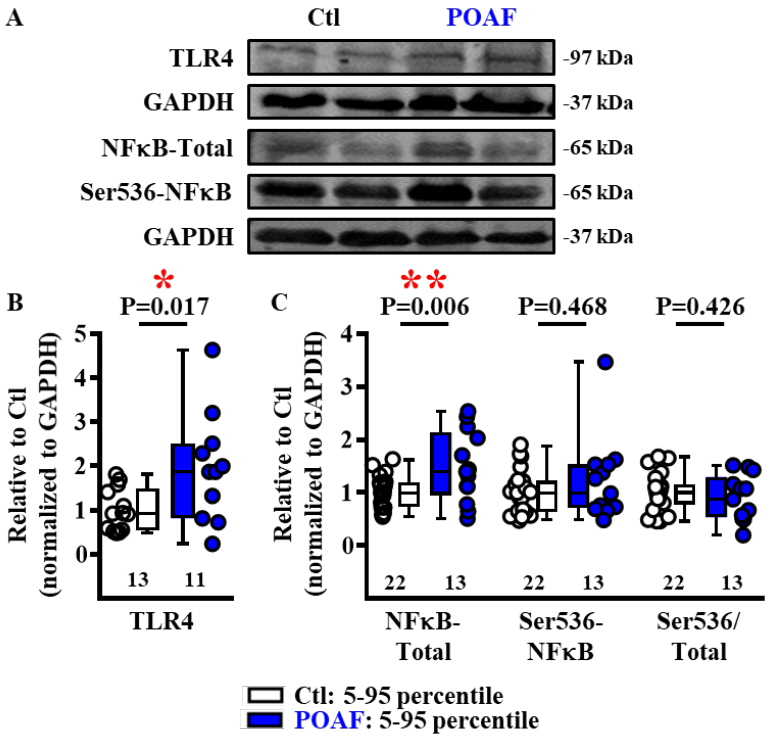

Figure 13: TLR4/NFκB pathway in atrial whole-tissue homogenates from POAF patients. Representative Western blots of TLR4, NFκB-Total and Ser536-NFκB (**A**). Quantitative analysis of TLR4 (**B**), NFκB-Total, Ser536-NFκB and the ratio between total and phosphorylated NFκB (**C**) in whole-atrial tissue lysates from POAF and Ctl patients. GAPDH was used as a loading control. *P<0.05, **P<0.01 vs. Ctl (= patients in sinus rhythm); numbers indicate number of patients. GAPDH = Glyceraldehyde 3-phosphate dehydrogenase; NFκB-Total = nuclear factor 'kappa-light-chain-enhancer' of activated B-cells; Ser536-NFκB = phosphorylated NFκB; Ser536/Total = ratio between the phosphorylated and the total (protein) NFκB; POAF = post-operative atrial fibrillation; TLR4 = toll-like receptor 4.

4.2.2.5 Triggering of the NLRP3 inflammasome complex in atrial whole-tissue homogenates from POAF patients

Protein levels of the purinergic receptor (P2X7R), which activation is considered the main triggering mechanism of the NLRP3 inflammasome in immune-competent cells (Savio et al., 2018) , were upregulated (Ctl: 1.000 ± 0.082, n = 18 vs. POAF: 1.59 ± 0.176, n = 13; P = 0.002) (**Figure 14**), pointing to increased NLRP3 triggering in POAF patients.

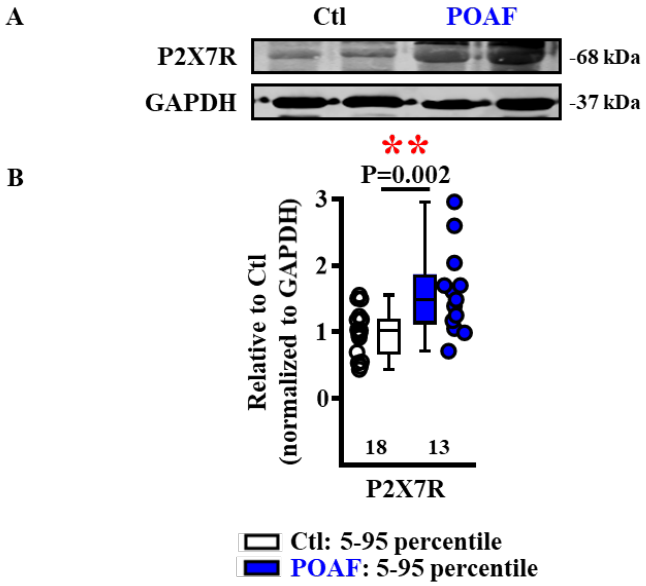

Figure 14: P2X7R in atrial whole-tissue homogenates from POAF patients. Representative Western blots of P2X7R (**A**) and quantitative analysis of human atrial whole-tissue lysates from POAF Ctl patients (**B**). GAPDH was used as a loading control. **P<0.01 vs. Ctl (= patients in sinus rhythm); numbers indicate number of patients. GAPDH = Glyceraldehyde 3-phosphate dehydrogenase; P2X7R = purinergic receptor; POAF = post-operative atrial fibrillation.

4.2.3 NLRP3 inflammatory signaling in atrial whole-tissue homogenates from PAF patients

4.2.3.1 NLRP3 inflammasome components in atrial whole-tissue homogenates from PAF patients

We next assessed the protein levels of the NLRP3 inflammasome components in PAF patients (**Figure 15**). There was no significant change in the protein levels of the two NLRP3 isoforms (100 kDa: Ctl: 1.000 ± 0.098, n = 18 vs. PAF: 1.161 ± 0.134, n = 28; P = 0.392; 125 kDa: Ctl: 1.000 ± 0.094, n = 18 vs. PAF: 0.938 ± 0.092, n = 28; P = 0.441) and ASC monomers (Ctl: 1.000 ± 0.082, n = 15 vs. PAF: 1.102 ± 0.083, n = 20; P = 0.867). Pro-Casp1 (Ctl: 1.000 ± 0.096, n = 14 vs. PAF: 1.103 ± 0.096, n = 23; P = 0.609), as well as its active forms Casp1-p33 (Ctl: 1.000 ± 0.085, n = 14 vs. PAF: 1.197 ± 0.146, n = 23; P = 0.631) and Casp1-p20 (Ctl: 1.000 ± 0.057, n = 14 vs. PAF: 1.331 ± 0.141, n = 23; P = 0.086), were also unchanged in PAF compared to Ctl patients.

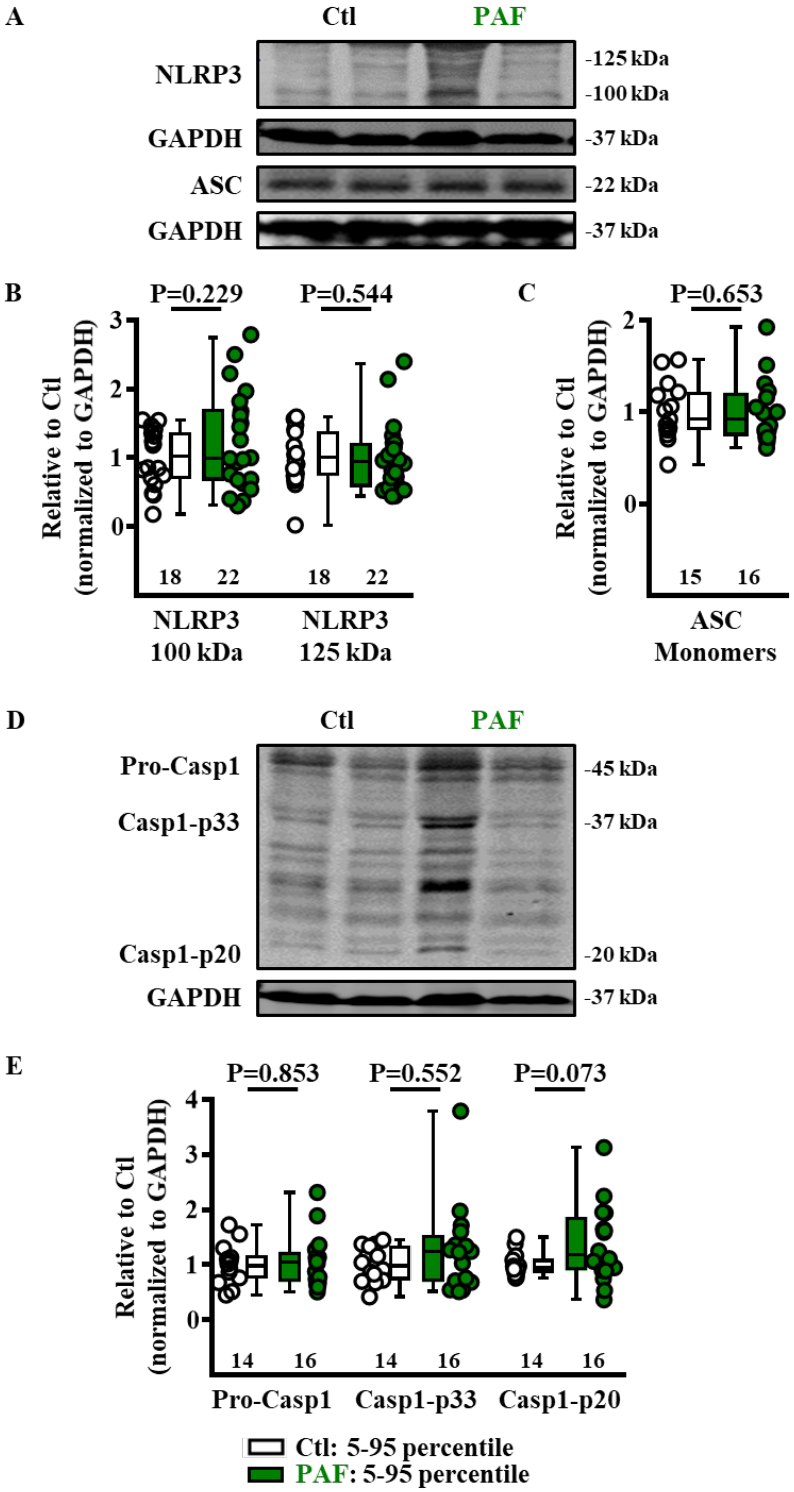

Figure 15: Components of the NLRP3 inflammasome in atrial whole-tissue homogenates from PAF patients. Representative Western blots of NLRP3 and ASC (A), pro-Casp1 and its active forms Casp1-p33 and Casp1-p20 (D), as well as quantitative analysis of atrial whole-tissue lysates from PAF and Ctl patients (B, C and E). GAPDH was used as a loading control. Ctl = patients in sinus rhythm; numbers indicate number of patients. ASC = apoptosis-associated speck-like protein containing a CARD domain; Casp1-p33 or -p20 = active caspase-1; pro-Casp1 = pro-caspase-1; GAPDH = Glyceraldehyde 3-phosphate dehydrogenase; NLRP3 = NACHT, LRR and PYD domains containing binding protein 3; PAF = paroxysmal atrial fibrillation.

4.2.3.2 Activation of GSDMD in atrial whole-tissue homogenates from PAF patients

We studied whether GSDMD is upregulated in patients with PAF compared to Ctl patients (**Figure 16**). We could demonstrate that GSDMD-FL protein levels (Ctl: 1.000 ± 0.059, n = 12 vs. PAF: 1.542 ± 0.203, n = 13; P = 0.021) were significantly increased in PAF and had a strong tendency towards upregulation of GSDMD-NT (Ctl: 1.000 ± 0.118, n = 12 vs. PAF: 1.408 ± 0.118, n = 13; P = 0.064). Protein levels of GSDMD-CT were comparable in both groups (Ctl: 1.000 ± 0.155, n = 12 vs. PAF: 1.303 ± 0.216, n = 13; P = 0.274).

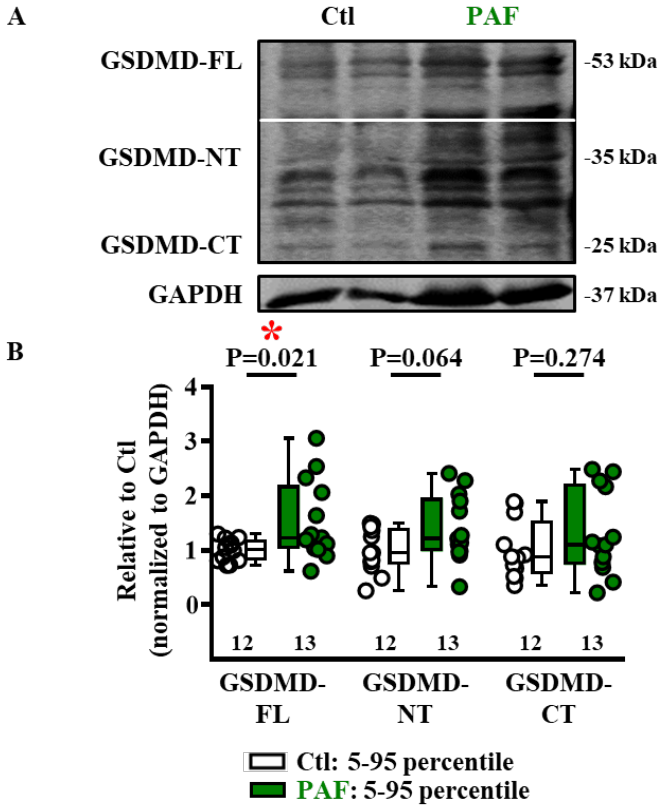

Figure 16: GSDMD in PAF atrial whole-tissue homogenates. Representative Western blots of GSDMD-FL, GSDMD-NT and GSDMD-CT (**A**), as well as quantitative analysis of atrial whole-tissue lysates from patients with PAF compared to Ctl (**B**). GAPDH was used as a loading control. *P<0.05 vs. Ctl (= patients in sinus rhythm); numbers indicate number of patients. GAPDH = Glyceraldehyde 3-phosphate dehydrogenase; GSDMD-CT = C-terminus of gasdermin D; GSDMD-FL = full-length gasdermin D; GSDMD-NT = N-terminus of gasdermin D; PAF = paroxysmal atrial fibrillation.

4.2.3.3 Maturation of cytokines in atrial whole-tissue homogenates from PAF patients

We also measured the protein levels of IL-1β, IL-18 and their precursors in both PAF and Ctl patients (**Figure 17**). Pro-IL-1β (Ctl: 1.000 ± 0.184, n = 11 vs. PAF: 1.100 ± 0.226, n = 17; P = 0.755), IL-1β (Ctl: 1.000 ± 0.164, n = 11 vs. PAF: 1.138 ± 0.218, n = 17; P = 0.781), pro-IL-

18 (Ctl: 1.000 ± 0.120, n = 12 vs. PAF: 0.988 ± 0.128, n = 13; P = 0.949) and IL-18 (Ctl: 1.000 ± 0.266, n = 12 vs. PAF: 1.276 ± 0.332, n = 13; P = 0.503) were all unchanged.

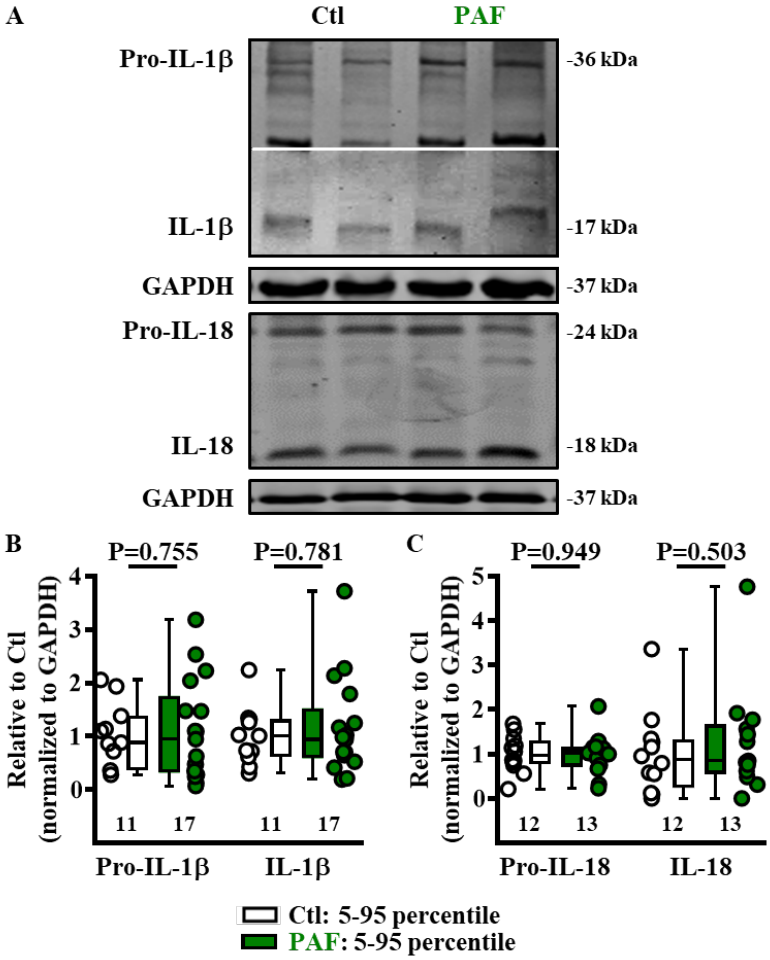

Figure 17: Maturation of IL-1β and IL-18 in atrial whole-tissue homogenates from PAF patients. Representative Western blots of IL-1β and IL-18 and their precursors (**A**), as well as quantitative analysis of atrial whole-tissue lysates from PAF Ctl patients (**B**). GAPDH was used as a loading control. Ctl = patients in sinus rhythm; numbers indicate number of patients. GAPDH = Glyceraldehyde 3-phosphate dehydrogenase; (Pro-)IL-18 = (pro-)interleukin-18; (Pro-)IL-1β = (pro-)interleukin-1β; PAF = paroxysmal atrial fibrillation.

4.2.3.4 Priming of the NLRP3 inflammasome complex in atrial whole-tissue homogenates from PAF patients

We then tested whether the main pathway for the priming of the NLRP3 inflammasome was more active in PAF patients (**Figure 18**). We detected a significant activation of the TLR4/NFκB priming pathway in PAF patients resulting from a borderline significant increase in protein levels of total NFκB (Ctl: 1.000 ± 0.070, n = 7 vs. PAF: 1.311 ± 0.141, n = 6; P = 0.051) and a significantly increased Ser536-phosphorylated NFκB protein (Ctl: 1.000 ± 0.097, n = 7 vs. PAF: 1.996 ± 0.348, n = 6; P = 0.022), along with a significant upregulation in relative

phosphorylation (activation) levels (Ctl: 1.000 ± 0.091, n = 7 vs. PAF: 1.419 ± 0.166, n = 6; P = 0.035).

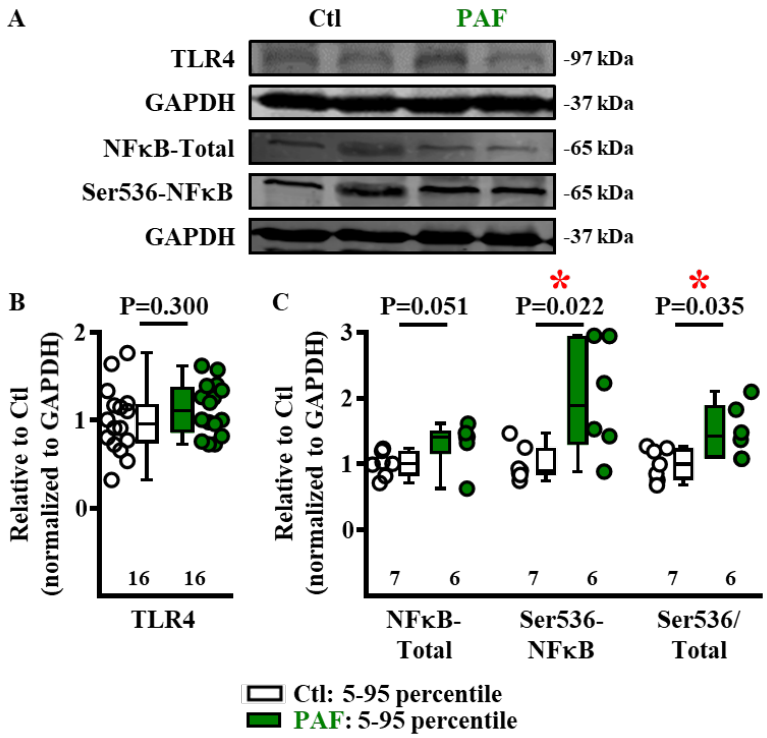

Figure 18: Activation of the TLR4/NFκB pathway in atrial whole-tissue homogenates from PAF patients. Representative Western blots of TLR4, NFκB-Total and Ser536-NFκB (**A**). Quantitative analysis of TLR4 (**B**), NFκB-Total, Ser536-NFκB and their ratio (**C**) in atrial whole-tissue lysates from PAF and Ctl patients. GAPDH was used as a loading control. Ctl = patients in sinus rhythm; numbers indicate number of patients. GAPDH = Glyceraldehyde 3-phosphate dehydrogenase; NFκB-Total = nuclear factor 'kappa-light-chain-enhancer' of activated B-cells; Ser536-NFκB = phosphorylated NFκB; Ser536/Total = ratio between the phosphorylated and the total (protein) NFκB; POAF = post-operative atrial fibrillation; PAF = paroxysmal atrial fibrillation; TLR4 = toll-like receptor 4.

4.2.3.5 Triggering of the NLRP3 complex in atrial whole-tissue homogenates from PAF patients

Similar to patients with POAF (**Figure 14**), the protein levels of P2X7R were significantly increased in PAF compared to Ctl patients (Ctl: 1.000 ± 0.212, n = 8 vs. PAF: 2.098 ± 0.315, n = 12; P = 0.019) (**Figure 19**).

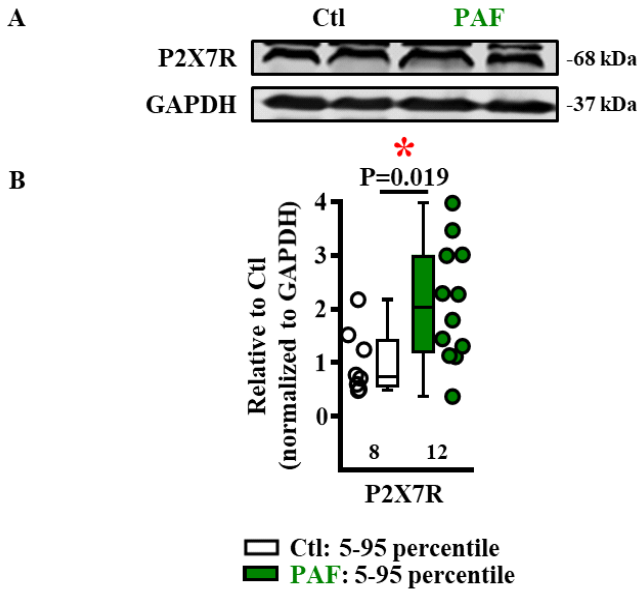

Figure 19: P2X7R in atrial whole-tissue homogenates from PAF patients. Representative Western blots of P2X7R (**A**) and quantitative analysis of atrial whole-tissue lysates from PAF and Ctl patients (**B**). GAPDH was used as a loading control. *P<0.05 vs. Ctl (= patients in sinus rhythm); numbers indicate number of patients. GAPDH = Glyceraldehyde 3-phosphate dehydrogenase; P2X7R = purinergic receptor; PAF = paroxysmal atrial fibrillation.

4.2.4 NLRP3 inflammatory signaling in atrial whole-tissue homogenates from CAF patients

4.2.4.1 NLRP3 inflammasome complex in atrial whole-tissue homogenates from CAF patients

First, we assessed the protein levels of the NLRP3 inflammasome components in patients with CAF (**Figure 20**). There was no significant difference in protein levels of the two NLRP3 proteins (100 kDa: Ctl: 1.000 ± 0.056, n = 16 vs. CAF: 1.142 ± 0.100, n = 24; P = 0.287; 125 kDa: Ctl: 1.000 ± 0.122, n = 14 vs. CAF: 1.344 ± 0.209, n = 24; P = 0.435). In contrast, the ASC monomers were upregulated in CAF compared to Ctl patients (Ctl: 1.000 ± 0.116, n = 13 vs. CAF: 1.439 ± 0.150, n = 11; P = 0.029). The protein levels of pro-Casp1 (Ctl: 1.000 ± 0.117, n = 9 vs. CAF: 1.019 ± 0.075, n = 17; P = 0.889) and its active forms Casp1-p33 (Ctl: 1.000 ± 0.098, n = 9 vs. CAF: 0.905 ± 0.078, n = 17; P = 0.472) and Casp1-p20 (Ctl: 1.000 ± 0.181, n = 9 vs. CAF: 1.311 ± 0.148, n = 17; P = 0.214) were comparable in CAF and Ctl patients.

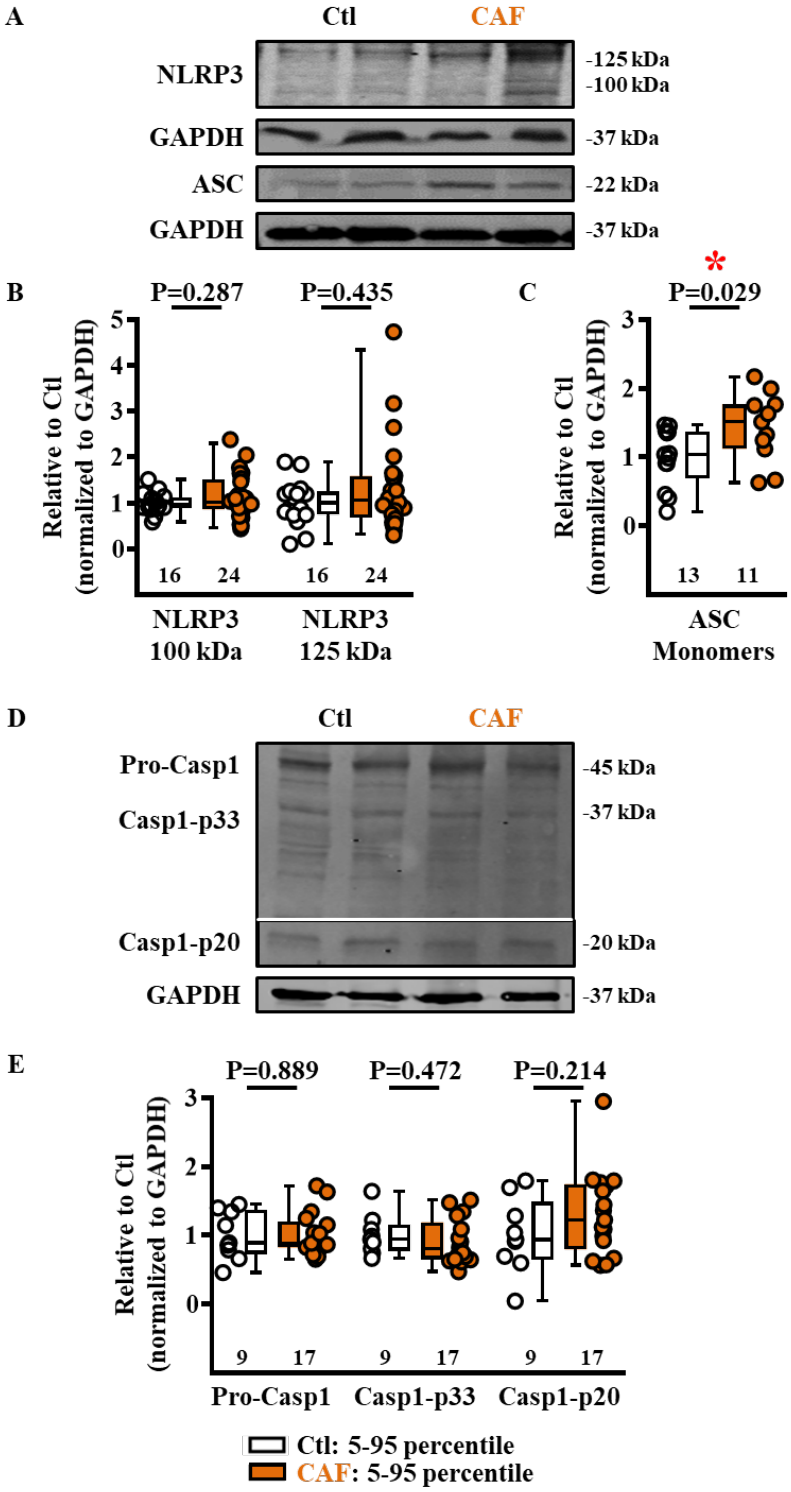

Figure 20: Components of the NLRP3 inflammasome in atrial whole tissue homogenates from CAF patients. Representative Western blots of NLRP3 and ASC (**A**) and pro-Casp1 and its active forms Casp1-p33 and Casp1-p20 (**D**), as well as quantitative analysis of atrial whole-tissue lysates from CAF and Ctl patients (**B, C** and **E**). GAPDH was used as a loading control. *P<0.05 vs. Ctl (= patients in sinus rhythm); numbers indicate number of patients. ASC = apoptosis-associated speck-like protein containing a CARD domain; CAF = long-standing persistent (chronic) atrial fibrillation; Casp1-p33 or -p20 = active caspase-1 forms; pro-Casp1 = pro-caspase-1; GAPDH = Glyceraldehyde 3-phosphate dehydrogenase; NLRP3 = NACHT, LRR and PYD domains containing binding protein 3.

4.2.4.2 Activation of GSDMD in atrial whole-tissue homogenates from CAF patients

The protein levels of GSDMD-FL protein (Ctl: 1.000 ± 0.100, n = 9 vs. CAF: 0.967 ± 0.114, n = 15; P = 0.847) and its CT fragment (Ctl: 1.000 ± 0.190, n = 9 vs. CAF: 1.090 ± 0.125, n = 15; P = 0.684) were similar between CAF and Ctl patients. However, there was a non-significant tendency towards upregulation of the pore-forming GSDMD-NT (Ctl: 1.000 ± 0.123, n = 9 vs. CAF: 1.745 ± 0.294, n = 15; P = 0.072) in CAF vs. Ctl patients (**Figure 21**).

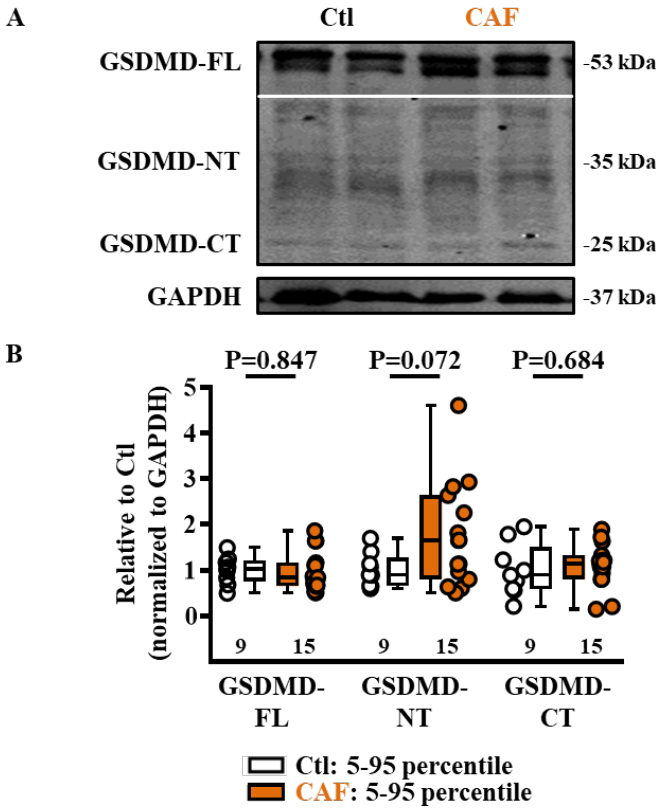

Figure 21: GSDMD in atrial whole-tissue homogenates from CAF patients. Representative Western blots of GSDMD-FL, GSDMD-NT and GSDMD-CT (**A**), as well as quantitative analysis of atrial whole-tissue lysates from CAF compared to Ctl patients (**B**). GAPDH was used as a loading control. Ctl = patients in sinus rhythm; numbers indicate number of patients. CAF = long-standing persistent (chronic) atrial fibrillation; GAPDH = Glyceraldehyde 3-phosphate dehydrogenase; GSDMD-CT = C-terminus of gasdermin D; GSDMD-FL = full-length gasdermin D; GSDMD-NT = N-terminus of gasdermin D.

4.2.4.3 Expression and maturation of interleukins in atrial whole-tissue homogenates from CAF patients

In CAF patients, the protein levels of the precursors pro-IL-1β (Ctl: 1.000 ± 0.134, n = 14 vs. CAF: 1.234 ± 0.263, n = 11; P = 0.767), pro-IL-18 (Ctl: 1.000 ± 0.136, n = 12 vs. CAF: 1.091 ± 0.101, n = 13; P = 0.592) and their active forms IL-1β (Ctl: 1.000 ± 0.088, n = 14 vs. CAF: 0.866 ± 0.124, n = 11; P = 0.267) and IL-18 (Ctl: 1.000 ± 0.141, n = 12 vs. CAF: 1.156 ± 0.201, n = 13; P = 0.542) showed no significant differences compared to Ctl patients (**Figure 22**).

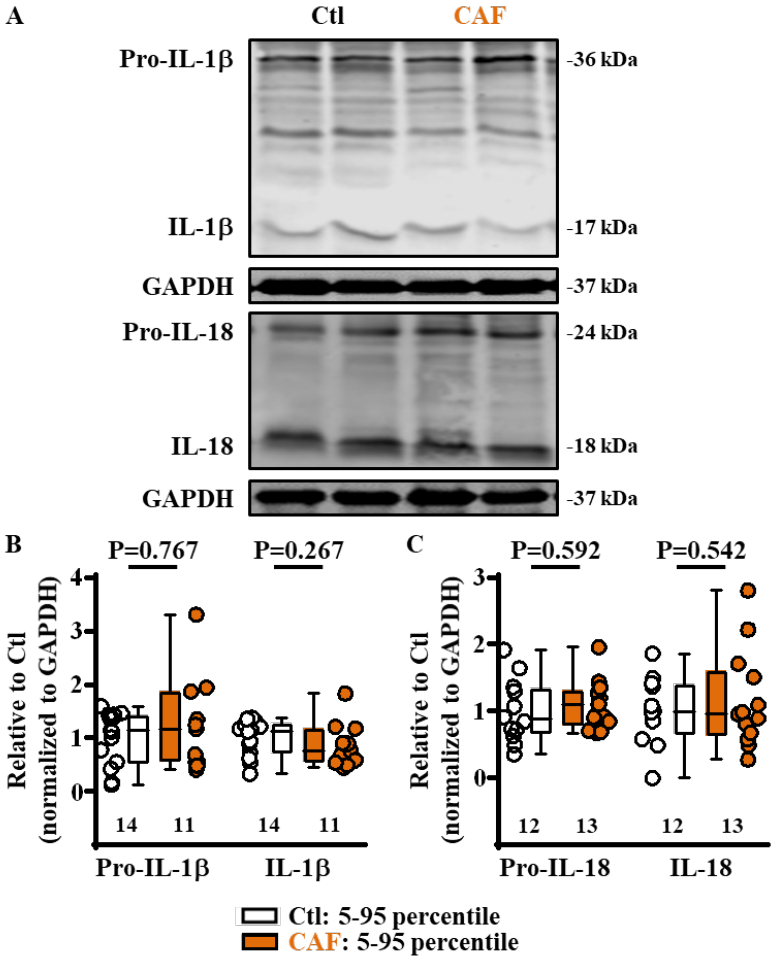

Figure 22: Protein levels of IL-1β and IL-18 **in atrial whole-tissue homogenates from CAF patients.** Representative Western blots of IL-1β and IL-18 and their precursors – pro-IL-1β and pro-IL-18 (**A**), as well as quantitative analysis of atrial whole-tissue lysates from CAF and Ctl patients (**B**). GAPDH was used as a loading control. Ctl = patients in sinus rhythm; numbers indicate number of patients. CAF = long-standing persistent (chronic) atrial fibrillation; GAPDH = Glyceraldehyde 3-phosphate dehydrogenase; (Pro-)IL-18 = (pro-) interleukin-18; (Pro-)IL-1β = (pro-)interleukin-1β.

4.2.4.4 Priming of the NLRP3 inflammasome complex in atrial whole-tissue homogenates from CAF patients

Immunoblotting of whole-tissue lysates from CAF patients showed an upregulation of the TLR4/NFκB priming pathway (**Figure 23**). The protein levels of TLR4 (Ctl: 1.000 ± 0.070, n = 11 vs. CAF: 1.283 ± 0.097, n = 13; P = 0.032) were significantly increased. NFκB-Total was unchanged (Ctl: 1.000 ± 0.130, n = 6 vs. CAF: 1.626 ± 0.330, n = 7; P = 0.294), whereas the phosphorylation of NFκB was higher in CAF vs. Ctl patients (Ctl: 1.000 ± 0.176, n = 6 vs. CAF: 1.570 ± 0.177, n = 8; P = 0.035). However, the relative Ser536-phosphorylation of NFκB was similar in both groups (Ctl: 1.000 ± 0.158, n = 6 vs. CAF: 1.078 ± 0.130, n = 7; P = 0.445).

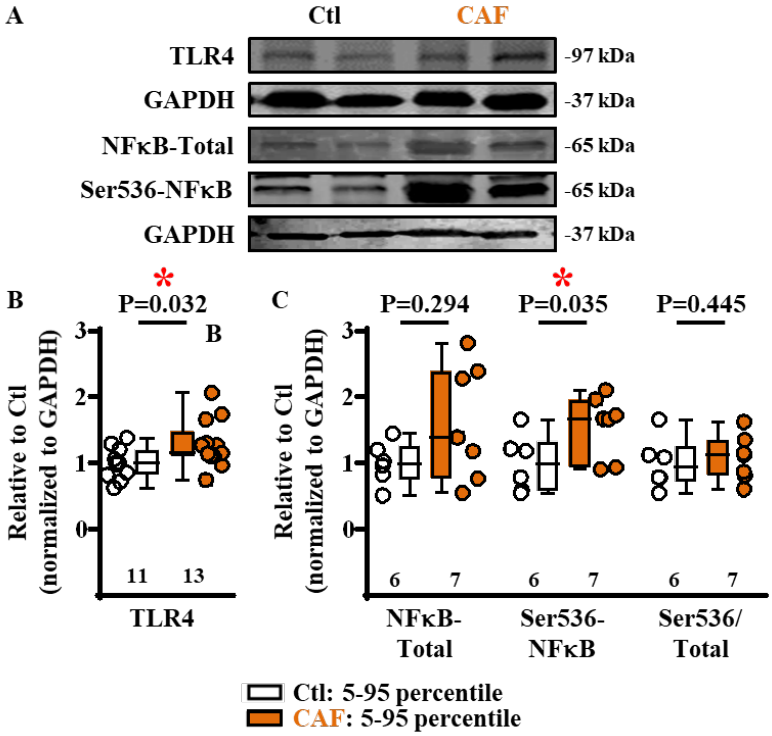

Figure 23: Proteins levels of the TLR4/NFκB priming pathway in atrial whole-tissue homogenates from CAF patients. Representative Western blots of TLR4, NFκB-Total and Ser536-NFκB (**A**). Quantitative analysis of TLR4 (**B**), NFκB-Total, Ser536-NFκB and their ratio (**C**) in atrial whole-tissue lysates from CAF and Ctl patients. GAPDH was used as a loading control. *P<0.05 vs. Ctl (= patients in sinus rhythm); numbers indicate number of patients. CAF = long-standing persistent (chronic) atrial fibrillation; GAPDH = Glyceraldehyde 3-phosphate dehydrogenase; NFκB-Total = nuclear factor 'kappa-light-chain-enhancer' of activated B-cells; Ser536-NFκB = phosphorylated NFκB; Ser536/Total = ratio between the phosphorylated and the total (protein) NFκB; POAF = post-operative atrial fibrillation; TLR4 = toll-like receptor 4.

4.2.4.5 Triggering of the NLRP3 inflammasome in atrial whole-tissue homogenates from CAF patients

Immunoblotting revealed a strong upregulation of the protein levels of P2X7R in CAF compared to Ctl patients (Ctl: 1.000 ± 0.270, n = 5 vs. CAF: 2.912 ± 0.807, n = 8; P = 0.029) (**Figure 24**).

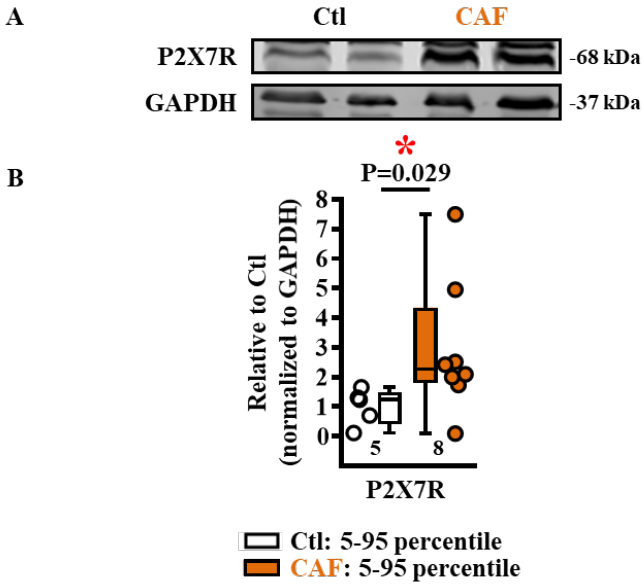

Figure 24: Protein levels of NLRP3 triggering P2X7R in atrial whole-tissue homogenates from CAF patients. Representative Western blots of P2X7R (**A**) and quantitative analysis of atrial whole-tissue lysates from CAF and Ctl patients (**B**). GAPDH was used as a loading control. *P<0.05 vs. Ctl (= patients in sinus rhythm); numbers indicate number of patients. CAF = long-standing persistent (chronic) atrial fibrillation; GAPDH = Glyceraldehyde 3-phosphate dehydrogenase; P2X7R = purinergic receptor.

4.3 Atrial infiltration of immune cells in AF

Since the NLRP3 inflammasome complex is a key source of inflammatory signaling in immune-competent cells, particularly in macrophages (Takeuchi & Akira, 2010), we investigated whether enhanced immune-cell infiltration occurs in patients with different AF forms. For this purpose, the protein levels of established inflammatory markers such as F4/80, CD68, CD206 and CD11b were assessed in atrial whole-tissue lysates from patients with POAF, PAF or CAF (**Figure 25**). There were no significant differences between the protein levels of the M2 macrophage marker CD206, in patients with POAF (Ctl: 1.000 ± 0.092, n = 19 vs. POAF: 1.118 ± 0.127, n = 17; P = 0.451), PAF (Ctl: 1.000 ± 0.084, n = 8 vs. PAF: 0.965 ± 0.113, n = 8; P = 0.809) or CAF (Ctl: 1.000 ± 0.165, n = 8 vs. CAF: 1.005 ± 0.107, n = 11; P = 0.977) compared to Ctl patients. Similarly, protein levels of the leucocyte marker CD11b were unchanged in POAF (Ctl: 1.000 ± 0.249, n = 8 vs. POAF: 1.832 ± 0.778, n = 8; P = 0.645), PAF (Ctl: 1.000 ± 0.203, n = 8 vs. PAF: 0.990 ± 0.227, n = 7; P > 0.999) or CAF (Ctl: 1.000 ± 0.105, n = 7 vs. CAF: 0.892 ± 0.185, n = 7; P = 0.710) compared to Ctl patients. The protein levels of CD68 were significantly increased in POAF patients (Ctl: 1.000 ± 0.059, n = 15 vs. POAF: 1.369 ± 0.104, n = 13; P = 0.003), but unchanged in PAF patients (Ctl: 1.000 ± 0.069, n = 7 vs. PAF: 0.992 ± 0.081, n = 8; P = 0.778) and CAF patients (Ctl: 1.000 ± 0.106, n = 6 vs. CAF: 1.185 ± 0.139, n = 10; P = 0.313). Because CD68 is highly expressed by a variety of cells, the protein expression of the highly specific macrophage marker F4/80 was also assessed in all 3 forms of AF. F4/80 levels were unchanged in PAF and CAF patients (Ctl: 1.000 ± 0.394, n = 6 vs. PAF: 1.389 ± 0.331, n = 7; P = 0.533), (Ctl: 1.000 ± 0.229, n = 7 vs. CAF: 2.828 ± 1.010, n = 7; P = 0.128), but were strongly upregulated in POAF patients (Ctl: 1.000 ± 0.389, n = 8 vs. POAF: 3.359 ± 0.852, n = 8; P = 0.025), clearly indicating that increased macrophage infiltration likely contributes to the upregulation of the NLRP3 inflammasome system in the atria of POAF patients.

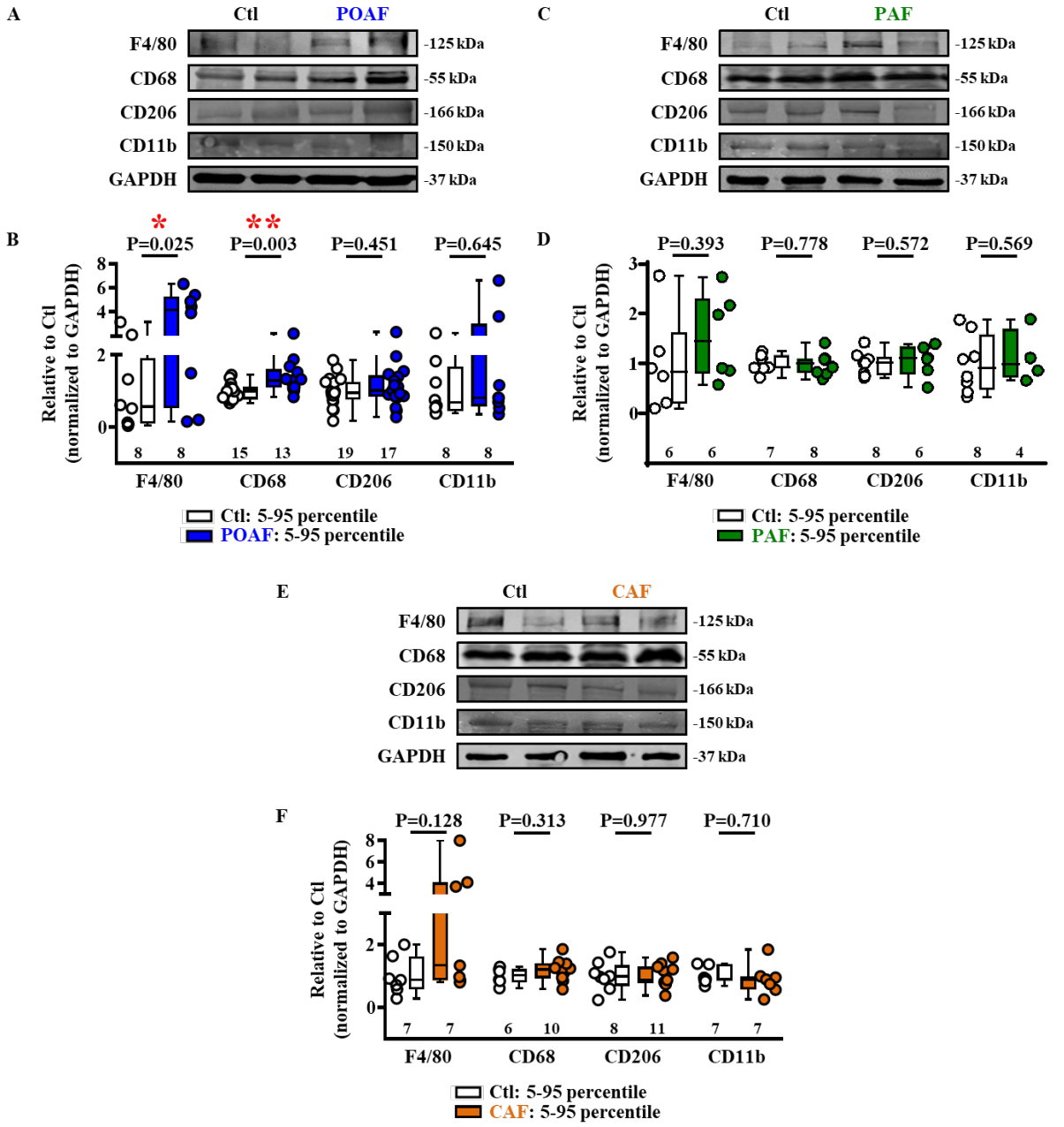

Figure 25: Expression of immune cell markers in atrial whole-tissue homogenates from patients with different forms of AF. Representative Western blots of F4/80, CD68, CD206 and CD11b, as well as quantitative analysis of atrial whole-tissue lysates from patients with POAF (A, B), PAF (C, D) or CAF (E, F) compared to Ctl. GAPDH was used as a loading control. *P<0.05, **P<0.01 vs. Ctl (= patients in sinus rhythm); numbers indicate number of patients. CD68 = cluster of differentiation (macrophage marker); CD206 = cluster of differentiation 206 (macrophage marker); Cd11b = cluster of differentiation 11b (leukocyte marker); F4/80 = EGF-like module-containing mucin-like hormone receptor-like 1 (macrophage marker); GAPDH = Glyceraldehyde 3-phosphate dehydrogenase; PAF = paroxysmal atrial fibrillation; POAF = post-operative atrial fibrillation; CAF == long-standing persistent (chronic) atrial fibrillation.

4.4 The NLRP3 inflammasome in human atrial cardiomyocytes (HAM) from patients with different forms of AF

The results we obtained in whole-tissue lysates from patients with different forms of AF do not allow to differentiate the source (immune vs non-immune cells) of NLRP3 inflammasome activation. Furthermore, in atrial whole-tissue lysates there was no significant upregulation of markers of inflammatory cells in PAF and CAF patients, pointing to non-immune cell sources of NLRP3 inflammasome activation in AF. Therefore, we tested the hypothesis that HAMs might be one major source of upregulated sterile inflammatory signaling in the atria of AF patients. For this purpose, we used HAM-enriched fractions of atrial samples from PAF, CAF and POAF patients, which were previously collected and stored in the atrial tissue bank of Univ.-Prof. Dr. med. Dobromir Dobrev at the Institute of Pharmacology in Essen.

4.4.1 Verification of purity of human atrial cardiomyocytes' fractions and validation of antibodies

4.4.1.1 Verification of purity of HAM-enriched cell fractions

HAM-enriched fractions were obtained as previously described (Graf et al., 2005; Heijman et al., 2018) using BSA gradient sedimentation for separation of HAM from non-HAM, mostly atrial cardiofibroblasts (CF). Validation of the HAM fraction was assessed by immunoblotting of calsequestrin (CSQ), a cardiomyocyte-specific protein. Immunoblotting with the highly specific macrophage/eosinophilic granulocyte marker F4/80 was performed to validate that the HAM-enriched fractions were not contaminated with immune cells (**Figure 26**). Atrial whole-tissue lysates and BMDM were used as positive and negative controls, respectively. The results showed that HAM are positive for CSQ (as were the whole-tissue lysates), whereas CF did not show any signal, which confirms the successful separation of HAM and CF. Most important, HAM and CF were negative for F4/80, whereas the BMDM showed the expected positive signal, which clearly validates the purity of HAM and the lack of immune cell contamination (**Figure 27**).

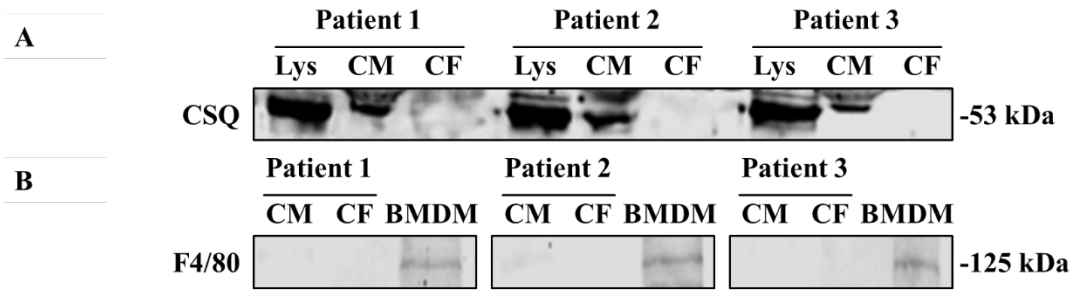

Figure 26: Purity of atrial HAM-enriched fractions. Atrial cardiomyocytes (CM) enriched cell fractions from 3 different patients in sinus rhythm are positive for calsequestrin (CSQ) (**A**) and negative for the highly-specific macrophage/eosinophilic granulocyte marker F4/80 (**B**). BMDM = mouse bone marrow-derived macrophages; CF = cardiofibroblasts; CM = cardiomyocytes; CSQ = calsequestrin; Lys = atrial whole-tissue lysate.

4.4.1.2 Validation of ASC and Caspase-1 antibodies in HAM-enriched cell fractions

Experiments with HAM highlighted the need to validate antibody specificity. For the validation of the ASC antibody, we used a compatible blocking peptide. The decrease of intensity of the detected bands after incubation with the blocking peptide confirmed the specificity of the bands. In HAM we were able to detect the expected ASC monomers at 22-24 kDa, but also dimers at ~50 kDa (**Figure 27**). The band representing the ASC dimers was strongly enhanced in comparison to the band of the ASC monomers in HAM suggesting the potential presence of ASC specks – a hallmark of inflammasome activation.

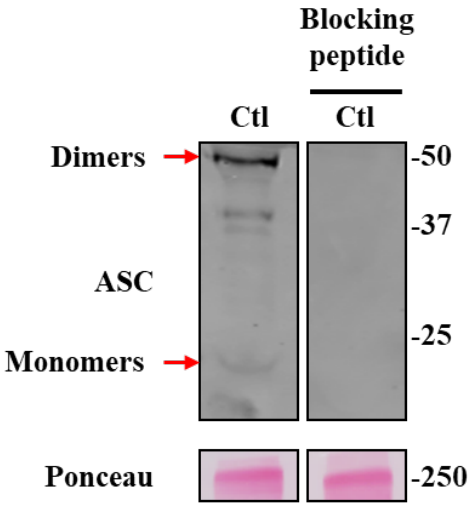

Figure 27: Validation of the specificity of the ASC antibody in HAM. Left, a representative Western blot showing ASC monomers (22-24 kDa) and dimers (~50 kDa) in HAM from a patient in SR. Right, the same blot incubated with both ASC antibody and blocking peptide in ratio 1:5 showing a strong decrease in intensity of the 2 ASC bands. Total protein levels at 250 kDa (Ponceau staining) were used as loading control. Ctl = patient in SR. ASC = Apoptosis-associated speck-like protein containing a CARD.

We also validated the Casp-1 antibody using HAM from both 2 Ctl (sinus rhythm) and 2 POAF patients. We were able to detect pro-Casp1 at 45 kDa and its active isoforms at p33, p20, and p10 kDa (**Figure 28**). The decrease of intensity of the detected bands after incubation with the blocking peptide confirmed the specificity of all bands.

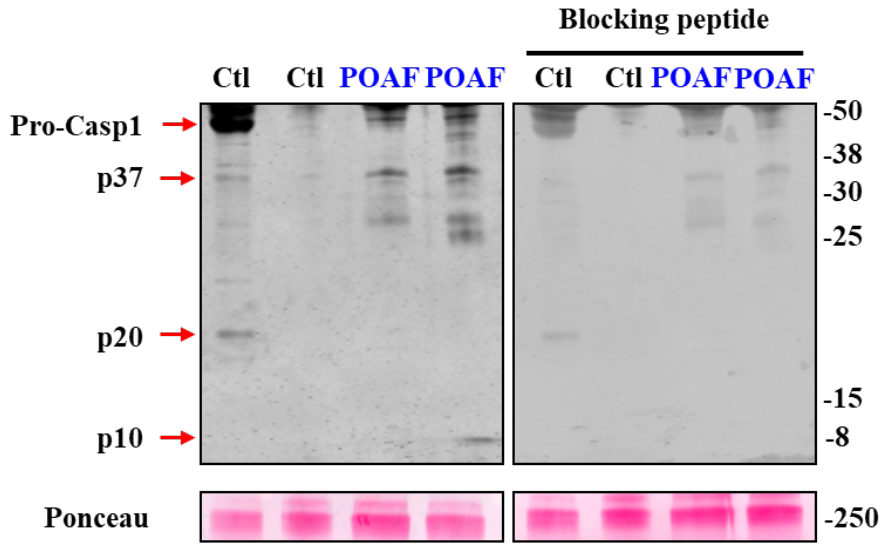

Figure 28: Validation of the specificity of the Casp1 antibody in HAM. Left, representative Western blot showing pro-Casp1, Casp1-p33, Casp1-p20 and Casp1-p10 in HAM from Ctl and POAF patients. Right, the same blot incubated with both Casp1 antibody and a blocking peptide in ratio 1:5 showing a strong decrease in intensity of all Casp1 bands. Total protein levels at 250 kDa (Ponceau staining) were used as loading control. Ctl = patients in sinus rhythm. Casp1-p33, -p20, and -p10 = active caspase-1 forms; pro-Casp1 = pro-caspase-1; HAM = human atrial cardiomyocyte; POAF = post-operative atrial fibrillation.

4.4.2 NLRP3 inflammatory signaling in HAM from POAF patients

4.4.2.1 NLRP3 inflammasome components in HAM from POAF patients

In contrast to atrial whole-tissue homogenates, HAM showed a positive signal only at 125 kDa. The protein expression of NLRP3 was similar in HAM of POAF compared to Ctl (125 kDa: Ctl: 1.000 ± 0.101, n = 16 vs. POAF: 1.129 ± 0.178, n = 16; P = 0.534). Unlike protein levels of ASC monomers, which were unchanged in the whole-tissue lysates from POAF versus Ctl patients, abundance of ASC dimers was strongly increased in HAM of patients prone to POAF (Ctl: 1.000 ± 0.163, n = 8 vs. POAF: 1.688 ± 0.143, n = 8; P = 0.007). We were unable to detect ASC monomers in HAM, most likely because these were below the detection limit of our Western blot conditions. The protein levels of pro-Casp1 (Ctl: 1.000 ± 0.132, n = 15 vs. POAF: 2.585 ± 0.675, n = 15; P = 0.005), Casp1-p33 (Ctl: 1.000 ± 0.167, n = 15 vs. POAF: 4.110 ± 0.861, n = 15; P = 0.0001) and Casp1-p10 (Ctl: 1.000 ± 0.212, n = 15 vs. POAF: 3.988 ± 0.800, n = 15; P = 0.001) were similarly upregulated. Casp1-p20 protein expression was numerically larger in HAM from POAF patients (Ctl: 1.000 ± 0.210, n = 15 vs. POAF: 2.559 ± 0.720, n = 15; P = 0.173), but this did not reach statistical significance (**Figure 29**).

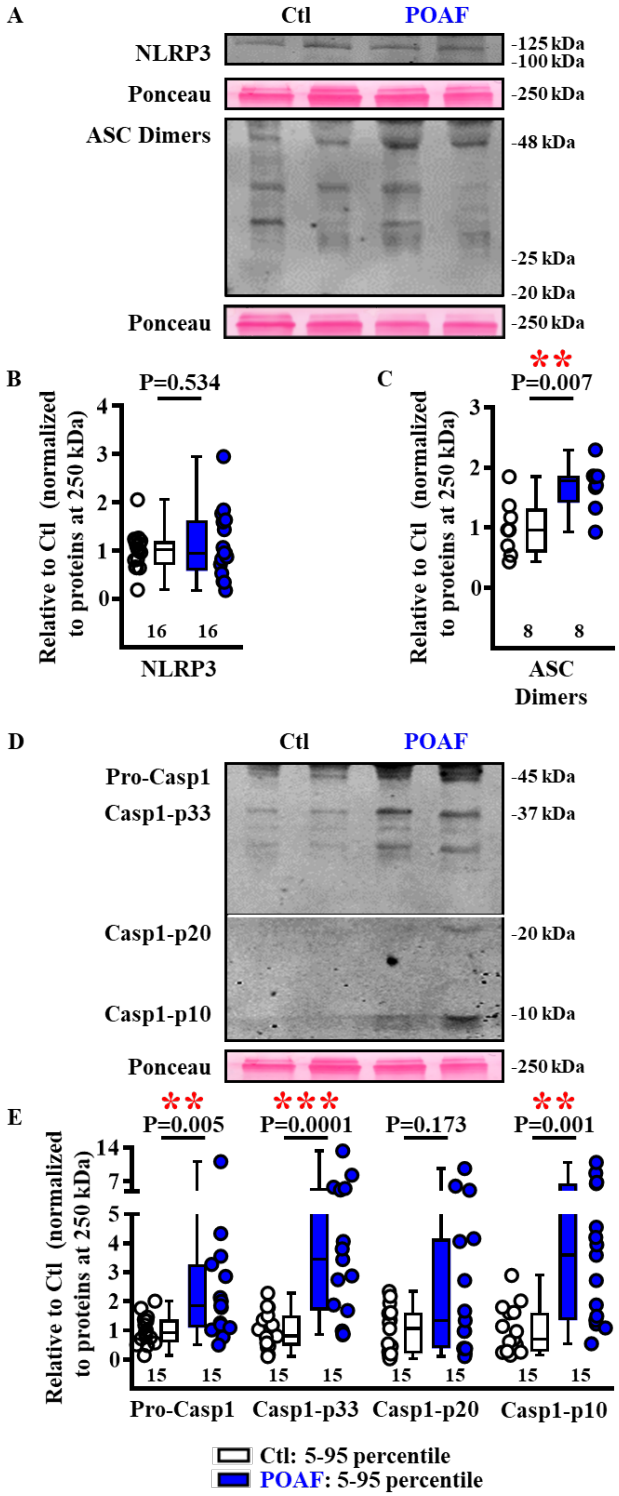

Figure 29: Components of NLRP3 inflammasome in HAM from POAF patients. Representative Western blots of NLRP3 and ASC (**A**), as well as pro-Casp1 and its active forms Casp1-p33, -p20, and -p10 (**D**), along with their quantified protein levels (**B**, **C** and **E**) in human atrial cardiomyocytes from POAF compared to Ctl patients. Total protein-levels at 250 kDa (Ponceau staining) were used as loading control. **P<0.01, ***P<0.001 vs. Ctl (= patients in sinus rhythm); numbers indicate number of patients. ASC = apoptosis-associated speck-like protein containing a CARD domain; Casp1-p33, -p20, -p10 = active caspase-1 forms; pro-Casp1 = pro-caspase-1; NLRP3 = NACHT, LRR and PYD domains containing binding protein 3; POAF = post-operative atrial fibrillation.

4.4.2.2 Activation pattern of GSDMD in HAM of POAF patients

Having detected an upregulation of Casp-1 in POAF, we assessed whether this resulted in an increased cleavage (activation) of GSDMD. We found that the protein levels of GSDMD-FL (Ctl: 1.000 ± 0.123, n = 12 vs. POAF: 2.404 ± 0.572, n = 9; P = 0.013), GSDMD-NT (Ctl: 1.000 ± 0.163, n = 12 vs. POAF: 3.980 ± 0.857, n = 9; P = 0.0009), and GSDMD-CT (Ctl: 1.000 ± 0.184, n = 12 vs. POAF: 1.990 ± 0.349, n = 9; P = 0.014) were all upregulated in HAM from POAF compared to Ctl patients, which is consistent with the results from whole-tissue lysates (**Figure 30**).

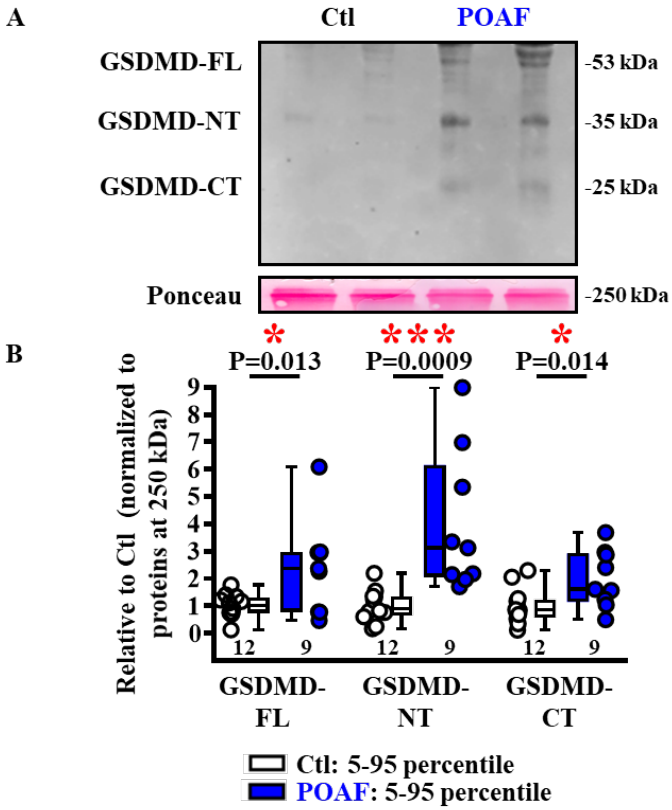

Figure 30: GSDMD in HAM from POAF patients. Representative Western blots of GSDMD-FL, GSDMD-NT and GSDMD-CT (**A**), as well as quantified protein levels (**B**) in human atrial cardiomyocytes from POAF compared to Ctl patients. Total protein levels at 250 kDa (Ponceau staining) were used as loading control. *P<0.05, ***P<0.001 vs. Ctl (= patients in sinus rhythm); numbers indicate number of patients. GSDMD-CT = C-terminus of gasdermin D; GSDMD-FL = full-length gasdermin D; GSDMD-NT = N-terminus of gasdermin D; POAF = post-operative atrial fibrillation.

4.4.2.3 Maturation of cytokines in HAM from POAF patients

We next assessed whether the higher Casp-1 activity is associated with an increased maturation of cytokines. The protein expression Pro-IL-1β was upregulated in HAM from POAF patients (pro-IL-1β: Ctl: 1.000 ± 0.183, n = 15 vs. POAF: 3.250 ± 0.840, n = 12; P = 0.007), whereas

the active isoform was significantly decreased (IL-1β: Ctl: 1.000 ± 0.224, n = 15 vs. POAF: 0.713 ± 0.373, n = 12; P = 0.005) (**Figure 31**), most likely because of an increase in GSDMD-mediated cytokine release from HAM.

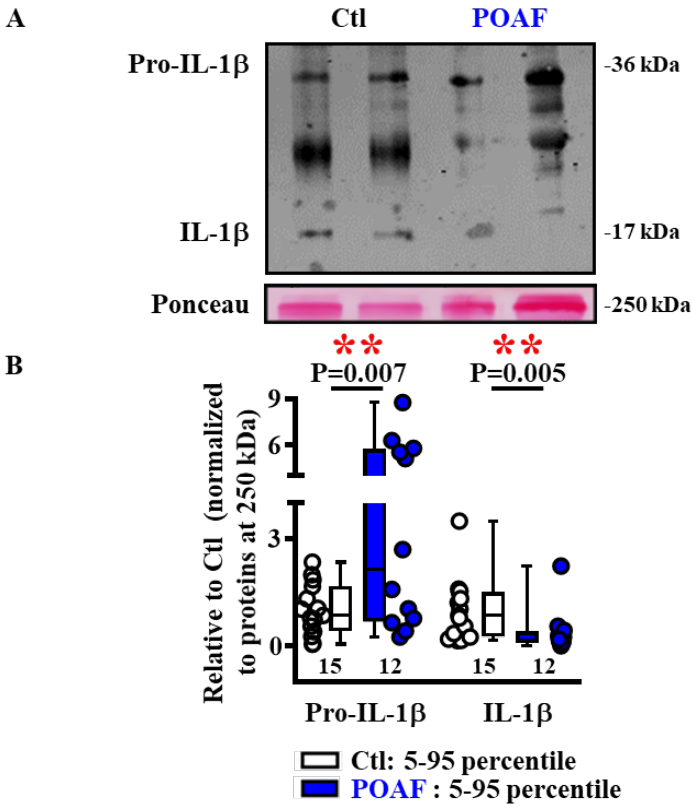

Figure 31: Maturation of IL-1β in HAM from POAF patients. Representative Western blots of pro-IL-1β and IL-1β (**A**), along with their quantified protein levels (**B**) in human atrial cardiomyocytes from POAF in comparison to Ctl patients. Total protein levels at 250 kDa (Ponceau staining) were used as loading control. **P<0.01 vs. Ctl (= patients in sinus rhythm); numbers indicate number of patients. (Pro-)IL-1β = (pro-)interleukin-1β; POAF = post-operative atrial fibrillation.

4.4.3 NLRP3 inflammatory signaling in HAM from PAF patients

4.4.3.1 NLRP3 inflammasome components in HAM from PAF patients

Similar to HAM from POAF patients, HAM from PAF patients showed only the full-length NLRP3 at 125 kDa and ASC as dimers. The protein levels of NLRP3 (Ctl: 1.000 ± 0.053, n = 7 vs. PAF: 1.247 ± 0.166, n = 8; P = 0.231) and ASC (Ctl: 1.000 ± 0.234, n = 8 vs. PAF: 1.429 ± 0.146, n = 7; P = 0.157) were unchanged in PAF compared to Ctl patients. Contrary to the results in whole-tissue lysates from PAF patients, pro-Casp1 (Ctl: 1.000 ± 0.129, n = 8 vs. PAF: 1.718 ± 0.280, n = 8; P = 0.035), Casp1-p33 (Ctl: 1.000 ± 0.086, n = 8 vs. PAF: 2.392 ± 0.366, n = 8; P = 0.002) and Casp1-p10 (Ctl: 1.000 ± 0.307, n = 8 vs. PAF: 8.290 ± 2.068, n = 8; P = 0.003) were strongly upregulated in HAM from PAF patients. Interestingly Casp1-p20 (Ctl: 1.000 ± 0.104, n = 8 vs. PAF: 0.536 ± 0.219, n = 8; P = 0.077) showed a non-significant tendency to decrease in PAF in comparison to Ctl (**Figure 32**), perhaps because of an increase in GSDMD-mediated release into the extracellular space (Lieberman et al., 2019).

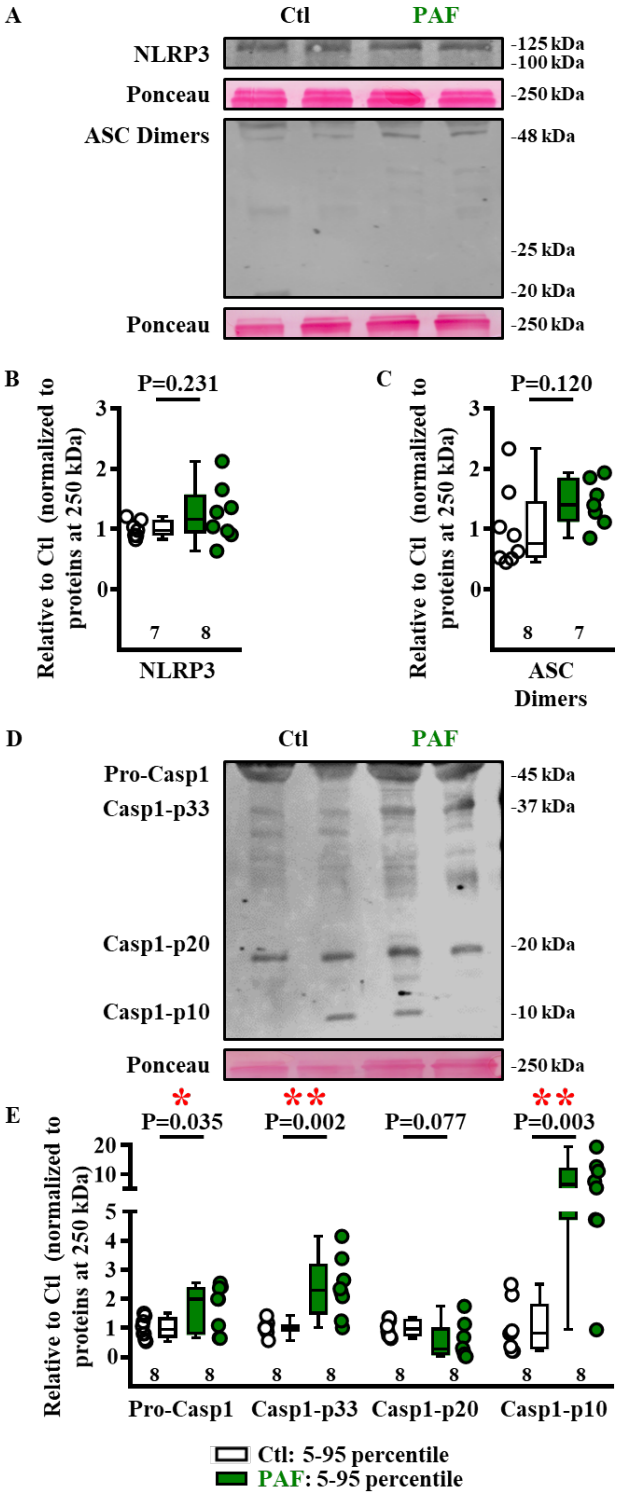

Figure 32: Components of NLRP3 inflammasome in PAF HAM. Representative Western blots of NLRP3 and ASC (**A**), as well as pro-Casp1 and its active forms Casp1-p33, -p20, and -p10 (**D**), along with their quantified protein levels (**B**, **C** and **E**) in human atrial cardiomyocytes from PAF compared to Ctl patients. Total protein levels at 250 kDa (Ponceau staining) were used as loading control. *P<0.05, **P<0.01 vs. Ctl (= patients in sinus rhythm); numbers indicate number of patients. ASC = apoptosis-associated speck-like protein containing a CARD domain; Casp1-p33, -p20, and -p10 = active caspase-1 forms; pro-Casp1 = pro-caspase-1; NLRP3 = NACHT, LRR and PYD domains containing binding protein 3; PAF = paroxysmal atrial fibrillation.

4.4.3.2 Activation of GSDMD in HAM from PAF patients

Consistent with the results obtained in whole-tissue lysates from PAF patients, the protein levels of GSDMD-FL (Ctl: 1.000 ± 0.173, n = 8 vs. PAF: 2.878 ± 0.609, n = 7; P = 0.005) were significantly higher in HAM from PAF versus Ctl patients. Also the cleaved forms GSDMD-NT (Ctl: 1.000 ± 0.217, n = 8 vs. PAF: 1.796 ± 0.338, n = 7; P = 0.072) and GSDMD-CT (Ctl: 1.000 ± 0.148, n = 8 vs. PAF: 2.662 ± 0.463, n = 7; P = 0.003) were upregulated in PAF compared to Ctl patients (**Figure 33**).

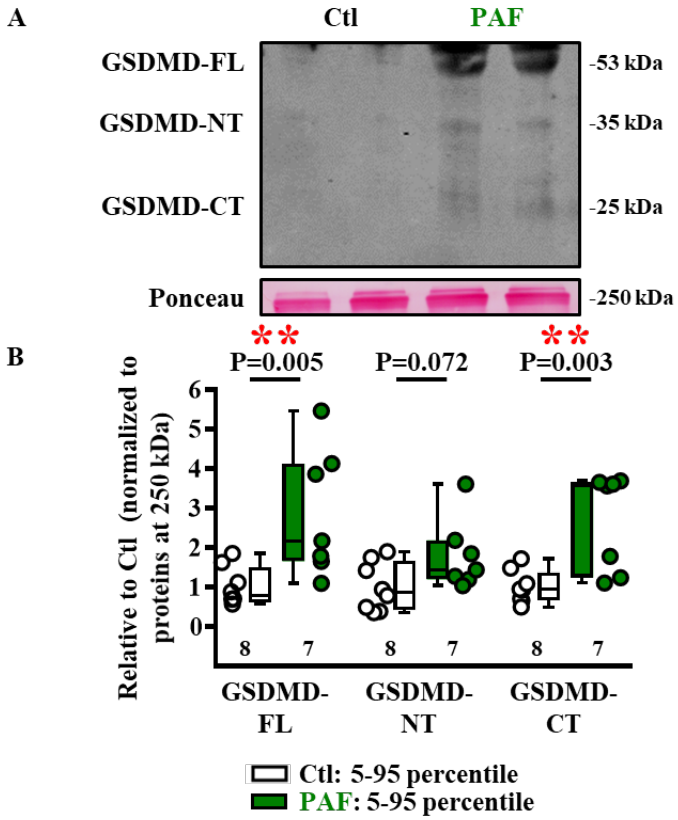

Figure 33: GSDMD in HAM from PAF patients. Representative Western blots of GSDMD-FL, GSDMD-NT and GSDMD-CT (**A**), as well as quantified protein levels (**B**) in human atrial cardiomyocytes from PAF compared to Ctl patients. Total protein levels at 250 kDa (Ponceau staining) were used as loading control. **P<0.01 vs. Ctl (= patients in sinus rhythm); numbers indicate number of patients. GSDMD-CT = C-terminus of gasdermin D; GSDMD-FL = full-length gasdermin D; GSDMD-NT = N-terminus of gasdermin D; PAF = paroxysmal atrial fibrillation.

4.4.3.3 Maturation of cytokines in PAF HAM

Similar to the results obtained HAM from POAF patients (**Figure 31**), the protein expression of the precursor of IL-1β was strongly upregulated (pro-IL-1β: Ctl: 1.000 ± 0.099, n = 8 vs. PAF: 2.457 ± 0.460, n = 8; P = 0.007), whereas the levels of its active form tended to decrease (IL-1β: Ctl: 1.000 ± 0.081, n = 8 vs. PAF: 0.627 ± 0.181, n = 8; P = 0.082) in HAM from PAF compared to Ctl patients (**Figure 34**).

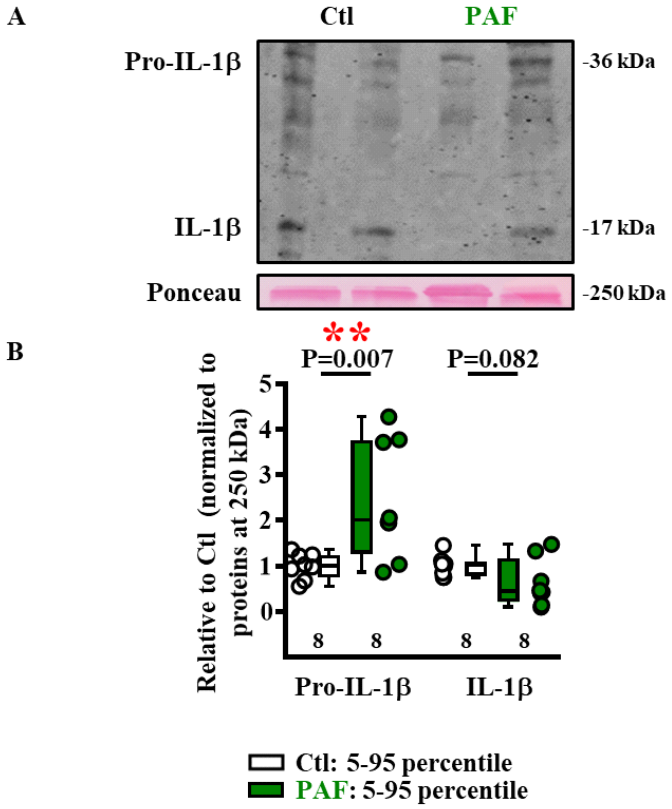

Figure 34: Maturation of IL-1β in HAM from PAF patients. Representative Western blots of pro-IL-1β and IL-1β (**A**), as well as quantified protein levels (**B**) in human atrial cardiomyocytes from PAF compared to Ctl patients. Total protein-levels at 250 kDa (Ponceau staining) were used as loading control. **P<0.01 vs. Ctl (= patients in sinus rhythm); numbers indicate number of patients. (Pro-)IL-1β = (pro-)interleukin-1β; PAF = paroxysmal atrial fibrillation.

4.4.4 NLRP3 inflammatory signaling in HAM from CAF patients

4.4.4.1 NLRP3 inflammasome components in HAM from CAF patients

Protein expression of the NLRP3 inflammasome components were assessed also in HAM from CAF patients (**Figure 35**). There was no significant change in protein levels of NLRP3 (125 kDa: Ctl: 1.000 ± 0.147, n = 11 vs. CAF: 1.262 ± 0.297, n = 10; P = 0.423) and ASC dimers in CAF compared to SR patients (Ctl: 1.000 ± 0.189, n = 8 vs. CAF: 1.446 ± 0.210, n = 8; P = 0.137). However, similar to results in HAM from PAF patients, protein levels of pro-Casp1 (Ctl: 1.000 ± 0.315, n = 10 vs. CAF: 9.809 ± 4.161, n = 12; P = 0.009), its active forms Casp1-p33 (Ctl: 1.000 ± 0.262, n = 10 vs. CAF: 3.499 ± 0.894, n = 12; P = 0.004) and Casp1-p20 (Ctl: 1.000 ± 0.274, n = 10 vs. CAF: 4.789 ± 1.501, n = 12; P = 0.011) were all significantly increased in HAM from CAF versus Ctl patients. Protein expression of Casp1-p10 also showed a tendency to strong upregulation, which did not reach the conventional level of statistical significance (Ctl: 1.000 ± 0.277, n = 10 vs. CAF: 3.584 ± 1.276, n = 12; P = 0.093).

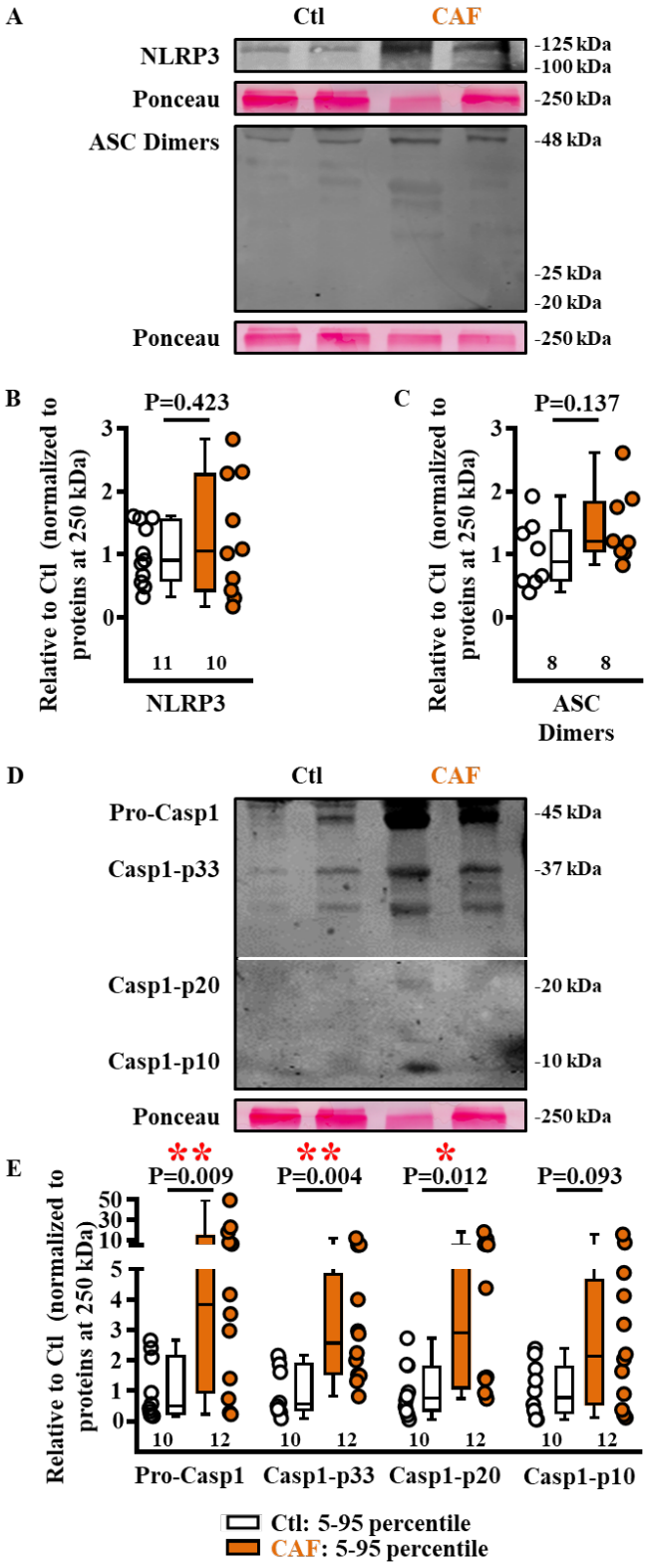

Figure 35: Components of the NLRP3 inflammasome in HAM from CAF patients. Representative Western blots of NLRP3 and ASC (**A**), as well as pro-Casp1 and its active forms Casp1-p33, -p20, and -p10 (**D**), along with their quantified protein levels (**B**, **C** and **E**) in human atrial cardiomyocytes from CAF and Ctl patients. Total protein levels at 250 kDa (Ponceau staining) were used as loading control. *P<0.05, **P<0.01 vs. Ctl (= patients in sinus rhythm); numbers indicate number of patients. ASC = apoptosis-associated speck-like protein containing a CARD domain; CAF = long-standing persistent (chronic) atrial fibrillation; Casp1-p33, -p20,

and -p10 = active caspase-1 forms; pro-Casp1 = pro-caspase-1; NLRP3 = NACHT, LRR and PYD domains containing binding protein 3.

4.4.4.2 Activation of GSDMD in HAM from CAF patients

In contrast to the unchanged GSDMD activation in atrial whole-tissue lysates, HAM from CAF patients showed a strong GSDMD activation compared to Ctl cells. Although the protein levels of GSDMD-FL were unchanged (Ctl: 1.000 ± 0.264, n = 8 vs. CAF: 1.131 ± 0.304, n = 8; P = 0.750), those of its pore-forming domain GSDMD-NT (Ctl: 1.000 ± 0.272, n = 8 vs. CAF: 5.974 ± 1.051, n = 8; P = 0.0004) together with its GSDMD-CT product (Ctl: 1.000 ± 0.210, n = 8 vs. CAF: 4.322 ± 0.851, n = 8; P = 0.002) showed a significant increase in CAF compared to SR patients (**Figure 36**).

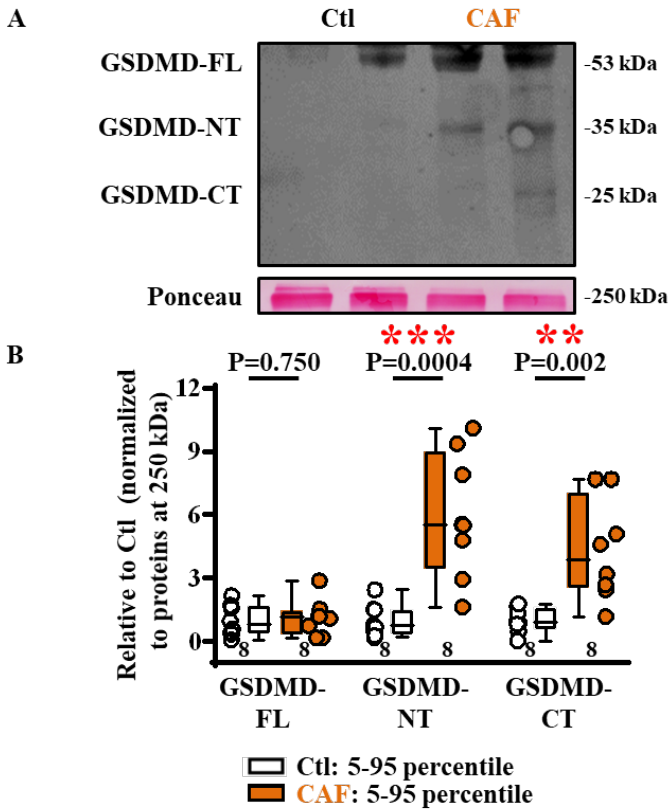

Figure 36: GSDMD in CAF HAM. Representative Western blots of GSDMD-FL, GSDMD-NT and GSDMD-CT (**A**), as well as quantified protein levels (**B**) in human atrial cardiomyocytes from CAF and Ctl patients. Total protein-levels at 250 kDa (Ponceau staining) were used as loading control. **P<0.01, ***P<0.001 vs. Ctl (= patients in sinus rhythm); numbers indicate number of patients. CAF = long-standing persistent (chronic) atrial fibrillation; GSDMD-CT = C-terminus of gasdermin D; GSDMD-FL = full-length gasdermin D; GSDMD-NT = N-terminus of gasdermin D.

4.4.4.3 Maturation of cytokines in HAM from CAF patients

In HAM from CAF patients we could detect a very strong upregulation of the pro-IL-1β protein levels (Ctl: 1.000 ± 0.230, n = 8 vs. CAF: 6.771 ± 1.399, n = 7; P = 0.0003). This was not associated with differences in protein expression of cleaved (active) IL-1β in CAF vs. Ctl (Ctl: 1.000 ± 0.334, n = 8 vs. CAF: 1.969 ± 0.574, n = 7; P = 0.231), potentially reflecting a bias by greater release of IL-1β through upregulated GSDMD plasma membrane pores (**Figure 37**).

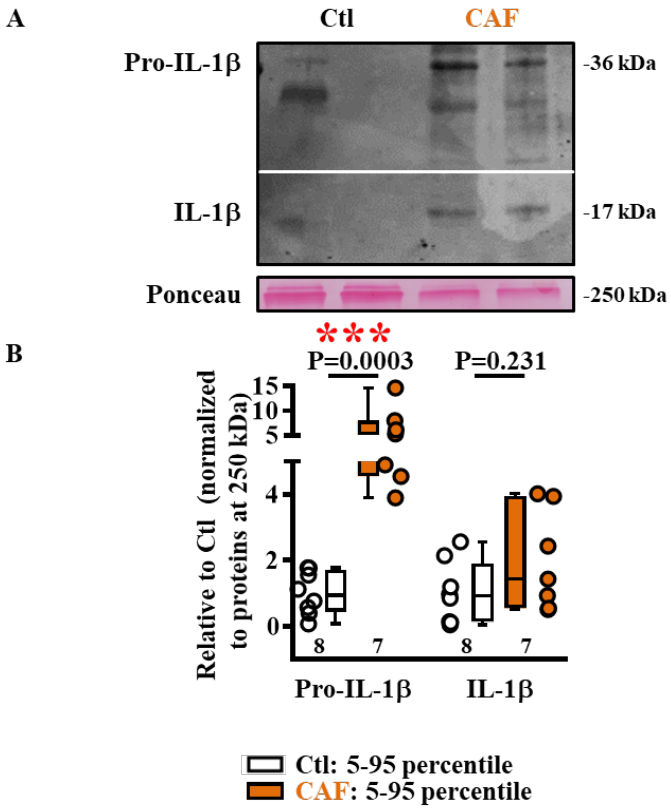

Figure 37: Maturation of IL-1β in HAM from CAF patients. Representative Western blots of pro-IL-1β and IL-1β (**A**), as well as quantified protein levels (**B**) in human atrial cardiomyocytes from CAF and Ctl patients. Total protein levels at 250 kDa (Ponceau staining) were used as loading control. ***P<0.001 vs. Ctl (= patients in sinus rhythm); numbers indicate number of patients. CAF = long-standing persistent (chronic) atrial fibrillation; (Pro-)IL-1β = (pro-)interleukin-1β.

4.5 Influence of other clinical parameter on NLRP3 inflammasome system

AF patients showed strong expression of activated components of the NLRP3-inflammasome system in human atrial whole-tissue homogenates as well as HAM. Given the differences in clinical parameters between Ctl and AF patients (**Table 18-19**), we investigated the potential influence of selected clinical parameters on the expression levels of the individual proteins. We applied 2-way ANOVA analyses to study the specific impact of individual clinical parameters together with their interaction effect with AF type (**Table 26-27**). Controlling for HLP, LAD

or medication like nitrates, DHP and digitalis did not alter the results between the groups. However, we observed a significant association between NFκB-Total levels and LVEF, as well as between GSDMD-FL levels and lipid lowering drugs (LLD) including significant interaction effects for both in whole-tissue lysate of PAF patients (**Figure 38**). In patient samples of CAF patients used for HAM experiments, there was a significant association between Casp-p33 levels and β-blocker including their significant interaction (**Figure 39**).

Table 26: Summary of clinical parameter statistics in atrial whole-tissue homogenates (HMG). Overview of P-values for two-way ANOVA analyses with factors rhythm (Ctl vs. POAF; Ctl. vs. PAF; or Ctl vs. CAF) and angiotensin-converting enzyme (ACE) inhibitors, hyperlipidemia (HLP), left ventricular ejection fraction (LVEF), left-atrial diameter (LAD), use of nitrates (NO), use of lipid-lowering drugs (LLD), or use of digitalis (no vs. yes) for expression levels of NLRP3-inflammasome components. P-values <0.05 have been indicated in purple. P = N/A indicates the inability to perform two-way ANOVA due to an insufficient number of patients in one or more of the subgroups.

	POAF HMG	PAF HMG					CAF HMG		
Parameter	**ACE**	**HLP**	**LVEF**	**LAD**	**NO**	**LLD**	**LVEF**	**LAD**	**Dig.**
NLRP3 100 kDa	P=0.760	P=0.368	P=0.235	P=0.369	P=N/A	P=0.582	P=0.797	P=N/A	P=N/A
NLRP3 125 kDa	P=0.747	P=0.654	P=0.516	P=0.643	P=N/A	P=0.297	P=0.876	P=N/A	P=N/A
ASC Monomers	P=0.711	P=0.726	P=0.982	P=N/A	P=N/A	P=0.497	P=0.542	P=N/A	P=N/A
Pro-Casp1	P=0.138	P=0.849	P=0.935	P=0.066	P=N/A	P=0.611	P=0.174	P=N/A	P=N/A
Casp1-p33	P=0.525	P=0.362	P=0.328	P=0.169	P=N/A	P=0.805	P=0.797	P=N/A	P=N/A
Casp1-p20	P=0.145	P=0.229	P=0.758	P=0.239	P=N/A	P=0.525	P=0.199	P=N/A	P=N/A
GSDMD-FL	P=0.664	P=N/A	P=0.979	P=N/A	P=N/A	P=0.047	P=0.471	P=N/A	P=N/A
GSDMD-NT	P=0.563	P=N/A	P=0.472	P=N/A	P=N/A	P=0.898	P=0.117	P=N/A	P=N/A
GSDMD-CT	P=0.261	P=N/A	P=0.151	P=N/A	P=N/A	P=0.755	P=0.466	P=N/A	P=N/A
Pro-IL-1β	P=0.578	P=0.350	P=0.265	P=0.942	P=N/A	P=0.716	P=0.330	P=N/A	P=N/A
IL-1β	P=0.098	P=0.662	P=0.456	P=0.452	P=N/A	P=0.466	P=0.793	P=N/A	P=N/A
Pro-IL-18	P=0.185	P=N/A	P=0.824	P=N/A	P=N/A	P=0.213	P=0.316	P=N/A	P=N/A
IL-18	P=0.063	P=N/A	P=0.540	P=N/A	P=N/A	P=0.879	P=0.084	P=N/A	P=N/A
TLR4	P=0.162	P=0.396	P=0.938	P=N/A	P=N/A	P=0.765	P=0.697	P=N/A	P=N/A
NFκB-Total	P=0.677	P=N/A	P=0.002	P=N/A	P=N/A	P=0.187	P=0.725	P=N/A	P=N/A
Ser536-NFκB	P=0.599	P=N/A	P=0.101	P=N/A	P=N/A	P=0.283	P=0.389	P=N/A	P=N/A
Total/Ser536	P=0.825	P=N/A	P=0.921	P=N/A	P=N/A	P=0.777	P=0.534	P=N/A	P=N/A
P2X7R	P=0.870	P=0.991	P=0.563	P=0.148	P=N/A	P=0.289	P=0.521	P=N/A	P=N/A
F4/80	P=N/A	P=0.347	P=N/A	P=N/A	P=N/A	P=0.229	P=0.527	P=N/A	P=N/A

CD68	P=N/A	P=N/A	P=0.573	P=N/A	P=N/A	P=0.633	P=0.475	P=N/A	P=N/A
CD206	P=0.576	P=0.630	P=N/A	P=N/A	P=N/A	P=0.296	P=0.558	P=N/A	P=N/A
CD11b	P=N/A	P=0.583	P=N/A	P=N/A	P=N/A	P=0.725	P=0.708	P=N/A	P=N/A

Table 27: Summary of clinical parameter statistics in human atrial cardiomyocytes (HAM). Overview of P-values for two-way ANOVA analyses with factors rhythm (Ctl vs. POAF; Ctl vs. PAF; or Ctl vs. CAF) and hyperlipidemia (HLP), left-atrial diameter (LAD), use of β-blockers (β-bl.), use of dihydropyridines (DHP), or use of digitalis (Dig.; no vs. yes) for expression levels of NLRP3-inflammasome components. P-values <0.05 have been indicated in purple. P = N/A indicates the inability to perform two-way ANOVA due to an insufficient number of patients in one or more of the subgroups.

	POAF HAM	PAF HAM			CAF HAM			
Parameter	**HLP**	**LAD**	**β-bl.**	**DHP**	**LAD**	**Dig.**	**β-bl.**	**DHP**
NLRP3 125 kDa	P=0.642	P=N/A	P=0.963	P=N/A	P=N/A	P=0.221	P=0.331	P=0.122
ASC Dimers	P=0.664	P=N/A	P=0.260	P=N/A	P=N/A	P=0.475	P=N/A	P=0.718
Pro-Casp1	P=0.608	P=N/A	P=0.115	P=N/A	P=N/A	P=0.459	P=0.795	P=0.929
Casp1-p33	P=0.250	P=N/A	P=0.319	P=N/A	P=N/A	P=0.689	P=0.001	P=0.419
Casp1-p20	P=0.911	P=N/A	P=0.644	P=N/A	P=N/A	P=0.810	P=0.888	P=0.770
Casp1-p10	P=0.415	P=N/A	P=0.846	P=N/A	P=N/A	P=0.361	P=0.846	P=0.917
GSDMD-FL	P=0.366	P=N/A	P=0.387	P=N/A	P=N/A	P=0.893	P=N/A	P=0.890
GSDMD-NT	P=0.935	P=N/A	P=0.223	P=N/A	P=N/A	P=0.140	P=N/A	P=0.392
GSDMD-CT	P=0.330	P=N/A	P=0.180	P=N/A	P=N/A	P=0.154	P=N/A	P=0.681
Pro-IL-1β	P=0.645	P=N/A	P=0.809	P=N/A	P=N/A	P=N/A	P=N/A	P=0.967
IL-1β	P=0.614	P=N/A	P=0.547	P=N/A	P=N/A	P=N/A	P=N/A	P=0.694

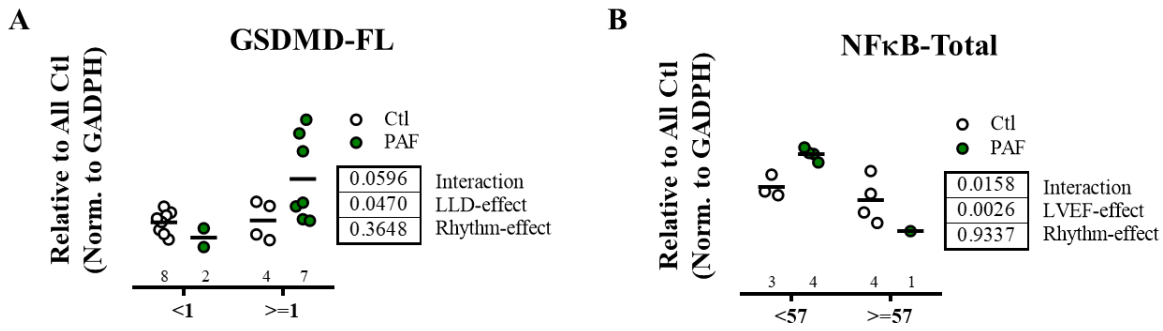

Figure 38: Effect lipid-lowering drugs (LLD) and left-ventricular ejection fraction (LVED) on expression of NLRP3-inflammasome components in HMG from PAF patients. There was a significant increase of GSDMD-FL in PAF patients taking LLD (A). There was an upregulation of NFκB in PAF patients with LVEF ≤ 57 %, but a significant decrease in NFκB with LVEF ≥ 57 % (B). GAPDH = Glyceraldehyde 3-phosphate dehydrogenase; GSDMD-FL = full-length gasdermin D; NFκB-Total = nuclear factor 'kappa-light-chain-enhancer' of activated B-cells; PAF = paroxysmal atrial fibrillation.

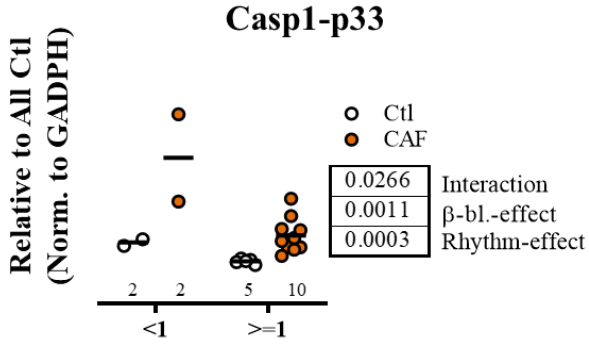

Figure 39: Effect of β-blockers on Casp-1 expression in HAM from CAF patients. There was a significant upregulation of Casp1-p33 in CAF patients regardless of the usage of β-blockers. β-bl. = β-blockers; CAF = chronic atrial fibrillation; Casp1-p33 = active caspase-1; GAPDH = Glyceraldehyde 3-phosphate dehydrogenase.

5 DISCUSSION

This work demonstrates a potential role of the NLRP3 inflammasome in AF pathophysiology. We studied the NLRP3 inflammasome in atrial whole-tissue homogenates and atrial cardiomyocytes from patients undergoing open-heart surgery. We were able to detect an enhanced NLRP3 inflammasome activation in both atrial tissue and HAM from patients with different forms of AF, particularly in those prone to POAF. Together, our results provide novel insight into the AF-promoting atrial substrate involving an upregulation of the NLRP3 inflammasome in AF patients, pointing to a mechanistic link between NLRP3 inflammasome signaling in HAM and AF pathogenesis. These data might help to develop novel approaches for efficient anti-AF therapy.

5.1 Previous work related to cardiac NLRP3 inflammasome

Available data on innate inflammation signaling complexes in the atrium are very limited. Recently, we could demonstrate a causal link between the NLRP3 inflammasome complex and the pathophysiology of PAF and CAF (Yao et al., 2018). Most important, we were able to show that NLRP3 inflammasome activity was enhanced in non-immune cells, particularly in HAM and fibroblasts. We then generated a mouse knockin model with cardiomyocyte-restricted constitutive activation of the NLPR3 complex (Yao et al., 2018). These mice showed increased incidence of premature atrial contractions and were more susceptible to inducible AF as compared to wild-type mice. Furthermore, the specific NLRP3 complex inhibitor MCC950 normalized the susceptibility of these mice to AF. These data revealed that cardiomyocyte (CM)-restricted activation of NLRP3 in mice promotes both ectopic firing and an AF-maintaining substrate, ultimately promoting AF (Yao et al., 2018).

In prior studies, activation of the autonomic nervous system, oxidative stress and inflammation were shown to be major triggers and perpetuators of AF (Harada et al., 2015; Linz et al., 2019). In particular, systematic inflammation is believed to play a pivotal role in POAF pathophysiology. Although data from a clinically-relevant animal model implicated acute inflammation in the formation of reentry, spontaneous AF is not reported. Hence, induction of spontaneous AF might require additional factors (such as DAD-triggered activity) acting on the reentry substrate (Ishii et al., 2017; Ishii et al., 2005). Despite the increasing evidence suggesting an association of inflammatory markers with AF progression, it remains questionable whether inflammatory signaling mechanisms play a direct role in AF formation (Cheng et al., 2012; Gungor et al., 2013; Wu et al., 2014). In addition, there are inconsistencies whether elevated pre-operative inflammatory markers correlate with POAF occurrence (Goette et al., 2002; Jacob et al., 2014; Pretorius et al., 2007; Ucar et al., 2007).

After revealing a multi-functional role of inflammatory signaling in promoting AF pathophysiology in mice, here we tested the hypothesis that enhanced atrial NLRP3-related signaling contributes to a pre-existing vulnerable substrate in patients undergoing open-heart surgery and later develop POAF or patients who already have PAF or CAF. For this purpose, immunoblotting was performed for the relevant proteins of the NLRP3 system. Their specific antibodies were validated with the help of blocking peptides or short-hairpin RNA-mediated knockdown used in atrial whole-tissue lysates, HAM or HL-1 cells (**Figures 6-8; 27-29**). We discovered that patients that go on to develop POAF or have a history of AF exhibit enhanced activation of the NLRP3 inflammasome, potentially contributing to the arrhythmogenic substrate. In addition, the NLRP3 inflammasome is predominantly activated in HAM, particularly in those prone to develop POAF. A data summary and a schematic representation of the activation of the NLRP3 inflammasome in HMG compared to HAM from patients with different AF forms are provided in **Table 28** and **Figure 39**, respectively. The combined findings clearly show that the number of alterations of the NLRP3 inflammasome system is higher in HAM than in HMG, with all forms of AF showing NLRP3 activation in HAM, although the strongest activation was noted in patients with POAF (**Figure 39**). The potential interpretation and implications of these findings for AF pathophysiology and therapy are discussed below.

Table 28: Overview of the different (protein) expression of the NLRP3 inflammasome cascade's components and products in both human atrial homogenates (HMG) and human atrial cardiomyocytes (HAM).

	HMG		HAM	
	Components	Products	Components	Products
POAF	NLRP3 *	IL-1β	NLRP3	Pro-IL-1β **
	ASC	IL-18	ASC **	IL-1β **
	Pro-Casp1	Casp1 *	Pro-Casp1 ***	Casp1 ***
	GSDMD-FL *	-NT *	GSDMD-FL ***	-NT ***
PAF	NLRP3	IL-1β	NLRP3	Pro-IL-1β **
	ASC	IL-18	ASC	IL-1β
	Pro-Casp1	Casp1	Pro-Casp1 **	Casp1 **
	GSDMD-FL *	-NT	GSDMD-FL **	-NT **
CAF	NLRP3	IL-1β	NLRP3	Pro-IL-1β ***
	ASC *	IL-18	ASC	IL-1β
	Pro-Casp1	Casp1	Pro-Casp1 **	Casp1 **
	GSDMD-FL	-NT	GSDMD-FL	-NT ***

ASC = apoptosis-associated speck-like protein containing a CARD domain; CAF = chronic atrial fibrillation; (Pro-)Casp1 = (pro-)caspase-1; GSDMD-FL = full-length gasdermin D; GSDMD-NT = N-terminus of gasdermin D; (Pro-)IL-18 = (pro-)interleukin-18; (Pro-)IL-1β = (pro-)interleukin-1β; NLRP3 = NACHT, LRR and PYD domains containing binding protein 3; PAF = paroxysmal atrial fibrillation; POAF = post-operative atrial fibrillation.

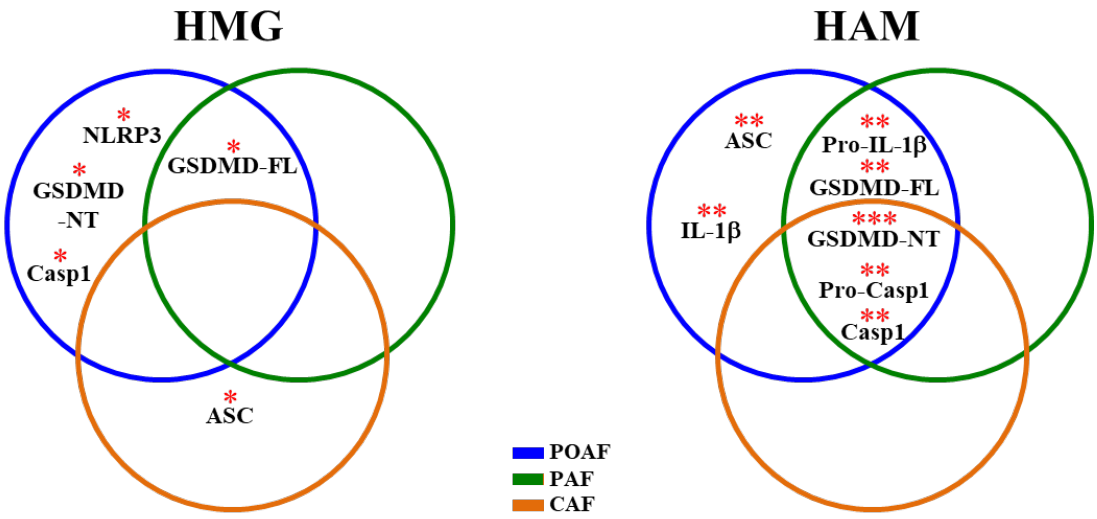

Figure 39: Schematic representation of the NLRP3 inflammasome activation in AF. Significant upregulation of the components and products of the NLRP3 inflammasome activation in HMG (left) and HAM (right) from POAF, PAF and CAF patients. ASC = apoptosis-associated speck-like protein containing a CARD domain; CAF = chronic atrial fibrillation; (Pro-)Casp1 = (pro-)caspase-1; GSDMD-FL = full-length gasdermin D; GSDMD-NT = N-terminus of gasdermin D; (Pro-)IL-1β = (pro-)interleukin-1β; NLRP3 = NACHT, LRR and PYD domains containing binding protein 3; PAF = paroxysmal atrial fibrillation; POAF = post-operative atrial fibrillation.

5.2 Enhanced activation of the NLRP3 inflammasome in atrial whole-tissue homogenates from AF patients

The physiological levels of the NLRP3 transcript are relatively low in the heart, small intestine, colon and kidney, compared to other organs, especially to the lymphatic system (spleen, lymph nodes) (Lech et al., 2010). Nevertheless, we could identify various components of the NLRP3 inflammasome system in atrial whole-tissue lysates from patients with different forms of AF using the Western blot technique.

The analysis of the immunoblotting in POAF atrial whole-tissue lysates showed increased NLRP3 (100 kDa) and Casp1 (p33, p20) as well as upregulated GSDMD (FL and NT), pointing to increased priming of the NLRP3 inflammasome in the atria of POAF patients. This was not the case for PAF whereby only GSDMD-FL was significantly upregulated and Casp1 was surprisingly unchanged. However, upregulated GSDMD could be a result of a non-canonical pathway activation by Casp4/5/11. The non-significant difference among small cytosolic molecules such as IL-1β, IL-18, Casp1, and ASC between Ctl patients and AF patients might partially reflect an early degradation or secretion through the NT-pores.

Work in immune cells has established that NLRP3 contains a leucine-rich repeat (LRR) domain, which although dispensable for the canonical activation of the NLRP3 inflammasome, amplifies the self-catalytic oligomerization and thus activation of NLRP3 (Hafner-Bratkovic et al., 2018). Thus the presence of the shorter (~100 kDa) NLRP3 variant in the human atrium could represent a protective mechanism to decrease sensitivity to endogenous triggers and prevent autoinflammation in the heart (Hafner-Bratkovic et al., 2018). Overall, the lack of transcriptional NLRP3 priming in PAF and CAF suggests that other non-transcriptional mechanisms of NLRP3 activation must exist which regulate the activation of NLRP3 in the atrium. Subsequent work should address the potential activation mechanisms of NLRP3 in PAF and CAF patients. Although the protein levels of ASC monomers were upregulated in CAF patients, it is known that the baseline amount of ASC protein in macrophages is sufficient for activation of the NLRP3 inflammasome and does not require transcriptional priming (Schroder et al., 2012; Sutterwala et al., 2014).

The protein levels of the two major mediators of transcriptional NLRP3 inflammasome priming, TLR4 and NFκB, were upregulated in all forms of AF, pointing to increased transcriptional priming of the NLRP3 inflammasome in AF. Similarly, a strong protein expression of P2X7R was also noted in POAF, PAF and CAF, suggesting also enhanced triggering of the NLRP3 inflammasome in human AF.

To determine whether the activation of NLRP3 inflammatory signaling in AF involves contamination by immune cells, we measured the protein levels of established proinflammatory markers in atrial whole-tissue lysates from patients with either POAF (**Figure 24**), PAF (**Figure 25**) or CAF (**Figure 26**). The protein expression of the macrophage markers F4/80 and CD68 were increased in POAF patients, suggesting that the increase in NLRP3 inflammasome activity is at least in part due to an enhanced atrial infiltration of macrophages in patients prone to POAF. Macrophage markers were not upregulated in PAF and CAF patients, suggesting that the enhanced NLRP3 activation does not involve increased infiltration by immune cells. Overall, exclusive NLRP3 inflammasome activation in macrophages is insufficient to increase AF-inducibility in mice, whereas cardiomyocyte-restricted constitutive NLRP3 inflammasome activation enhances the susceptibility of mice to AF (Yao et al., 2018). Of note, the HAM we studied in patients with different AF forms were not contaminated by macrophages (**Figure 27**), suggesting that like in mice the constitutive NLRP3 inflammasome activation in HAM from AF patients could contribute to AF pathophysiology.

5.3 Upregulation of the NLRP3 inflammasome in HAM from AF patients

Next, we studied the NLRP3 inflammasome cascade in HAM where we detected an activation of the NLRP3 inflammasome in all AF forms. Importantly, this upregulation of the NLRP3 system was quantitatively stronger in HAM than in atrial HMG (**Table 28**, **Figure 39**). Unexpectedly, in HAM we were able to detect only the full-length (~125 kDa) LLR-domain containing NLRP3. Our data suggest that the NLRP3 protein might exist in different forms in the different atrial cell types. As mentioned before in section 4.2.2.1, the 100 kDa band is considered a variant lacking LRR, whereas the 125 kDa band likely corresponds to the full-length NLRP3 protein (Hafner-Bratkovic et al., 2018). The presence of only the latter band in HAM suggests a cell-type specific NLRP3 inflammasome activation, the consequences of which should be studied in detail in subsequent work.

Emerging evidence suggest that the NIMA-related kinase 7 (NEK7) could play an essential role in the activation of the NLRP3 inflammasome in immune cells (Swanson et al., 2019).

NEK7 is a serine-threonine kinase which traditionally is involved in mitosis, but which was recently shown to directly interact with the NLRP3, thereby promoting its oligomerization and facilitating the association with ASC and Casp1 (Swanson et al., 2019). Thus, NEK7 is candidate activation mechanism of NLRP3 in AF patients that should also be studied in future work.

One major new finding of present work is that the protein levels of pro-Casp1 and its active forms (p33, p20 and p10) were strongly increased in POAF, PAF and CAF patients. We were unable to detect ASC monomers in HAM-fractions, but we detected an upregulation of ASC dimers in POAF patients, which might have also contributed to the activation of the NLRP3 system. Consequently, GSDMD was activated in all AF forms, with its activation being strongest in POAF patients. The protein levels of pro-IL-1β were increased in settings of POAF, PAF and CAF, pointing to enhanced transcriptional priming in HAM of AF patients. Surprisingly, its cleaved form IL-1β remained unchanged in PAF/CAF and was significantly downregulated in POAF. The comparable protein amount of small cytosolic molecules such as IL-1β, IL-18, and Casp1, along with lack of detectable ASC monomers could be most likely explained with their increased efflux through the NT-pore (10-18 nm inner diameter) of activated GSDMD, which dissipates ion gradients (Gaidt et al., 2016a; Rogers et al., 2019).

Recent findings from our group demonstrated that the NLRP3 inflammasome activation could contribute to the evolution of a pre-existing arrhythmogenic substrate that allows the induction and accommodation of AF in response to appropriate postoperative triggers in patients prone to POAF (Heijman et al., 2020). By mimicking post-operative inflammation with acute IL-1β application to HAMs under patch-clamp conditions, we could observe an increased occurrence of potentially proarrhythmic spontaneous Ca^{2+}-release events in HAM from POAF patients. These results along with the recent data pointing to CaMKIIδ as a direct upstream activator of the NLRP3 inflammasome support the idea that the NLRP3 inflammasome complex might constitute a mechanism which directly links inflammatory and Ca^{2+} signaling cascades thereby creating a cellular substrate for AF (Heijman et al., 2020; Willeford et al., 2018).

Given the emerging number of associations between NLRP3 and cardiovascular diseases and the potential proarrhythmogenic potential of upregulated NLRP3 system, the NLRP3 inflammasome is increasingly considered as a potential therapeutic target for cardiovascular diseases. Direct and indirect inhibitors of the NLRP3 inflammasome cascade are increasingly developed (Swanson et al., 2019). Unfortunately, the precise mechanisms of action of putative NLRP3 inhibitors are still elusive, making it difficult to avoid off-target effects. A successful

IL-1 signaling inhibition was achieved with the use of biologicals (canakinumab, anakinra and rilonacept) (Dinarello et al., 2012). However, this type of blockade is not organ-specific and could cause substantial detrimental effects. The most promising approach is direct targeting of NLRP3 with small molecule inhibitors such as MCC950, which inhibits both the canonical and non-canonical pathways of NLRP3-inflammasome activation. Although the therapeutic potential of MCC950 has been demonstrated in a number of preclinical immunopathological models, including atherosclerosis and cardiac arrhythmias, MCC950 might cause hepatic toxicity. Although many more small molecules are in clinical development, the only approved inhibitor to date is tranilast, which prevents the NLRP3-NLRP3 interaction and thus its activation by binding to the NACHT domain (Swanson et al., 2019). Whether small molecular NLRP3 inhibitors could represent an effective anti-AF approach should be demonstrated in clinical trials with appropriate AF patient cohorts.

5.4 Limitations

Several limitations should be considered when interpreting the results presented in this thesis. First, patient follow-up was part of routine clinical care and based on symptoms and ECG-monitoring. As such, Ctl patients may have experienced undetected brief POAF episodes. Furthermore, occurrence of asymptomatic PAF before surgery could not be ruled out for some patients. Given the limitations of current AF animal models, work performed with human atrial tissue is essential to better understand AF pathophysiology. However, its limited availability restricted the number of experiments that could be done. For example, tissue is only available from patients undergoing open heart surgery, which may have different risk factors from the general population of AF patients. Moreover, due to the limited accessibility of human left atrial samples, this work was restricted to right atrial appendages only. Because of the diversity of the patients' clinical profile, the results demonstrate some (expected) variability. Therefore, false negative results could not be excluded. The complex interplay of risk factors together with the limited number of samples in individual subgroups also complicate the identification of clinical variables associated with the NLRP3 inflammasome remodeling that we identified in the different forms of AF, likely contributing to the absence of significant interactions in the two-way ANOVA analysis with different clinical variables (**Tables 26-27**).

From an experimental perspective, the BSA used for the preparation of HAM-fractions, precluded the detection of proteins involved in the activation of the NLRP3 inflammasome like P2X7R, NFκB and TLR4 due to their similar molecular weight with BSA. However, we studied these proteins in whole-tissue lysates and the results make it likely that similar changes might

occur in HAM, a hypothesis that needs verification in subsequent work. We performed Western blot only; immunostaining could provide a better understanding of the exact location of the inflammasome activation in HAM. In order to further investigate the mechanism of the NLRP3 inflammatory signaling, extensive experimental work about the alternative priming and triggering pathways of the NLRP3-inflammasome complex is required. Similarly, future functional experiments in HAM are needed to assess the potential proarrhythmic mechanisms mediated by NLRP3 inflammasome activation that we identified.

5.5 Conclusions

This study demonstrated a link between the innate inflammation signaling complex / NLRP3 inflammasome and clinical AF. We could show that NLRP3 inflammasome activation was particularly enhanced in HAM. Thus we discovered a novel paradigm of inflammatory signaling in non-immune cells. Furthermore, we studied the various priming and triggering mechanisms and could show complex activation patterns of the NLRP3-inflammasome system in different forms of AF. Our results provide new insights that could lead to the development of novel anti-AF strategies directed at targeting pre-existing arrhythmogenic substrates created by NLRP3 inflammasome activation. We speculate that a selective NLRP3 inhibition could be beneficial for both the prevention and management of AF.

SUMMARY

Atrial fibrillation (AF) is the most common sustained arrhythmia in developed countries, affecting more than 33 million people worldwide. It leads to increased morbidity and mortality due to complications like stroke, hemodynamic instability, heart failure and cardiomyopathy. AF represents a major public health problem negatively affecting quality of life. Traditionally, AF is defined as paroxysmal (episodes < 7 days; PAF), persistent (episodes > 7 days) and long-standing persistent ("chronic"; CAF). In addition, AF commonly occurs after surgery: post-operative atrial fibrillation (POAF). Post-operative inflammation has been suggested to be an important trigger of POAF and there is accumulating evidence for a potential role of inflammation in other forms of AF. However, the exact mechanistic role of inflammation in AF pathophysiology remains elusive.

As a well-known activator of inflammatory signaling, the "Nucleotide-binding and oligomerization (NACHT), Leucine-rich repeat (LRR) and Pyrin (PYD) domains containing protein 3" (NLRP3) inflammasome could contribute to AF. This thesis addressed the hypothesis that the NLRP3-inflammasome complex is more active in patients with AF, especially in those prone to POAF. The inflammasome components, products and activation pathways were examined using the Western blot technique in right atrial samples of 237 patients. Although protein levels of the inflammasome components - NLRP3, apoptosis-associated speck-like protein (ASC) and caspase-1 (Casp1) - were differently regulated in the distinct forms of AF compared to Ctl, in whole-tissue lysates AF patients showed significant upregulation of the major priming pathway toll-like receptor 4 (TLR4)/nuclear factor kappa-light-chain-enhancer of activated B cells (NFκB), followed by enhanced purinergic receptor subtype 7 (P2X7R) triggering mechanism. Protein expression of gasdermin D (GSDMD), an important effector of the NLRP3 inflammasome, was activated in POAF and PAF, but not CAF patients. Protein levels of the cytokines interleukin-1β and -18 (IL-1β, IL-18), the major products of the NLRP3 inflammasome, remained unchanged. We then performed immunoblotting of the same NLRP3 inflammasome proteins in human atrial cardiomyocytes (HAM)-enriched fractions from patients with POAF, PAF and CAF. It was discovered that the NLRP3 inflammasome was strongly activated in the AF groups vs. the Ctl group with the POAF group showing the strongest activation. Our results position human atrial cardiomyocytes as a major source of inflammatory signaling and indicate that cardiomyocyte NLRP3-inflammasome signaling may contribute to the formation of the AF-promoting vulnerable substrate.

ZUSAMMENFASSUNG

Vorhofflimmern (VHF) ist die häufigste Herzrhythmusstörung, die mit erhöhter Morbidität und Mortalität und mit einem hohen Risiko für Schlaganfälle, Herzinsuffizienz und Myokardischämie einhergeht. Es lassen sich verschiedenen Formen des VHF anhand der Dauer der Episoden unterscheiden: paroxysmales VHF (Episoden < 7 Tage; pVHF), persistierendes VHF (Episoden > 7 Tage) und länger andauerndes, chronisches VHF (cVHF). Post-operatives VHF (poVHF) tritt z.B. als Folge einer Herzoperation auf. Der postoperative Entzündungszustand des Körpers hierbei als Trigger für das Auftreten des poVHF verantwortlich sein könnte. Auch bei den anderen VHF-Formen wird zunehmend vermutet, dass Entzündungsprozesse eine wichtige Rolle spielen könnten. Der genaue Zusammenhang zwischen den Entzündungsvorgängen und der Pathophysiologie des VHF ist jedoch unvollständig geklärt. Ein wichtiger Auslöser von Entzündungsreaktionen ist das „Nukleotidbindung and Oligomerisierung (NACHT), Leucine-rich Repeat (LRR) und Pyrin (PYD) Domäne-beinhaltende Protein 3" (NLRP3) Inflammasom, das zur Pathophysiologie von VHF beitragen könnte. Im Rahmen dieser Studie haben wir deshalb untersucht, ob das NLRP3 Inflammasom bei Patienten mit VHF, insbesondere mit poVHF, vermehrt aktiviert ist. Gewebeproben wurden aus dem rechten Vorhof von 237 Patienten gewonnen und mittels Western Blot Technik hinsichtlich der Aktivierungskaskade sowie der Bestandteile und Produkte des NLRP3 Inflammasoms analysiert. Die Proteinexpression der Bestandteile des Inflammasoms NLRP3, Apoptose-assoziiertes speck-ähnliches Protein (ASC) und Caspase-1 (Casp1) war vergleichbar zwischen Patienten im Sinusrhythmus und Patienten mit verschiedenen Formen des VHF. Allerdings konnten wir ein erhöhtes *Priming* über die Toll-like Rezeptor 4 (TLR4) / nuclear factor kappa-light-chain-enhancer of activated B cells (NFκB) Signalkaskade, gefolgt vom verstärkten *Triggering*, vermittelt durch den Purinergen Rezeptor Subtyp 7 (P2X7R), nachweisen. Die Proteinexpression von Gasdermin D (GSDMD), einem wichtigen Effektor des NLRP3 Inflammasoms, war bei Patienten mit poVHF und pVHF signifikant gesteigert, nicht jedoch bei Patienten mit cVHF. Die Expression der Zytokine Interleukin-1β und -18 (IL-1β, IL-18), die Hauptprodukte des NLRP3-Inflammasoms, war bei allen VHF-Formen unverändert. Als nächstes untersuchten wir die Proteine des NLRP3 Inflammasoms mit Western Blot in isolierten atrialen Kardiomyozyten (HAM) von Patienten mit poVHF, pVHF und cVHF. Hier konnten wir bei allen untersuchten VHF-Gruppen eine starke Aktivierung des NLRP3 Inflammasoms im Vergleich zur Kontrollgruppe (Sinusrhythmus) nachwiesen, wobei die Aktivierung des NLRP3 Inflammasoms bei poVHF am stärksten ausfiel. Unsere Ergebnisse etablieren die Vorthofmyozyten als Hauptreservoir entzündlicher Vorgänge und deuten darauf hin, dass die Aktivierung des NLRP3 Inflammasoms in Kardiomyozyten die Entwicklung eines VHF-fördernden arrhythmogenen Substrats begünstigen könnte.

REFERENCES

1. Aglietti, R. A., Estevez, A., Gupta, A., Ramirez, M. G., Liu, P. S., Kayagaki, N., Ciferri, C., Dixit, V. M., Dueber, E. C. M. (2016): GsdmD p30 elicited by caspase-11 during pyroptosis forms pores in membranes. Proc Natl Acad Sci U S A 113, 7858-7863.

2. Ahlsson, A., Fengsrud, E., Bodin, L.,Englund, A. (2010): Postoperative atrial fibrillation in patients undergoing aortocoronary bypass surgery carries an eightfold risk of future atrial fibrillation and a doubled cardiovascular mortality. Eur J Cardiothorac Surg 37, 1353-1359.

3. Aziz, M., Jacob, A., Yang, W. L., Matsuda, A.,Wang, P. (2013): Current trends in inflammatory and immunomodulatory mediators in sepsis. J Leukoc Biol 93, 329-342.

4. Baroja-Mazo, A., Martin-Sanchez, F., Gomez, A. I., Martinez, C. M., Amores-Iniesta, J., Compan, V., Barbera-Cremades, M., Yague, J., Ruiz-Ortiz, E., Anton, J., Bujan, S., Couillin, I., Brough, D., Arostegui, J. I.,Pelegrin, P. (2014): The NLRP3 inflammasome is released as a particulate danger signal that amplifies the inflammatory response. Nat Immunol 15, 738-748.

5. Bauernfeind, F., Niepmann, S., Knolle, P. A.,Hornung, V. (2016): Aging-Associated TNF Production Primes Inflammasome Activation and NLRP3-Related Metabolic Disturbances. J Immunol 197, 2900-2908.

6. Bauernfeind, F. G., Horvath, G., Stutz, A., Alnemri, E. S., MacDonald, K., Speert, D., Fernandes-Alnemri, T., Wu, J., Monks, B. G., Fitzgerald, K. A., Hornung, V.,Latz, E. (2009): Cutting edge: NF-kappaB activating pattern recognition and cytokine receptors license NLRP3 inflammasome activation by regulating NLRP3 expression. J Immunol 183, 787-791.

7. Boucher, D., Monteleone, M., Coll, R. C., Chen, K. W., Ross, C. M., Teo, J. L., Gomez, G. A., Holley, C. L., Bierschenk, D., Stacey, K. J., Yap, A. S., Bezbradica, J. S.,Schroder, K. (2018): Caspase-1 self-cleavage is an intrinsic mechanism to terminate inflammasome activity. J Exp Med 215, 827-840.

8. Broz, P.,Dixit, V. M. (2016): Inflammasomes: mechanism of assembly, regulation and signalling. Nat Rev Immunol 16, 407-420.

9. Broz, P., Newton, K., Lamkanfi, M., Mariathasan, S., Dixit, V. M.,Monack, D. M. (2010): Redundant roles for inflammasome receptors NLRP3 and NLRC4 in host defense against Salmonella. J Exp Med 207, 1745-1755.

10. Bryan, N. B., Dorfleutner, A., Rojanasakul, Y.,Stehlik, C. (2009): Activation of inflammasomes requires intracellular redistribution of the apoptotic speck-like protein containing a caspase recruitment domain. J Immunol 182, 3173-3182.

11. Burnstock, G. (2016): P2X ion channel receptors and inflammation. Purinergic Signal 12, 59-67.

12. Burnstock, G.,Knight, G. E. (2018): The potential of P2X7 receptors as a therapeutic target, including inflammation and tumour progression. Purinergic Signal 14, 1-18.

13. Chen, K. W., Gross, C. J., Sotomayor, F. V., Stacey, K. J., Tschopp, J., Sweet, M. J.,Schroder, K. (2014): The neutrophil NLRC4 inflammasome selectively promotes IL-1beta maturation without pyroptosis during acute Salmonella challenge. Cell Rep 8, 570-582.

14. Cheng, T., Wang, X. F., Hou, Y. T.,Zhang, L. (2012): Correlation between atrial fibrillation, serum amyloid protein A and other inflammatory cytokines. Mol Med Rep 6, 581-584.

15. Dick, M. S., Sborgi, L., Ruhl, S., Hiller, S.,Broz, P. (2016): ASC filament formation serves as a signal amplification mechanism for inflammasomes. Nat Commun 7, 11929.

16. Dinarello, C. A., Simon, A.,van der Meer, J. W. (2012): Treating inflammation by blocking interleukin-1 in a broad spectrum of diseases. Nat Rev Drug Discov 11, 633-652.

17. Ding, J., Wang, K., Liu, W., She, Y., Sun, Q., Shi, J., Sun, H., Wang, D. C.,Shao, F. (2016): Pore-forming activity and structural autoinhibition of the gasdermin family. Nature 535, 111-116.

18. Dobrev, D., Aguilar, M., Heijman, J., Guichard, J. B.,Nattel, S. (2019): Postoperative atrial fibrillation: mechanisms, manifestations and management. Nat Rev Cardiol 16, 417-436.

19. Evavold, C. L., Ruan, J., Tan, Y., Xia, S., Wu, H.,Kagan, J. C. (2018): The Pore-Forming Protein Gasdermin D Regulates Interleukin-1 Secretion from Living Macrophages. Immunity 48, 35-44 e36.

20. Fernandes-Alnemri, T., Kang, S., Anderson, C., Sagara, J., Fitzgerald, K. A.,Alnemri, E. S. (2013): Cutting edge: TLR signaling licenses IRAK1 for rapid activation of the NLRP3 inflammasome. J Immunol 191, 3995-3999.

21. Fernandes-Alnemri, T., Wu, J., Yu, J. W., Datta, P., Miller, B., Jankowski, W., Rosenberg, S., Zhang, J.,Alnemri, E. S. (2007): The pyroptosome: a supramolecular assembly of ASC dimers mediating inflammatory cell death via caspase-1 activation. Cell Death Differ 14, 1590-1604.

22. Filardo, G., Damiano, R. J., Jr., Ailawadi, G., Thourani, V. H., Pollock, B. D., Sass, D. M., Phan, T. K., Nguyen, H.,da Graca, B. (2018): Epidemiology of new-onset atrial fibrillation following coronary artery bypass graft surgery. Heart 104, 985-992.

23. Franchi, L., Eigenbrod, T.,Nunez, G. (2009): Cutting edge: TNF-alpha mediates sensitization to ATP and silica via the NLRP3 inflammasome in the absence of microbial stimulation. J Immunol 183, 792-796.

24. Friedrichs, K., Baldus, S.,Klinke, A. (2012): Fibrosis in Atrial Fibrillation - Role of Reactive Species and MPO. Front Physiol 3, 214.

25. Gaidt, M. M., Ebert, T. S., Chauhan, D., Schmidt, T., Schmid-Burgk, J. L., Rapino, F., Robertson, A. A., Cooper, M. A., Graf, T.,Hornung, V. (2016a): Human Monocytes Engage an Alternative Inflammasome Pathway. Immunity 44, 833-846.

26. Gaidt, M. M.,Hornung, V. (2016b): Pore formation by GSDMD is the effector mechanism of pyroptosis. EMBO J 35, 2167-2169.

27. Goette, A., Juenemann, G., Peters, B., Klein, H. U., Roessner, A., Huth, C.,Rocken, C. (2002): Determinants and consequences of atrial fibrosis in patients undergoing open heart surgery. Cardiovasc Res 54, 390-396.

28. Graf, E. M., Bock, M., Heubach, J. F., Zahanich, I., Boxberger, S., Richter, W., Schultz, J. H.,Ravens, U. (2005): Tissue distribution of a human Ca v 1.2 alpha1 subunit splice variant with a 75 bp insertion. Cell Calcium 38, 11-21.

29. Groslambert, M.,Py, B. F. (2018): Spotlight on the NLRP3 inflammasome pathway. J Inflamm Res 11, 359-374.

30. Gungor, B., Ekmekci, A., Arman, A., Ozcan, K. S., Ucer, E., Alper, A. T., Calik, N., Yilmaz, H., Tezel, T., Coker, A.,Bolca, O. (2013): Assessment of interleukin-1 gene cluster polymorphisms in lone atrial fibrillation: new insight into the role of inflammation in atrial fibrillation. Pacing Clin Electrophysiol 36, 1220-1227.

31. Hafner-Bratkovic, I., Susjan, P., Lainscek, D., Tapia-Abellan, A., Cerovic, K., Kadunc, L., Angosto-Bazarra, D., Pelegrin, P.,Jerala, R. (2018): NLRP3 lacking the leucine-rich repeat domain can be fully activated via the canonical inflammasome pathway. Nat Commun 9, 5182.

32. Harada, M., Van Wagoner, D. R.,Nattel, S. (2015): Role of inflammation in atrial fibrillation pathophysiology and management. Circ J 79, 495-502.

33. Heijman, J., Kirchner, D., Kunze, F., Chretien, E. M., Michel-Reher, M. B., Voigt, N., Knaut, M., Michel, M. C., Ravens, U.,Dobrev, D. (2018): Muscarinic type-1 receptors contribute to IK,ACh in human atrial cardiomyocytes and are upregulated in patients with chronic atrial fibrillation. Int J Cardiol 255, 61-68.

34. Heijman, J., Muna, A. P., Veleva, T., Molina, C. E., Sutanto, H., Tekook, M., Wang, Q., Abu-Taha, I. H., Gorka, M., Kunzel, S., El-Armouche, A., Reichenspurner, H., Kamler, M., Nikolaev, V., Ravens, U., Li, N., Nattel, S., Wehrens, X. H. T.,Dobrev, D. (2020): Atrial Myocyte NLRP3/CaMKII Nexus Forms a Substrate for Postoperative Atrial Fibrillation. Circ Res 127, 1036-1055.

35. Heijman, J., Voigt, N., Nattel, S.,Dobrev, D. (2014): Cellular and molecular electrophysiology of atrial fibrillation initiation, maintenance, and progression. Circ Res 114, 1483-1499.

36. Huang, X., Feng, Y., Xiong, G., Whyte, S., Duan, J., Yang, Y., Wang, K., Yang, S., Geng, Y., Ou, Y.,Chen, D. (2019): Caspase-11, a specific sensor for intracellular lipopolysaccharide recognition, mediates the non-canonical inflammatory pathway of pyroptosis. Cell Biosci 9, 31.

37. Ishii, Y., Schuessler, R. B., Gaynor, S. L., Hames, K.,Damiano, R. J., Jr. (2017): Postoperative atrial fibrillation: The role of the inflammatory response. J Thorac Cardiovasc Surg 153, 1357-1365.

38. Ishii, Y., Schuessler, R. B., Gaynor, S. L., Yamada, K., Fu, A. S., Boineau, J. P.,Damiano, R. J., Jr. (2005): Inflammation of atrium after cardiac surgery is associated with inhomogeneity of atrial conduction and atrial fibrillation. Circulation 111, 2881-2888.

39. Iyer, S. S., He, Q., Janczy, J. R., Elliott, E. I., Zhong, Z., Olivier, A. K., Sadler, J. J., Knepper-Adrian, V., Han, R., Qiao, L., Eisenbarth, S. C., Nauseef, W. M., Cassel, S. L.,Sutterwala, F. S. (2013): Mitochondrial cardiolipin is required for Nlrp3 inflammasome activation. Immunity 39, 311-323.

40. Jacob, K. A., Nathoe, H. M., Dieleman, J. M., van Osch, D., Kluin, J.,van Dijk, D. (2014): Inflammation in new-onset atrial fibrillation after cardiac surgery: a systematic review. Eur J Clin Invest 44, 402-428.

41. Jamilloux, Y., Lefeuvre, L., Magnotti, F., Martin, A., Benezech, S., Allatif, O., Penel-Page, M., Hentgen, V., Seve, P., Gerfaud-Valentin, M., Duquesne, A., Desjonqueres, M., Laurent, A., Remy-Piccolo, V., Cimaz, R., Cantarini, L., Bourdonnay, E., Walzer, T., Py, B. F., Belot, A.,Henry, T. (2018): Familial Mediterranean fever mutations are hypermorphic mutations that specifically decrease the activation threshold of the Pyrin inflammasome. Rheumatology (Oxford) 57, 100-111.

42. Juliana, C., Fernandes-Alnemri, T., Kang, S., Farias, A., Qin, F.,Alnemri, E. S. (2012): Non-transcriptional priming and deubiquitination regulate NLRP3 inflammasome activation. J Biol Chem 287, 36617-36622.

43. Karmakar, M., Katsnelson, M., Malak, H. A., Greene, N. G., Howell, S. J., Hise, A. G., Camilli, A., Kadioglu, A., Dubyak, G. R.,Pearlman, E. (2015): Neutrophil IL-1beta processing induced by pneumolysin is mediated by the NLRP3/ASC inflammasome and caspase-1 activation and is dependent on K+ efflux. J Immunol 194, 1763-1775.

44. Karmakar, M., Katsnelson, M. A., Dubyak, G. R.,Pearlman, E. (2016): Neutrophil P2X7 receptors mediate NLRP3 inflammasome-dependent IL-1beta secretion in response to ATP. Nat Commun 7, 10555.

45. Karmakar, M., Minns, M., Greenberg, E. N., Diaz-Aponte, J., Pestonjamasp, K., Johnson, J. L., Rathkey, J. K., Abbott, D. W., Wang, K., Shao, F., Catz, S. D., Dubyak, G. R.,Pearlman, E. (2020): N-GSDMD trafficking to neutrophil organelles facilitates IL-1beta release independently of plasma membrane pores and pyroptosis. Nat Commun 11, 2212.

46. Kayagaki, N., Stowe, I. B., Lee, B. L., O'Rourke, K., Anderson, K., Warming, S., Cuellar, T., Haley, B., Roose-Girma, M., Phung, Q. T., Liu, P. S., Lill, J. R., Li, H., Wu, J., Kummerfeld, S., Zhang, J., Lee, W. P., Snipas, S. J., Salvesen, G. S., Morris, L. X., Fitzgerald, L., Zhang, Y., Bertram, E. M., Goodnow, C. C.,Dixit, V. M. (2015): Caspase-11 cleaves gasdermin D for non-canonical inflammasome signalling. Nature 526, 666-671.

47. Kayagaki, N., Warming, S., Lamkanfi, M., Vande Walle, L., Louie, S., Dong, J., Newton, K., Qu, Y., Liu, J., Heldens, S., Zhang, J., Lee, W. P., Roose-Girma, M.,Dixit, V. M. (2011): Non-canonical inflammasome activation targets caspase-11. Nature 479, 117-121.

48. Kayagaki, N., Wong, M. T., Stowe, I. B., Ramani, S. R., Gonzalez, L. C., Akashi-Takamura, S., Miyake, K., Zhang, J., Lee, W. P., Muszynski, A., Forsberg, L. S., Carlson, R. W.,Dixit, V. M. (2013): Noncanonical inflammasome activation by intracellular LPS independent of TLR4. Science 341, 1246-1249.

49. Kirchhof, P., Benussi, S., Kotecha, D., Ahlsson, A., Atar, D., Casadei, B., Castella, M., Diener, H. C., Heidbuchel, H., Hendriks, J., Hindricks, G., Manolis, A. S., Oldgren, J., Popescu, B. A., Schotten, U., Van Putte, B., Vardas, P., Agewall, S., Camm, J., Baron Esquivias, G., Budts, W., Carerj, S., Casselman, F., Coca, A., De Caterina, R., Deftereos, S., Dobrev, D., Ferro, J. M., Filippatos, G., Fitzsimons, D., Gorenek, B., Guenoun, M., Hohnloser, S. H., Kolh, P., Lip, G. Y., Manolis, A., McMurray, J., Ponikowski, P., Rosenhek, R., Ruschitzka, F., Savelieva, I., Sharma, S., Suwalski, P., Tamargo, J. L., Taylor, C. J., Van Gelder, I. C., Voors, A. A., Windecker, S., Zamorano, J. L.,Zeppenfeld, K. (2016): 2016 ESC Guidelines for the management of atrial fibrillation developed in collaboration with EACTS. Europace 18, 1609-1678.

50. Laemmli, U. K. (1970): Cleavage of structural proteins during the assembly of the head of bacteriophage T4. Nature 227, 680-685.

51. Latz, E. (2010): The inflammasomes: mechanisms of activation and function. Curr Opin Immunol 22, 28-33.

52. Lavrik, I. N., Golks, A.,Krammer, P. H. (2005): Caspases: pharmacological manipulation of cell death. J Clin Invest 115, 2665-2672.

53. Lech, M., Avila-Ferrufino, A., Skuginna, V., Susanti, H. E.,Anders, H. J. (2010): Quantitative expression of RIG-like helicase, NOD-like receptor and inflammasome-related mRNAs in humans and mice. Int Immunol 22, 717-728.

54. Lieberman, J., Wu, H.,Kagan, J. C. (2019): Gasdermin D activity in inflammation and host defense. Sci Immunol 4

55. Lin, K. M., Hu, W., Troutman, T. D., Jennings, M., Brewer, T., Li, X., Nanda, S., Cohen, P., Thomas, J. A.,Pasare, C. (2014): IRAK-1 bypasses priming and directly links TLRs to rapid NLRP3 inflammasome activation. Proc Natl Acad Sci U S A 111, 775-780.

56. Linz, D., Elliott, A. D., Hohl, M., Malik, V., Schotten, U., Dobrev, D., Nattel, S., Bohm, M., Floras, J., Lau, D. H.,Sanders, P. (2019): Role of autonomic nervous system in atrial fibrillation. Int J Cardiol 287, 181-188.

57. Liu, X., Zhang, Z., Ruan, J., Pan, Y., Magupalli, V. G., Wu, H.,Lieberman, J. (2016): Inflammasome-activated gasdermin D causes pyroptosis by forming membrane pores. Nature 535, 153-158.

58. Maesen, B., Nijs, J., Maessen, J., Allessie, M.,Schotten, U. (2012): Post-operative atrial fibrillation: a maze of mechanisms. Europace 14, 159-174.

59. Man, S. M.,Kanneganti, T. D. (2016): Converging roles of caspases in inflammasome activation, cell death and innate immunity. Nat Rev Immunol 16, 7-21.

60. Man, S. M., Karki, R.,Kanneganti, T. D. (2017): Molecular mechanisms and functions of pyroptosis, inflammatory caspases and inflammasomes in infectious diseases. Immunol Rev 277, 61-75.

61. Mangan, M. S. J., Olhava, E. J., Roush, W. R., Seidel, H. M., Glick, G. D.,Latz, E. (2018): Targeting the NLRP3 inflammasome in inflammatory diseases. Nat Rev Drug Discov 17, 588-606.

62. Martinon, F., Burns, K.,Tschopp, J. (2002): The inflammasome: a molecular platform triggering activation of inflammatory caspases and processing of proIL-beta. Mol Cell 10, 417-426.

63. Masumoto, J., Taniguchi, S., Ayukawa, K., Sarvotham, H., Kishino, T., Niikawa, N., Hidaka, E., Katsuyama, T., Higuchi, T.,Sagara, J. (1999): ASC, a novel 22-kDa protein, aggregates during apoptosis of human promyelocytic leukemia HL-60 cells. J Biol Chem 274, 33835-33838.

64. Medzhitov, R. (2008): Origin and physiological roles of inflammation. Nature 454, 428-435.

65. Melduni, R. M., Schaff, H. V., Bailey, K. R., Cha, S. S., Ammash, N. M., Seward, J. B.,Gersh, B. J. (2015): Implications of new-onset atrial fibrillation after cardiac surgery on long-term prognosis: a community-based study. Am Heart J 170, 659-668.

66. Miao, E. A., Leaf, I. A., Treuting, P. M., Mao, D. P., Dors, M., Sarkar, A., Warren, S. E., Wewers, M. D.,Aderem, A. (2010): Caspase-1-induced pyroptosis is an innate immune effector mechanism against intracellular bacteria. Nat Immunol 11, 1136-1142.

67. Misawa, T., Takahama, M., Kozaki, T., Lee, H., Zou, J., Saitoh, T.,Akira, S. (2013): Microtubule-driven spatial arrangement of mitochondria promotes activation of the NLRP3 inflammasome. Nat Immunol 14, 454-460.

68. Monie, T. P. (2017): The Canonical Inflammasome: A Macromolecular Complex Driving Inflammation. Subcell Biochem 83, 43-73.

69. Munoz-Planillo, R., Kuffa, P., Martinez-Colon, G., Smith, B. L., Rajendiran, T. M.,Nunez, G. (2013): K(+) efflux is the common trigger of NLRP3 inflammasome activation by bacterial toxins and particulate matter. Immunity 38, 1142-1153.

70. Netea, M. G., Nold-Petry, C. A., Nold, M. F., Joosten, L. A., Opitz, B., van der Meer, J. H., van de Veerdonk, F. L., Ferwerda, G., Heinhuis, B., Devesa, I., Funk, C. J., Mason, R. J., Kullberg, B. J., Rubartelli, A., van der Meer, J. W.,Dinarello, C. A. (2009): Differential requirement for the activation of the inflammasome for processing and release of IL-1beta in monocytes and macrophages. Blood 113, 2324-2335.

71. Piccini, A., Carta, S., Tassi, S., Lasiglie, D., Fossati, G.,Rubartelli, A. (2008): ATP is released by monocytes stimulated with pathogen-sensing receptor ligands and induces IL-1beta and IL-18 secretion in an autocrine way. Proc Natl Acad Sci U S A 105, 8067-8072.

72. Pretorius, M., Donahue, B. S., Yu, C., Greelish, J. P., Roden, D. M.,Brown, N. J. (2007): Plasminogen activator inhibitor-1 as a predictor of postoperative atrial fibrillation after cardiopulmonary bypass. Circulation 116, I1-7.

73. Ren, M., Li, X., Hao, L.,Zhong, J. (2015): Role of tumor necrosis factor alpha in the pathogenesis of atrial fibrillation: A novel potential therapeutic target? Ann Med 47, 316-324.

74. Ridker, P. M., MacFadyen, J. G., Thuren, T., Everett, B. M., Libby, P., Glynn, R. J.,Group, C. T. (2017): Effect of interleukin-1beta inhibition with canakinumab on incident lung cancer in patients with atherosclerosis: exploratory results from a randomised, double-blind, placebo-controlled trial. Lancet 390, 1833-1842.

75. Rogers, C., Erkes, D. A., Nardone, A., Aplin, A. E., Fernandes-Alnemri, T.,Alnemri, E. S. (2019): Gasdermin pores permeabilize mitochondria to augment caspase-3 activation during apoptosis and inflammasome activation. Nat Commun 10, 1689.

76. Ruhl, S.,Broz, P. (2015): Caspase-11 activates a canonical NLRP3 inflammasome by promoting K(+) efflux. Eur J Immunol 45, 2927-2936.

77. Sanders, M. G., Parsons, M. J., Howard, A. G., Liu, J., Fassio, S. R., Martinez, J. A.,Bouchier-Hayes, L. (2015): Single-cell imaging of inflammatory caspase dimerization reveals differential recruitment to inflammasomes. Cell Death Dis 6, e1813.

78. Savio, L. E. B., de Andrade Mello, P., da Silva, C. G.,Coutinho-Silva, R. (2018): The P2X7 Receptor in Inflammatory Diseases: Angel or Demon? Front Pharmacol 9, 52.

79. Sborgi, L., Ruhl, S., Mulvihill, E., Pipercevic, J., Heilig, R., Stahlberg, H., Farady, C. J., Muller, D. J., Broz, P.,Hiller, S. (2016): GSDMD membrane pore formation constitutes the mechanism of pyroptotic cell death. EMBO J 35, 1766-1778.

80. Schroder, K., Sagulenko, V., Zamoshnikova, A., Richards, A. A., Cridland, J. A., Irvine, K. M., Stacey, K. J.,Sweet, M. J. (2012): Acute lipopolysaccharide priming boosts inflammasome activation independently of inflammasome sensor induction. Immunobiology 217, 1325-1329.

81. Schroder, K.,Tschopp, J. (2010): The inflammasomes. Cell 140, 821-832.

82. Scott, L., Jr., Li, N.,Dobrev, D. (2019): Role of inflammatory signaling in atrial fibrillation. Int J Cardiol 287, 195-200.

83. Sharma, D.,Kanneganti, T. D. (2016): The cell biology of inflammasomes: Mechanisms of inflammasome activation and regulation. J Cell Biol 213, 617-629.

84. Sutterwala, F. S., Haasken, S.,Cassel, S. L. (2014): Mechanism of NLRP3 inflammasome activation. Ann N Y Acad Sci 1319, 82-95.

85. Swanson, K. V., Deng, M.,Ting, J. P. (2019): The NLRP3 inflammasome: molecular activation and regulation to therapeutics. Nat Rev Immunol 19, 477-489.

86. Takeuchi, O.,Akira, S. (2010): Pattern recognition receptors and inflammation. Cell 140, 805-820.

87. Ucar, H. I., Tok, M., Atalar, E., Dogan, O. F., Oc, M., Farsak, B., Guvener, M., Yilmaz, M., Dogan, R., Demircin, M.,Pasaoglu, I. (2007): Predictive significance of plasma levels of interleukin-6 and high-sensitivity C-reactive protein in atrial fibrillation after coronary artery bypass surgery. Heart Surg Forum 10, E131-135.

88. van de Veerdonk, F. L., Netea, M. G., Dinarello, C. A.,Joosten, L. A. (2011): Inflammasome activation and IL-1beta and IL-18 processing during infection. Trends Immunol 32, 110-116.

89. Van Tassell, B. W., Toldo, S., Mezzaroma, E.,Abbate, A. (2013): Targeting interleukin-1 in heart disease. Circulation 128, 1910-1923.

90. Van Wagoner, D. R.,Chung, M. K. (2018): Inflammation, Inflammasome Activation, and Atrial Fibrillation. Circulation 138, 2243-2246.

91. Volonte, C., Apolloni, S., Skaper, S. D.,Burnstock, G. (2012): P2X7 receptors: channels, pores and more. CNS Neurol Disord Drug Targets 11, 705-721.

92. von Moltke, J., Ayres, J. S., Kofoed, E. M., Chavarria-Smith, J.,Vance, R. E. (2013): Recognition of bacteria by inflammasomes. Annu Rev Immunol 31, 73-106.

93. Wakili, R., Voigt, N., Kaab, S., Dobrev, D.,Nattel, S. (2011): Recent advances in the molecular pathophysiology of atrial fibrillation. J Clin Invest 121, 2955-2968.

94. Wallach, D., Kang, T. B., Dillon, C. P.,Green, D. R. (2016): Programmed necrosis in inflammation: Toward identification of the effector molecules. Science 352, aaf2154.

95. Willeford, A., Suetomi, T., Nickle, A., Hoffman, H. M., Miyamoto, S.,Heller Brown, J. (2018): CaMKIIdelta-mediated inflammatory gene expression and inflammasome activation in cardiomyocytes initiate inflammation and induce fibrosis. JCI Insight 3

96. Wu, G., Cheng, M., Huang, H., Yang, B., Jiang, H.,Huang, C. (2014): A variant of IL6R is associated with the recurrence of atrial fibrillation after catheter ablation in a Chinese Han population. PLoS One 9, e99623.

97. Xiao, H., Li, H., Wang, J. J., Zhang, J. S., Shen, J., An, X. B., Zhang, C. C., Wu, J. M., Song, Y., Wang, X. Y., Yu, H. Y., Deng, X. N., Li, Z. J., Xu, M., Lu, Z. Z., Du, J., Gao, W., Zhang, A. H., Feng, Y.,Zhang, Y. Y. (2018): IL-18 cleavage triggers cardiac inflammation and fibrosis upon beta-adrenergic insult. Eur Heart J 39, 60-69.

98. Xu, Q., Bo, L., Hu, J., Geng, J., Chen, Y., Li, X., Chen, F.,Song, J. (2018): High mobility group box 1 was associated with thrombosis in patients with atrial fibrillation. Medicine (Baltimore) 97, e0132.

99. Yang, D., He, Y., Munoz-Planillo, R., Liu, Q.,Nunez, G. (2015): Caspase-11 Requires the Pannexin-1 Channel and the Purinergic P2X7 Pore to Mediate Pyroptosis and Endotoxic Shock. Immunity 43, 923-932.

100. Yao, C., Veleva, T., Scott, L., Jr., Cao, S., Li, L., Chen, G., Jeyabal, P., Pan, X., Alsina, K. M., Abu-Taha, I., Ghezelbash, S., Reynolds, C. L., Shen, Y. H., LeMaire, S. A., Schmitz, W., Muller, F. U., El-Armouche, A., Eissa, N. T., Beeton, C., Nattel, S., Wehrens, X. H. T., Dobrev, D.,Li, N. (2018): Enhanced Cardiomyocyte NLRP3 Inflammasome Signaling Promotes Atrial Fibrillation. Circulation 138(20), 2227-2242.

101. Zhou, R., Yazdi, A. S., Menu, P.,Tschopp, J. (2011): A role for mitochondria in NLRP3 inflammasome activation. Nature 469, 221-225.

102. Zoni-Berisso, M., Lercari, F., Carazza, T.,Domenicucci, S. (2014): Epidemiology of atrial fibrillation: European perspective. Clin Epidemiol 6, 213-220.

LIST OF FIGURES

LIST OF TABLES

NON-STANDARD ABBREVIATIONS AND ACRONYMS

ACE	Angiotensin-converting enzyme
AF	Atrial fibrillation
AGTR	Angiotensin-II receptor
APD	Action potential duration
ASC	Apoptosis-associated speck-like protein (containing a CARD)
ATP	Adenosine trisphosphate
BCA	Bicinchoninic acid
BMDM	Mouse bone marrow-derived macrophage
BMI	Body mass index
BSA	Bovine serum albumin
BSB	Bromophenol blue
CAF	Long-standing persistent (‘chronic’) atrial fibrillation
CARD	Caspase activation and recruitment domain
Casp1	Caspase 1
Casp4/5/11	Caspase 4/5/11
CD68	Cluster of differentiation 68
CD206	Cluster of differentiation 206
CD11b	Cluster of differentiation 11b
CF	Cardiac fibroblast
CM	Cardiomyocyte
CRP	C-reactive protein
CSQ	Calsequestrin
CT	C-terminus
Ctl	Control patients without atrial fibrillation
DAD	Delayed afterdepolarization
DAMP	Damage-associated molecular pattern
DDT	Dithiothreitol
DHP	Dihydropyridines
F4/80	EGF-like module-containing mucin-like hormone receptor-like 1

FADD	Fas-associated protein with death domain
FL	Full-length
GAPDH	Glyceraldehyde 3-phosphate dehydrogenase
GPRC	Protein-coupled receptor family C
GSDMD	Gasdermin D
HAM	Human atrial cardiomyocyte
HL-1	Immortalized mouse cardiac cell line
HMG	Homogenate
IκB	Endogenous inhibitor of NFκB
I_{Kur}	Ultra-rapid delayed-rectified K^+ current
(Pro-)IL-18	Interleukin-18
(Pro-)IL-1β	Interleukin-1β
IL-1R	Interleukin-1 receptor
IRAK4	Interleukin-1 receptor-associated kinase 4
LAD	Left atrial diameter
LPS	Lipopolysaccharide
LRR	Leucine-rich repeat
LVEF	Left ventricular ejection fraction
Lys	Atrial lysate
MPO	Myeloperoxidase
MyD88	Myeloid differentiation primary response 88
NACHT	Nucleotide-binding and oligomerization domain
NFκB	Nuclear factor kappa-light-chain-enhancer of activated B cells
NLR	Nod-like receptor
NLRP3	NACHT, LRR and PYD domains containing protein 3
NT	N-terminus
P2X7R	Purinergic receptor-7
PAF	Paroxysmal atrial fibrillation
PAMP	Pathogen-associated molecular pattern
POAF	Post-operative atrial fibrillation
PRR	Pattern recognition receptor

PYD	Pyrin domain
RIPK1/3	Receptor-interacting serine/threonine-protein kinase 1/3
(mt)ROS	(Mitochondrial) reactive oxygen species
RyR2	Ryanodine receptor 2
SDS	Sodium dodecyl sulfate
SR	Sinus rhythm
TBST	Tris-buffered saline with Tween20
THP1	human monocytic cell line Tohoku Hospital Pediatrics-1
TLR(4)	Toll-like receptor (4)
TNF-α	Tumor necrosis factor α
TNFR	Tumor necrosis factor receptor
TRIF	TIR domain-containing adapter-inducing interferon-β
TRIK	TIR-domain-containing adapter-inducing interferon-β

ACKNOWLEDGEMENTS

I wish to express my sincere appreciation to my supervisor and mentor, Univ.-Prof. Dr. med. Dobromir Dobrev, to whom I would be forever indebted for giving me this amazing opportunity to take part in such an important project. Without his persistent support, this work would have never been possible.

Next, I would like to express my deepest gratitude to the academic crew in our department, who has provided to me constant support from the very beginning to the very end. I could always rely on them for everything that came along. Special thanks go to Prof. Dr. Jordi Heijman. I whole-heartedly appreciate your great advice for my study that proved monumental towards the success of this work. I wish to show my gratitude to Prof. Dr. Anke Fender, Drs. Issam Abu-Taha and Marina Schäfer for teaching me the language of science. I would like to thank as well the numerous roommates of mine, sharing the same faith and although going through the same struggles as me, never let the positivity leave our room.

Furthermore, I wish to thank all the people from the technical personnel, whose assistance was a milestone in the completion of this project. A special thank goes to Ramona Nagel, who introduced me to laboratory work, as well as Simone Olesch and Bettina Mausa, who were working with me on various parts of the project. I would like to show my appreciation to Iris Weinbach for always looking after me like a guardian.

I would never forget all the people working in the Institute of Pharmacology in Essen, who happened to be my first family here in Germany. They introduced me to the culture and life here, took care of me and helped me immensely to integrate and find my place in the society. I would never forget you, who have tremendously contributed to my personal growth.

Last but not least I would like to pay my special regards to my family and friends. I want to thank my parents for making it possible for me to study and start a life abroad by supporting me both financially and mentally. I cannot express enough my gratitude to my father, Valentin, for his unstoppable motivation and dedication, and to my mother, Zhaneta, for being my rock and source of never ending love. To all my friends, here and in Bulgaria, I love you from the bottom of my heart.

CURRICULUM VITAE

Aus datenschutzrechtlichen Gründen ist der Lebenslauf in der Online-Version nicht enthalten

Publications:

07.2020	*Heijman J*, Muna P*, **Veleva T**, Molina C, Sutanto H, Tekook M, Wang Q, Abu- Taha I, Gorka M, Künzel S, El- Armouche A, Reichenspurner H, Kamler M, Nikolaev V, Ravens U, Li N, Nattel S, Wehrens X, Dobrev D.* Atrial Myocyte NLRP3/CAMKII Nexus Forms a Substrate for Post-Operative Atrial Fibrillation. ***Circ Res.*** (doi: 10.1161/CIRCRESAHA.120.316710) *equally contributed first authors.
07.2018	*Yao C*, **Veleva T***, Scott L Jr, Cao S, Li L, Chen G, Jeyabal P, Pan X, Alsina KM, Abu-Taha I, Ghezelbash S, Reynolds CL, Shen YH, LeMaire SA, Schmitz W, Müller FU, El-Armouche A, Eissa NT, Beeton C, Nattel S, Wehrens XHT, Dobrev D, Li N***.** Enhanced Cardiomyocyte NLRP3 Inflammasome Signaling Promotes Atrial Fibrillation. ***Circulation,*** doi: 10.1161/CIRCULATIONAHA.118.035202. *equally contributed first authors.

Awards:

04.2018	*Travel Award* 84. Jahrestagung der Deutsche Gesellschaft der Kardiologie in Mannheim, Germany.
06.2017	*Poster Award* 41st European Society of Cardiology Working Group on Cardiac Cellular Electrophysiology Meeting in Wien, Austria.

Published abstracts:

05.2018	***Veleva T**, Abu-Taha I, Schmidt C, Kamler M, Heijman J, Nattel S, Wehrens X, Li N, Dobrev D.* The Role of the NLRP3 Inflammasome in Atrial Fibrillation. 39th Heart Rhythm Society's Annual Scientific Sessions in Boston, MA, USA.
04.2018	***Veleva T**, Abu-Taha I, Schmidt C, Kamler M, Heijman J, Nattel S, Wehrens X, Li N, Dobrev D*. The Role of the NLRP3 Inflammasome in Postoperative Atrial Fibrillation. 84. Jahrestagung der Deutsche Gesellschaft der Kardiologie in Mannheim, Germany.
06.2017	***Veleva T**, Li N, Schmidt C, Abu-Taha I, Kamler M, Heijman J, Nattel S, Wehrens X*, *Dobrev D.* 41st European Society of Cardiology Working Group on Cardiac Cellular Electrophysiology Meeting in Wien, Austria.

Congress presentation:

06.2019	***Veleva T,** Schmidt C, Abu-Taha I, Kamler M, Heijman J, Wehrens X, Nattel S, Dobrev D.*

The Role of the NLRP3 Inflammasome in Postoperative Atrial Fibrillation.
15th Annual Scientific Congress of the European Cardiac Arrhythmia Society in Marseille, France.